T-1700

A TIME-DOMAIN ELECTROMAGNETIC SURVEY OF THE EAST RIFT ZONE, KILAUEA VOLCANO, HAWAII

By

Catherine King Skokan

T-1700

A Thesis submitted to the Faculty and the Board of Trustees of the Colorado School of Mines in partial fulfillment of the requirements for the degree of Doctor of Philosophy in Geophysical Engineering.

Signed: Catherine King Bokan
Student

Golden, Colorado

Date: Dec. 12, 1974

Approved: George V. Keller
Thesis Advisor

George V. Keller
Head of Department

Golden, Colorado

Date: Dec. 12, 1974

ABSTRACT

A time-domain electromagnetic survey was conducted over the East Rift Zone of Kilauea Volcano, Hawaii. The purpose of the survey was two-fold. First, the survey was intended to give greater insight into interpretation techniques of time-domain electromagnetic data. Secondly, a more complete picture of the geologic structure and hydrology of the Rift, with special emphasis on its geothermal potential, was to be gained.

To interpret the time-domain electromagnetic data, first the maximum-received voltages were converted to apparent resistivities and mapped. Next, the received transients were matched with a catalog of asymptotic curves. Then, theoretical layered-earth curves were calculated and the transients were again matched. Finally, use of a least-squares-fit computer program gave a more exact interpretation. Although the asymptotic curves have been calculated for no more than a three-layer case, the theoretical matching technique may be expanded to a greater number of layers.

A comparison of time-domain electromagnetic results with the results of conventional DC dipole mapping surveys shows that both measurements provide essentially the same resistivity information. Time-domain electromagnetic surveys, however, provide resistivity versus depth information as well.

After interpretation, a low-resistivity area of geothermal interest was outlined approximately seven kilometers south of the town of Pahoa.

TABLE OF CONTENTS

ILLUSTRATIONS

ACKNOWLEDGEMENTS

I wish to express my appreciation to Dr. G. V. Keller, my thesis advisor, for his help and guidance. For their criticism and participation on my committee, I am grateful to Drs. L. T. Grose, P. Romig, M. W. Major, and D. I. Dickinson.

Support for the survey was part of a Kilauea Volcano project funded by the National Science Foundation (NSF).

I wish to thank John Shupe, Director of the Hawaii Geothermal Project (University of Hawaii) for permission to use DC resistivity data from the Puna District. This project is also funded by NSF.

Finally, I want to thank my husband, Jack, for his criticism of the thesis and for his support during its preparation.

INTRODUCTION

Electromagnetic methods have been used in many geophysical surveys in an attempt to relate electrical conductivity variations with subsurface geologic structure. The earliest mention of an electromagnetic system for prospecting was in 1908. This method used a "black box" which emitted an inductive wave which would penetrate all but metallic substances. The areal extent of a conductive ore body at depth could be ascertained by passing this device over the surface of the ground (Popular Mechanics, 1908, p. 33-34). In the 1910's and 1920's, patents for loop-loop systems were issued in Europe and electromagnetic surveys were used to search for metallic ore deposits. The success of this method led to the development of a dipole-dipole (ELTRAN) system for oil detection in sedimentary basins. This method fell into disrepute when the theory for a layered-earth model was developed in the 1950's and it was found that the resolution to identify layers was not as good as anticipated (Vanyan, 1967, p. 9). Because of this, theoretical development of electromagnetic methods has been much slower than developments of the more popular direct-current methods.

There is a basic electromagnetic classification: frequency-domain and time-domain. With frequency-domain measurements, individual frequencies are transmitted and received. Because of this, very narrow band filtering can be used to reject noise. With time-domain measurements, a step change in current is transmitted and a transient is received. A wider band receiver is required to avoid distortion.

Both frequency- and time-domain electromagnetic measurements are inherently related through Fourier transforms.

mathematical modeling in the frequency-domain has been studied for the layered model more extensively than in the time-domain. In the literature, frequency-domain theory and interpretation have been developed by Keller and Frischknecht (1966), Frischknecht (1967), Keller (1968), Silva (1969), Prichard (1971), Daniels (1974) and others. Time-domain theory has had limited publications. A few of the published articles include those by Kaufman, et al. (1970), Vanyan (1967), Silva (1969), King (1971), and Isaev, et al. (1971). There have been even more infrequent applications of interpretations (Keller, 1970; Jackson and Keller, 1972). Time-domain electromagnetic interpretation techniques require more investigation so time-domain surveys may be utilized to their full potential.

A time-domain electromagnetic survey was conducted in the East Rift Zone of Kilauea Volcano, Hawaii, by students of the Colorado School of Mines. Three interpretation methods

were used to evaluate the East Rift data. First, a maximum-voltage resistivity map was plotted. Maximum-voltage resistivities are easily and quickly calculated in the field. For the remaining two interpretation procedures, a layered-earth model was used. Next, asymptotic curves were used to estimate resistivities and thicknesses for a sequence of layers. Finally, the field data were matched with computer-calculated multi-layered earth-model curves. This curve matching technique was carried out in both the time-domain and the frequency-domain. A least-squares-fit technique was used to find a closer multi-layer interpretation of the data.

Through this study, interpretation methods of time-domain electromagnetic data may be understood, and a more accurate representation of the hydrology and of the subsurface structure and geothermal potential of the East Rift Zone of Kilauea Volcano will result.

DESCRIPTION OF FIELD AREA

Background

The Island of Hawaii is composed of five volcanoes. The youngest, Kilauea, is an asymmetrical shield-shaped dome, and lies on the main rift zone which is also occupied by Kohala and Mauna Kea (Stearns, 1966, p. 128). The dome is cut by two zones of dikes which are characterized by fissures and cones. The eastern zone, the East Rift Zone (Stearns and Macdonald, 1946, p. 129), is also called the Puna Rift Zone. Figure 1 shows a map of the Island of Hawaii.

Ancient Hawaiian legend gives an account of the origin of the East Rift Zone of Kilauea. Kahavari, Chief of Puna, while celebrating the festival of Lono, announced a Holua (sliding) contest. In disguise, Pele, goddess of volcanoes, challenged Kahavari. Pele was badly beaten and, thinking that her sled was inferior, she asked to trade and try again. When Kahavari refused, Pele became angry and stamped her foot causing a river of lava to pour from the hill into the valley. Horrified, Kahavari recognized Pele and fled for the ocean. Coming to a chasm, he saw Pele riding the ap-

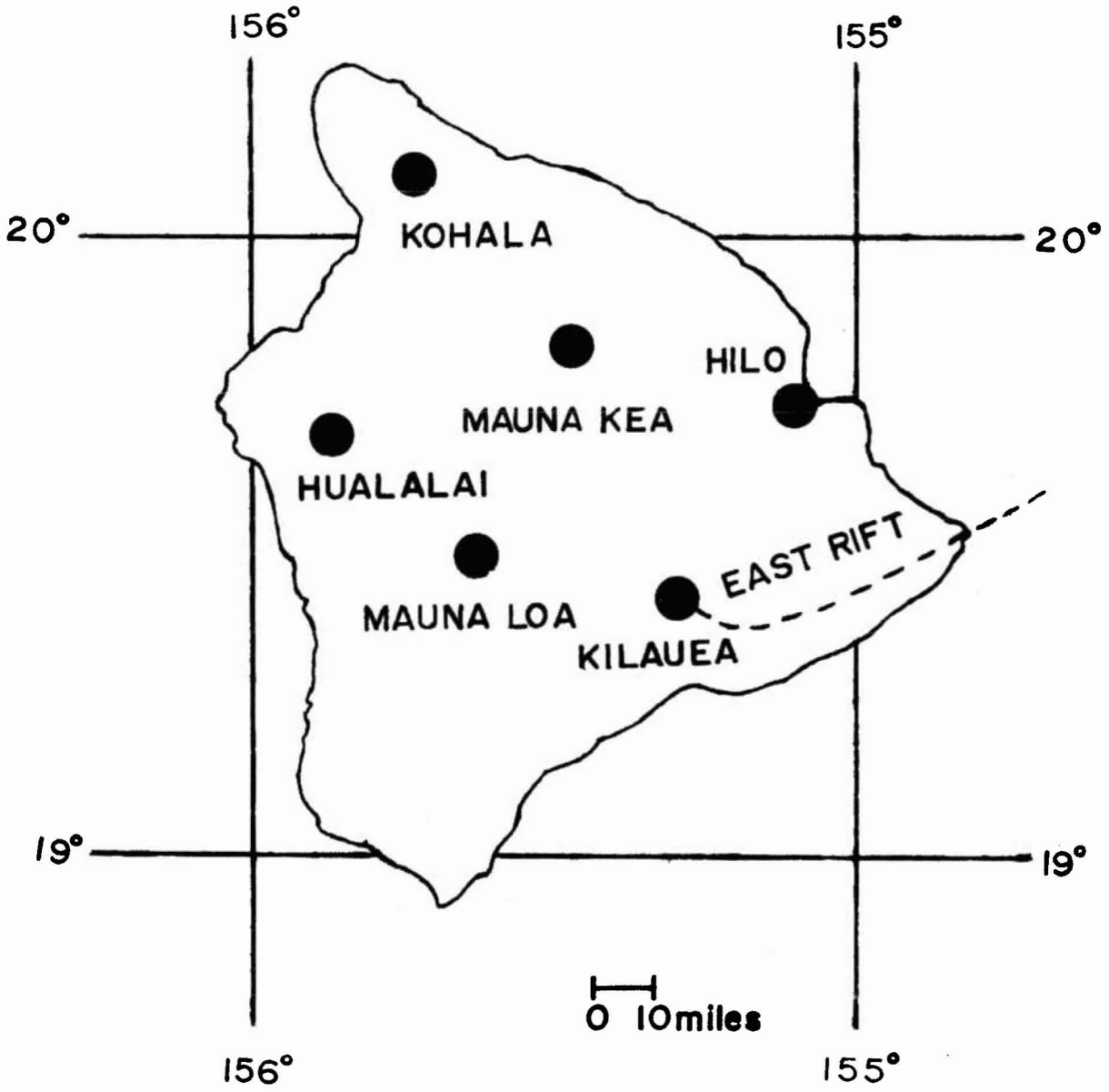

Figure 1. Map of the Island of Hawaii.

proaching lava. He crossed by making a bridge with his spear and safely reached the ocean. Kahavari fled to Oahu where he remained because of his fear of the unforgiving Goddess Pele. The East Rift of Puna remains as proof of the power and disposition of Pele (Kalakaua, 1888).

Geophysical Studies

Kilauea Volcano is the most active modern volcano in the world. As well as at the summit, many eruptions have occurred along the eastern section of its flank, the Puna Rift Zone. In recorded historic time, there were Puna eruptions in 1750, 1790, 1840, 1884, 1923-1924, 1955, and most recently in 1961. During the 1961 eruption, the town of Kapoho was destroyed by lava. Because many people live and work in the Puna District along the Rift, the U. S. Geological Survey has monitered both tilt and seismicity from the Hawaiian Volcanic Observatory. These measurements are carried out to find centers of inflation and seismic activity related to lava movements to try to locate the most likely time and area for the next eruption. Such evaluations are not generally concerned with explaining subsurface structures, hydrology, or the geothermal potential of the rift zone.

A few surveys either included or were concentrated in the East Rift Zone in the Puna District. A regional gravity

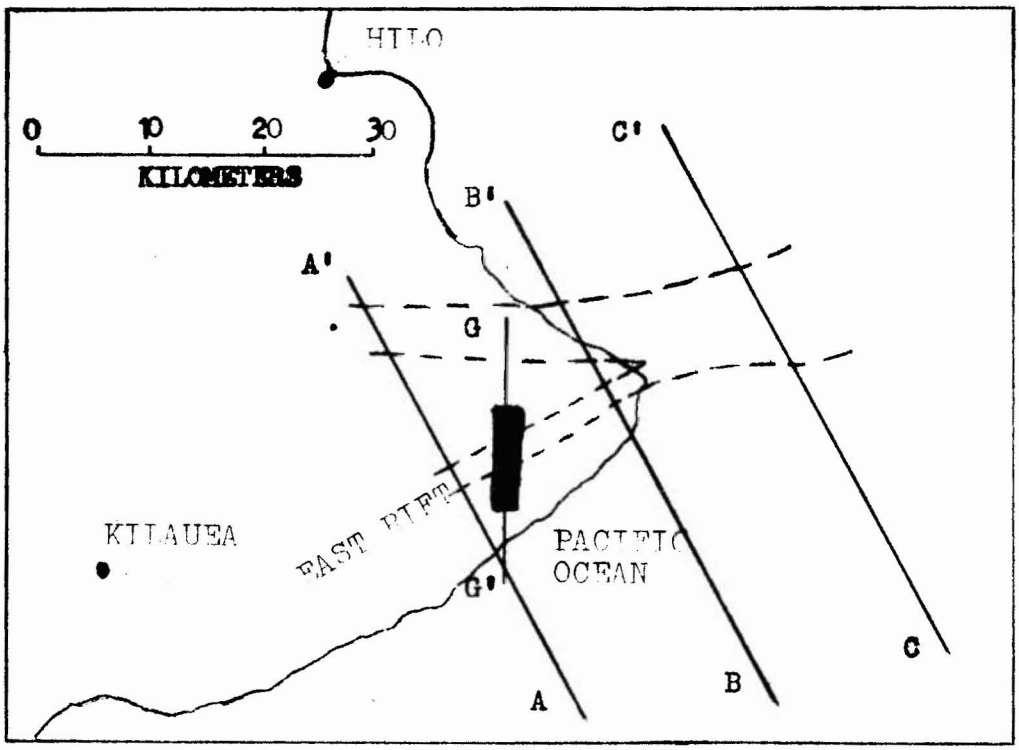

Figure 2. Location map of the gravity and magnetic profiles through the Puna District. The resultant dike positions are indicated. G-G' shows the position of a dike obtained from interpretation of the gravity data; A-A', B-B', and C-C' show the position of dikes obtained from interpretation of the magnetic data.

survey of the Island of Hawaii was conducted by Kinoshita, et al. Macdonald (1965) states that the gravity high along the Puna Rift shows dense material, such as dikes, at depth. Figure 2 illustrates the location of a cross section through the rift which was interpretated to show the dike complex.

Malahoff and McCoy (1967) confirm this dike concept with a magnetic survey. They, too, feel a composite dike or plug complex extends to considerable depths. Figure 2 also illustrates a set of cross sections through the East Rift Zone. Malahoff and McCoy (1967) believe that the northern dike system is related to a Mauna Loa rift while the shallow dike system is related to Kilauea. The two merge just off shore. This dike model agrees with the Puna Rift structure obtained from the gravity interpretation.

The USGS flew an IR survey in 1966 which covered a 15 km strip along the coast 1 km south of Cape Kumukahi. Near shore, anomalies show that the groundwater is warmer than the ocean water. This temperature is attributed to onshore volcanic activity (Fischer, et al., 1966). The University of Hawaii recently sponsored a DC resistivity survey of the East Rift to help evaluate its geothermal potential. The results of this survey will be compared to the electromagnetic surveys in the area. In 1972 and 1973, a time-domain electromagnetic survey was conducted over the eastern section of the rift to clarify structure with emphasis on the geothermal potential of the area.

Geologic Structure

Figure 3 is a geologic map of the East Rift. This rift extends from Kilauea southeastward for 7.3 km, then turns N65°E and continues beyond Cape Kumukahi into the ocean for 70 km, then disappears. The submarine portion of the rift is a prominent ridge which contains a composite plug or dike complex. Normal faults occur on the flanks of the ridge.

On land, the East Rift Zone is marked by many fissures, cones, and pit craters. Macdonald and Eaton (1964, p. 6) state that there are more than 70 lava vents on the surface and surely many hundred more which have been buried. Basaltic lava which flows from these vents has built a broad arch with its crest along the rift. This lava comes from Kilauea through a continuous series of lava tubes. Finch (1946) reasoned that the high number of pit craters are formed by engulfment into lava tubes. "The upper grouping of the craters is due to the intersection of the Puna Rift by a series of fissures trending NE-SW....Any such intersection....would be a favorable location for the development of pit craters" (p. 2).

Generally, vents occur on the northwest side of the

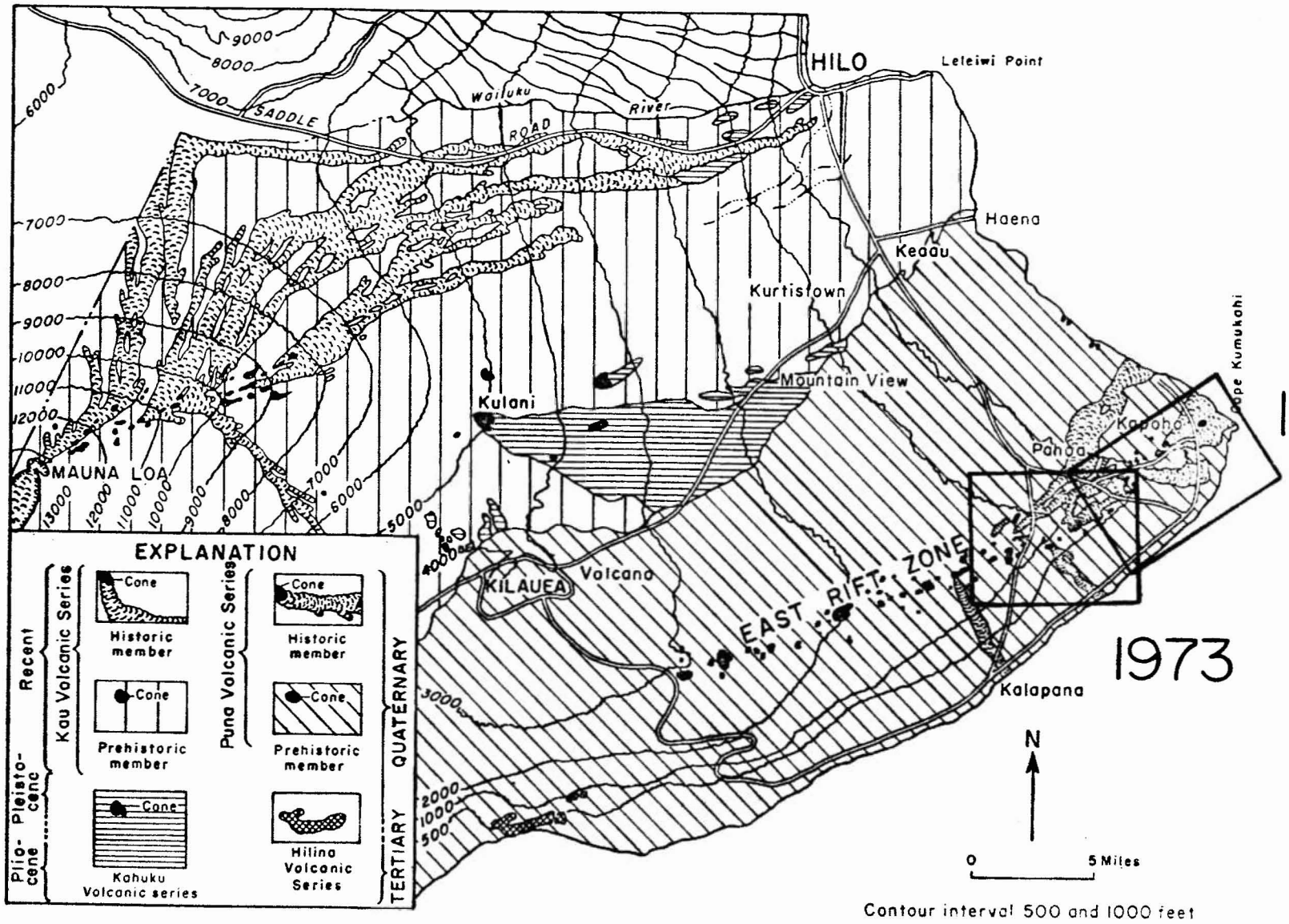

Figure 3. Generalized geologic map of the East Rift and surrounding areas (after Davis and Yamanaga, 1968, p. 5). Location of the 1972 and 1973 time-domain electromagnetic surveys are indicated.

rift and mark the zone of faulting and cracking. The southeast side is marked by cinder cones and is the area of most eruptive activity. Moore and Richter (1962) interpret this saying "that the rift zone dips southeastward, with the zone of faulting marking its actual surface intersection and the zone of cones formed by piercing its hanging wall" (p. 446). The south side of the rift zone is steep from faulting. Many en echelon fissures follow the rift. Figure 4 shows the relationship of these fissures, cinder cones and grabens on the eastern part of the rift.

The rift zone is bounded by grabens. The graben area has been filled repeatedly so that the total movement is not measureable; but it must be considerable. For example, in 1924, vertical movement of 10 to 12 feet was measured during an eruption (Finch, 1925). The rift is covered by alternating layers of ashes and flows of unknown thickness.

There are two basic concepts to explain the existence of the East Rift. Macdonald (1949, p. 63) believes that Kilauea results from the intersection of gravity faults in the flank of Mauna Loa with an easterly zone of fissuring. Moore feels that the rift is the result of large scale landsliding. He believes that the southern slope of Kilauea is sliding seaward, the fractures on which the movement is taking place steepening to near vertical to form the East Rift Zone, with graben collapse along the upper edge of the sliding block (Macdonald, 1965, p. 327). Magma

Figure 4. Block diagram showing the relationship between faulting, eruptive fissures, and cones in the eastern part of the Puna Rift (after Moore and Krivoy, 1964, p. 2042).

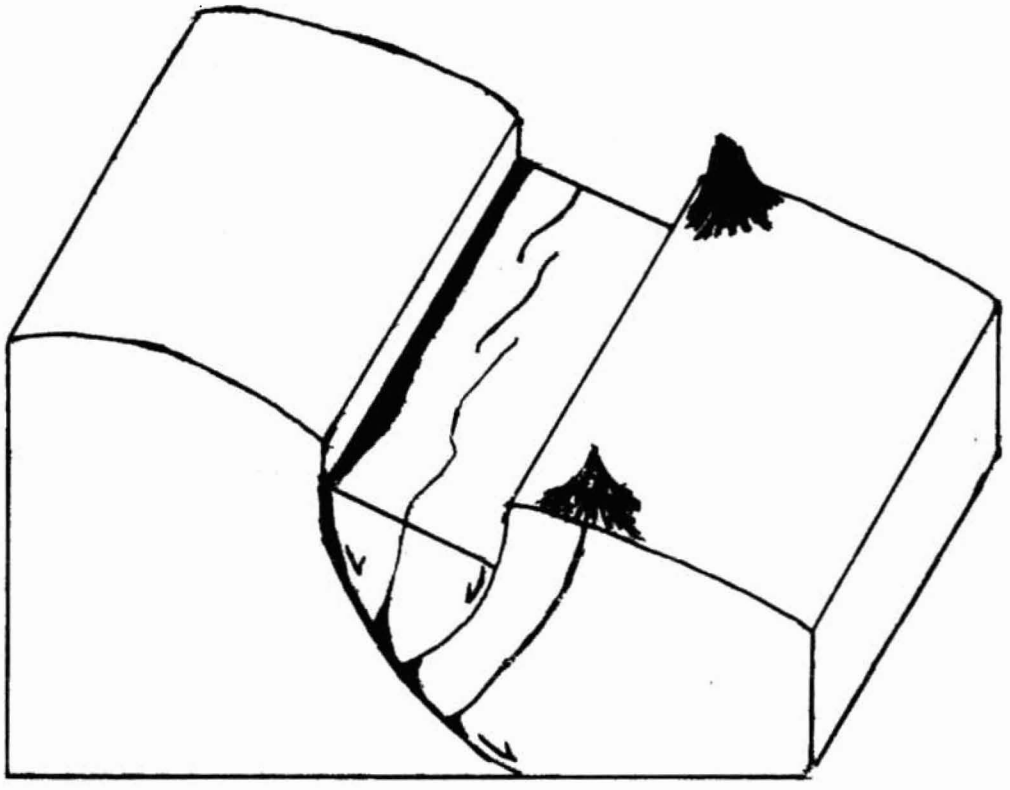

then rises through the fractures. Macdonald disagrees and cites the gravity anomaly found along the rift zone. This gravity high shows dense material, such as dikes, at depth. Macdonald interprets this as a continuation of the rift at depth. He feels the "most proable cause of the Hawaiian rift zone still appears to be inflation of the volcano by intrusion of magma within it" (Macdonald, 1965, p. 328). He claims that his theory is further supported by clay experiments in which cracking patterns extend from a center of inflation. Stearns (1966, p. 144) feels that "subsidence appears to be due to the spreading of the dome under the influence of gravity and dike injection, possibly aided by melting and absorption of rocks in the grabens by the magma".

Hydrology

The eastern section of the Island of Hawaii is underlain by basal groundwater with the exception of the East Rift Zone of Kilauea. Here groundwater is impounded at higher levels by dikes. Figure 5 is a generalized cross-section showing the groundwater levels within the East Rift Zone.

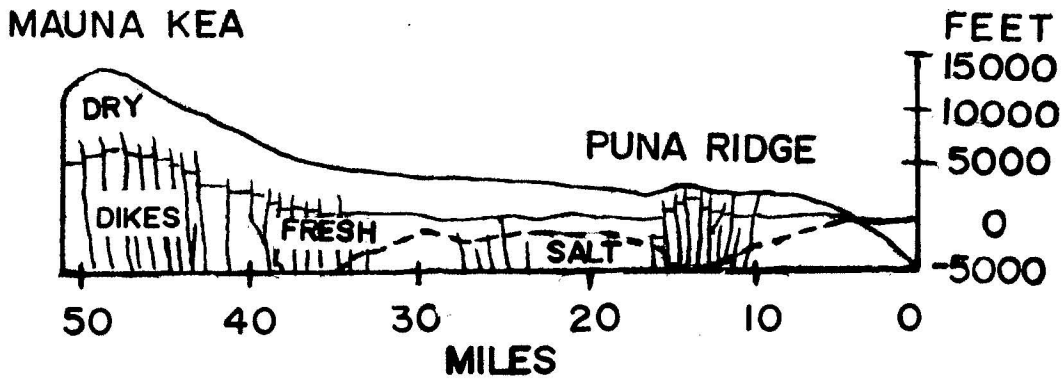

Figure 5. Generalized cross-section from Mauna Kea to the Puna Ridge showing fresh-and salt-water distribution (after Stearns and Macdonald, 1946, p. 225).

Throughout many parts of the Hawaiian Island chain, a Ghyben-Herzberg system is present. Figure 6 illustrates the Ghyben-Herzberg Principle: t = 40 h. t is the thickness of fresh water depressed below sea level; h is the height of fresh water above sea level.

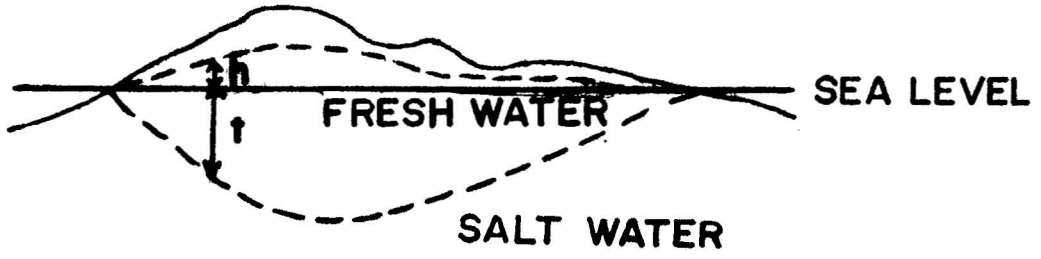

Figure 6. The Ghyben-Herzberg Principle showing the lense of fresh water depressed below sea level (after Stearns, 1966, p. 234).

A permeable lava-rock aquifer and impermeable coastal plain rock are necessary for development of such a system. Either a poorly developed or non-existent lense occurs when the rock structure is not fairly homogeneous or when the rocks have too low permeability. Although Ghyben-Herzberg systems are well developed in some areas, especially Pearl Harbor, there appears to be none in the East Rift Zone of Hawaii. In this area, the structure is unfavorable; the rocks are cut by numerous faults and dikes. These dikes also form a barrier to southward movement of groundwater from the north where the annual rainfall is great (Wentworth, 1947).

The annual rainfall near Hilo averages 200 inches/year. This level drops to 100 to 125 inches/year in the East Rift.

The normal gradient of the groundwater level in areas of heavy rainfall, such as here, is 4 feet/mile from shore (Duncan, 1942).

Numerous wells have been drilled in the survey area which reinforce this concept. Figure 7 shows the location of wells and shafts in the eastern section of the Puna Rift. Table 8 summarizes the data from these wells and shafts. With a few exceptions, most of the well water temperatures are cool or warm, but not hot. Davis, (1968, p. 30), when discussing water resources in Puna, notes some "sparse thermal anomalies to be seen on infrared images of near-shore water along the south shore suggests that much of the issuing groundwater is warmer than the surrounding sea water". Wells drilled by the Hawaii Thermal Power Company in 1961 confirm the presence of high temperatures (200°F to 215°F) in one part of the East Rift. But these temperatures are not high enough for a commercial geothermal system. Macdonald (1973) thinks the East Rift might yield a geothermal system but at depths considerably below sea level. Present wells have not penetrated this deep. A resistivity survey can penetrate much deeper and may show evidence of greater temperatures at depth.

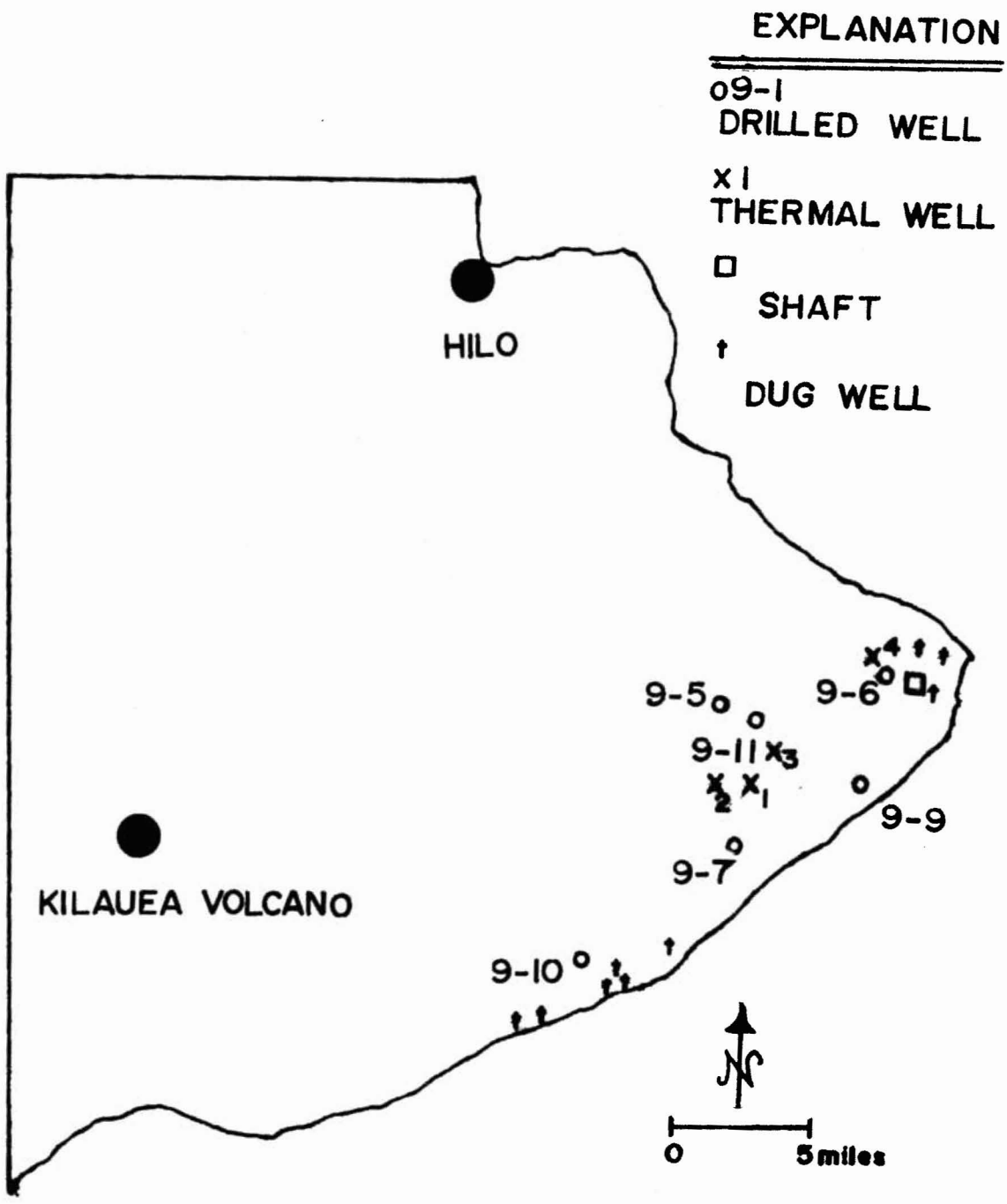

Figure 7. Map of the Puna District showing the location of wells drilled.

FIGURE 3 : TABULATION OF WELLS IN THE EASTERN PART OF THE PUNA DISTRICT, EAST RIFT ZONE

WELL NUMBER	ALTITUDE	DEPTH	WATER LEVEL ABOVE MSL	Cl CONT. (PPM)	BOTTOM T (F^{o})	COMMENTS	REFERENCE
Thermal 1	1,009	178			130	Lost tool in hole	1
Thermal 2	1,035	556			215	Lost tool in hole	1
Thermal 3	563	690			200	Steady temperature	1
Thermal 4	250	290			110	Strong circulation of sea water	1
9-5	705	754	18	6	*72	Taps water in pyroclastic material	2
9-6	287	337	3	350	92-94		2
9-7	752	802	3	90	*74	Fresh water	2
9-9	274	316	1	7,000	127-130	Very saline, unused	2
9-10	230	250	12	295	79	Unused	2
9-11	402	446	10	16	*74		2
□	38	41		2.6		Domestic use, shaft	2

\+ **The dug wells generally are about 30 feet deep. They have been used for either stock or industry. Most are brackish and some water levels vary with the tide.

1 Stearns, 1966, p. 248

2 Davis and Yamanaga, 1968, p. 30

* Dept. of Land and Natural Resources of Hawaii, 1970, p. 145-146

** Ibid., p. 155-157

FIELD EQUIPMENT

Current Source

A block diagram of the source equipment is illustrated in Figure 9. The power source used for the 1972 survey and for soundings EM3-1 through EM3-47 of the 1973 survey was a 30 KVA, water-cooled, Onan generator with an output of 220 volts. The generator output was stepped-up to 440, 660, or 880 volts with a three-phase transformer. The power source used for the remainder of the 1973 soundings was a 12.5 KVA, air-cooled, Onan generator with an output of 220 volts. Two series-connected, single-phase, transformers were used to step up the supply voltage to a maximum of 1,000 volts. The AC voltage from the transformers was rectified and an asymmetrical square wave was applied to the source electrodes. The square wave was applied to the electrodes through 12-gauge wire with a resistance of 1.6 Ω per 1,000 feet. The electrodes consisted of ten-foot lengths of galvanized steel pipe. Several pipes were buried in shallow trenches, soaked with salt water, and connected to form each grounding electrodes. The current between these

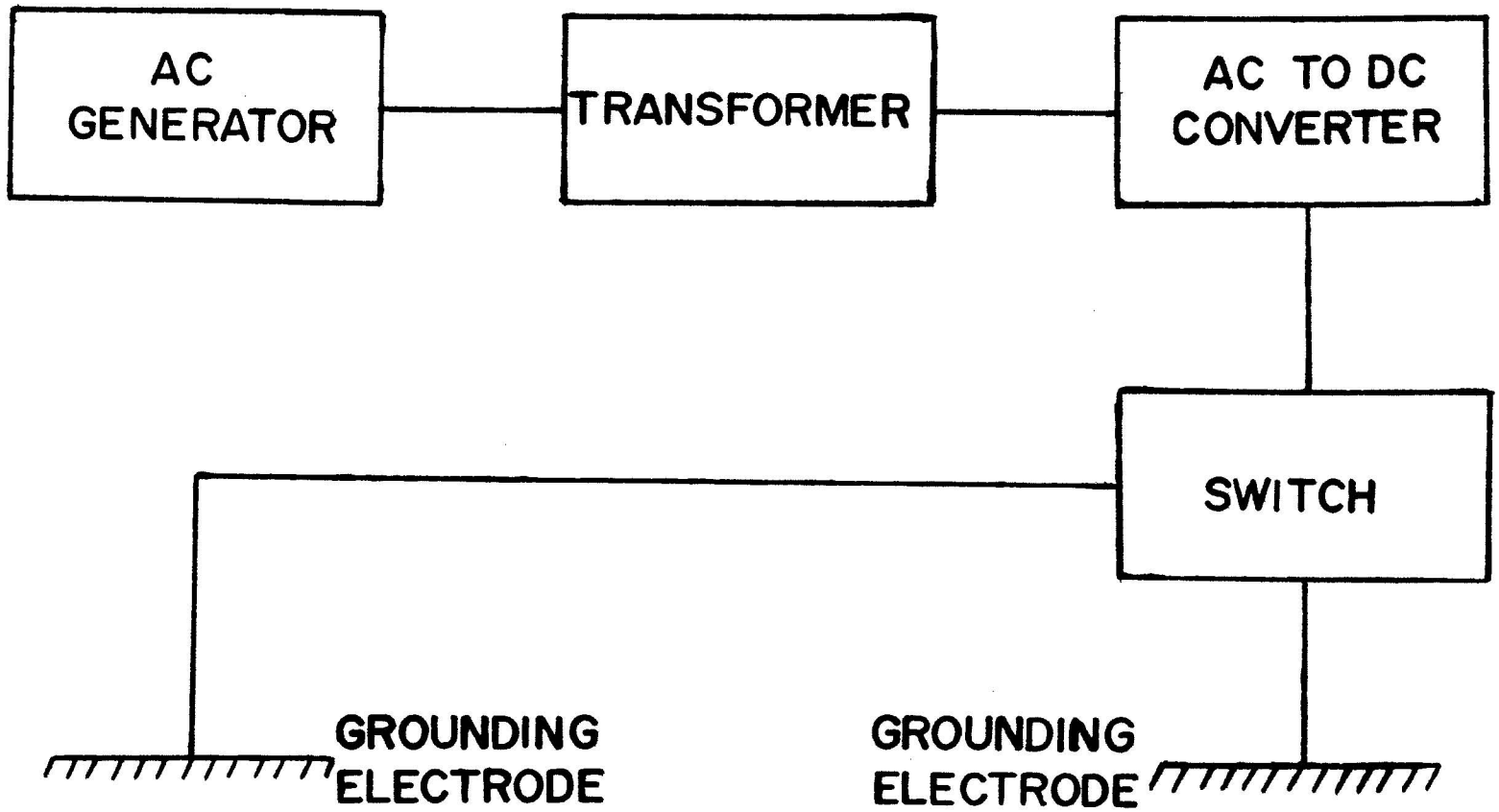

Figure 9. Block diagram showing the source configuration.

electrodes was recorded on an Esterline Angus T-171-B paper-and-ink chart recorder.

Voltage Receiver

A block diagram of the receiver equipment is illustrated in Figure 10. The vertical component of the changing magnetic field was detected with a square loop of 26 turns of wire, 250 feet on a side.

From the loop sensor, the received signal entered a signal conditioner. For the 1972 survey, the signal conditioner consisted of a 20-Hertz, low-pass, passive filter. For the 1973 survey, a White, 60-Hertz, band-reject, passive filter was used. In addition, a 5-Hertz, low-pass, passive filter was applied for soundings EM3-6 and EM3-17 through EM3-21. After the conditioner, the received voltage passed through an amplifier with a variable gain from 1 to 1,000. The amplified voltage was then recorded on a Gould Brush Mark 250 paper-and-ink, chart recorder with a High Gain DC Preamplifier Model 13-4215-62. The recorder has a maximum sensitivity of 10 microvolts/inch and a maximum recording speed of 0.2 seconds/inch. The Gould recorder has a flat frequency response from DC to 30-Hertz. (See Figure 11).

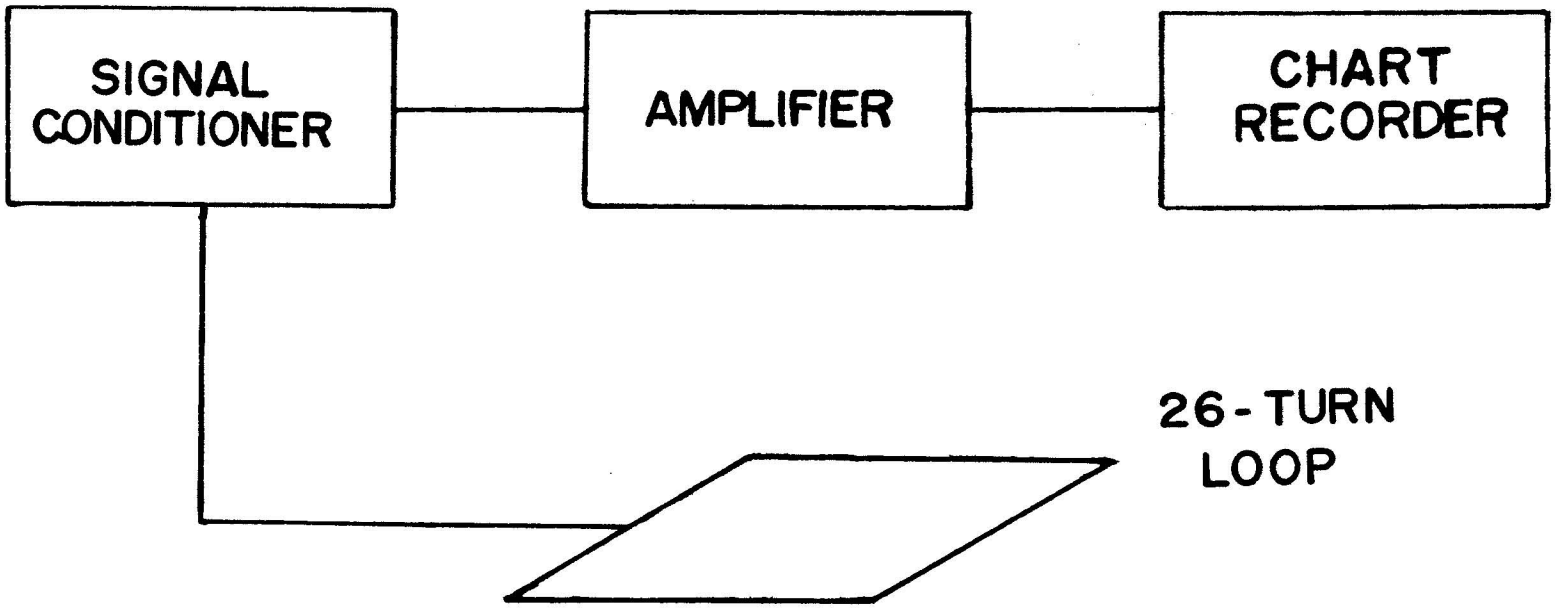

Figure 10. Block diagram showing the receiver configuration.

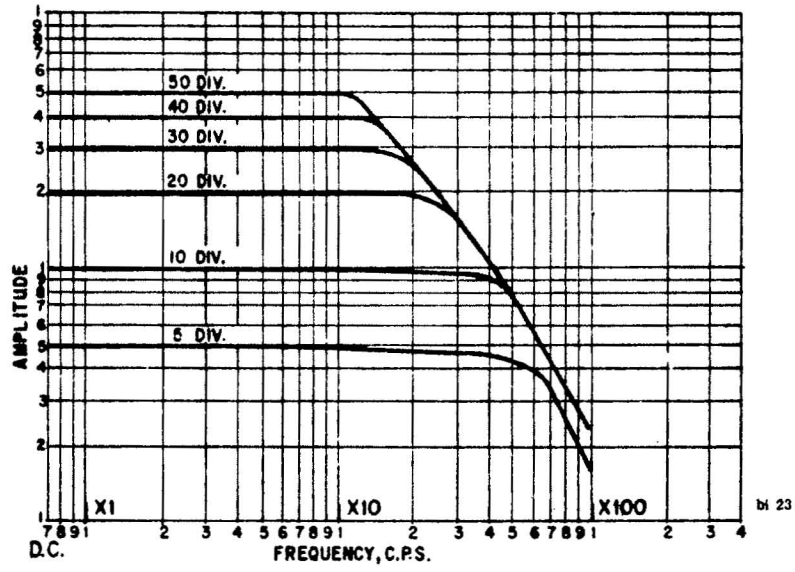

Figure 11. *Penmotor Frequency Response Curve*
(Gould Brush Mark 250 Recorder User's Manual, p. 1.4)
This illustrates that the response for most signals was linear to about 30 Hz. Therefore, the high frequency (early-time) portion of the curve is distorted.

DATA ACQUISITION AND PREPARATION

For the time-domain electromagnetic survey, a line source and loop receiver were used. There are three types of line sources: long line, short line, and a finite-length line. With a short line source, measurements are taken at a distance great enough (usually five source lengths) such that the source appears to be a dipole. When a long-wire source is used, its length is large compared to the offset distance so that it can be considered infinite. The finite length is intermediate.

The mathematical expression for a finite length source is very complicated and has not been developed. Vanyan (1967) stated that the dipole approximation worked well for distances from the source which are several times the depth to a boundry. Therefore, dipole approximations were used to interpret the time-domain electromagnetic data even though measurements were taken a distances less than five source lengths.

For the 1972 part of the project, three sources, 1.6-km, 2.0-km, and 1.4-km long were used. A 2.4-km long source provided current for the 1973 survey. A square wave with a 15-second period introduced between 5 and 15 amps of current

into the ground. Measurements of the transient magnetic field resulting from the current step were then made with a 1,000-foot loop of 26-conductor cable laid out in a square. Figure 12 illustrates a sample transient curve recorded in the field.

Recording stations were located with a density of one per square kilometer when possible. Recordings were not taken off the ends of the sources because the theoretical coupling drops off to zero. This can be seen from the equation which converts voltage to apparent resistivity: $V = F(\rho_a) \cdot \cos\theta$. As θ increases to 90° off the end of the source, $\cos\theta$, and therefore, the voltage becomes zero. Figures 13 and 14 illustrate the station and source locations for the two parts of the electromagnetic survey.

After the data were collected in the field, they were returned to the office for preparation for interpretation. First, a step response (Figure 15) had to be removed from the recorded signal so only the response of the earth remained. To achieve this, both the step response and the received transient were digitized. An 0.8 second length of each record was digitized at a 0.02 second time interval. The digitizer has a dynamic range of 60 db which, for quiet signals, provided an error in the voltage reading of less than 1%. The digitized information was then fed into a computer program for processing. For noisier signals, the data were

RUMENTS DIVISION CLEVELAND, OHIO PRINTED IN U.S.A.

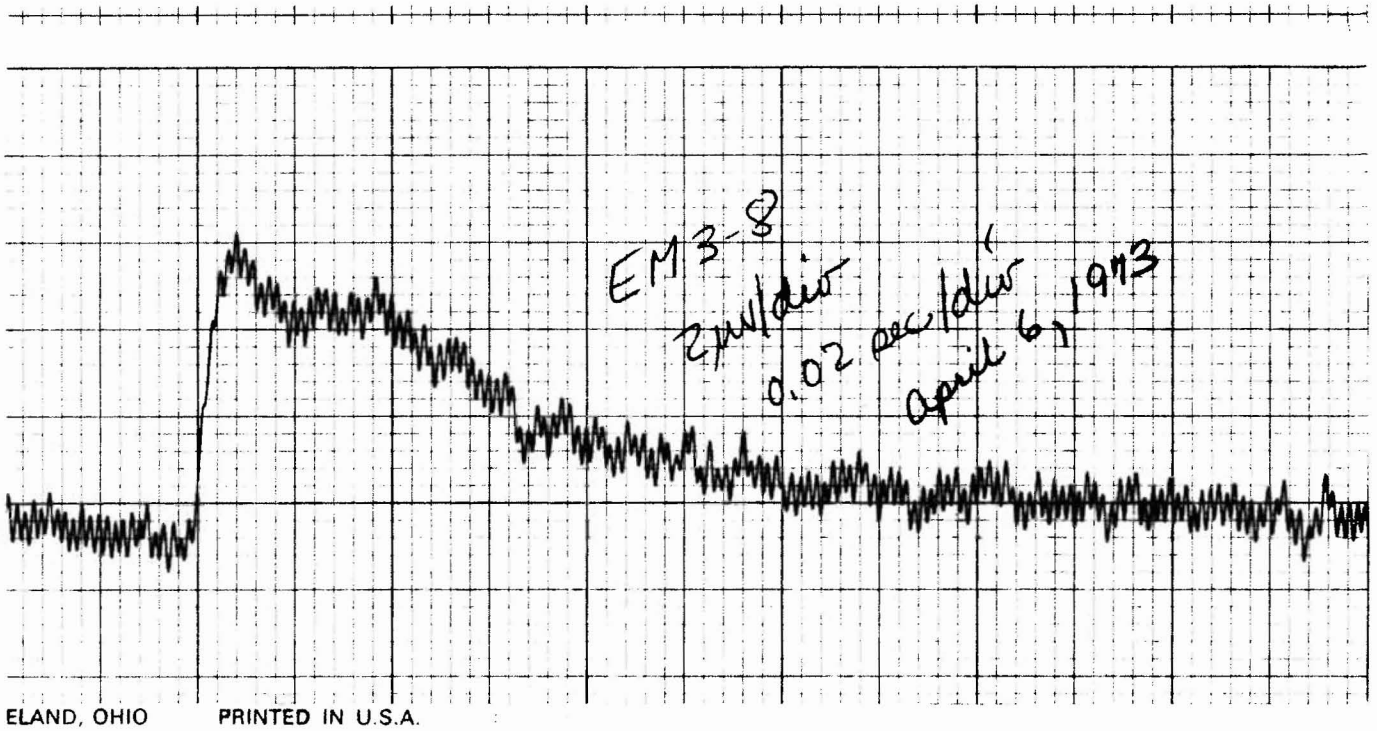

ELAND, OHIO PRINTED IN U.S.A.

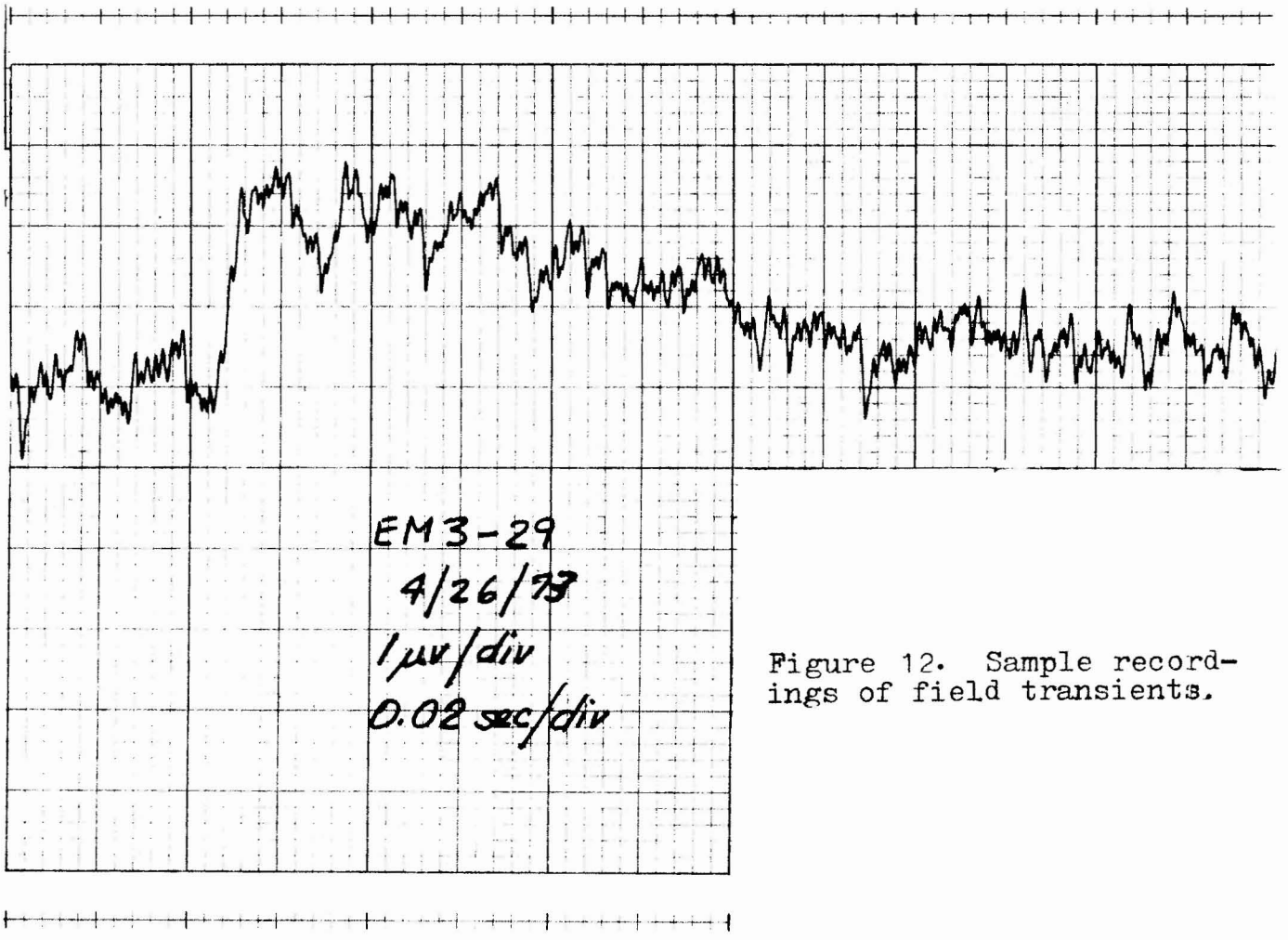

Figure 12. Sample recordings of field transients.

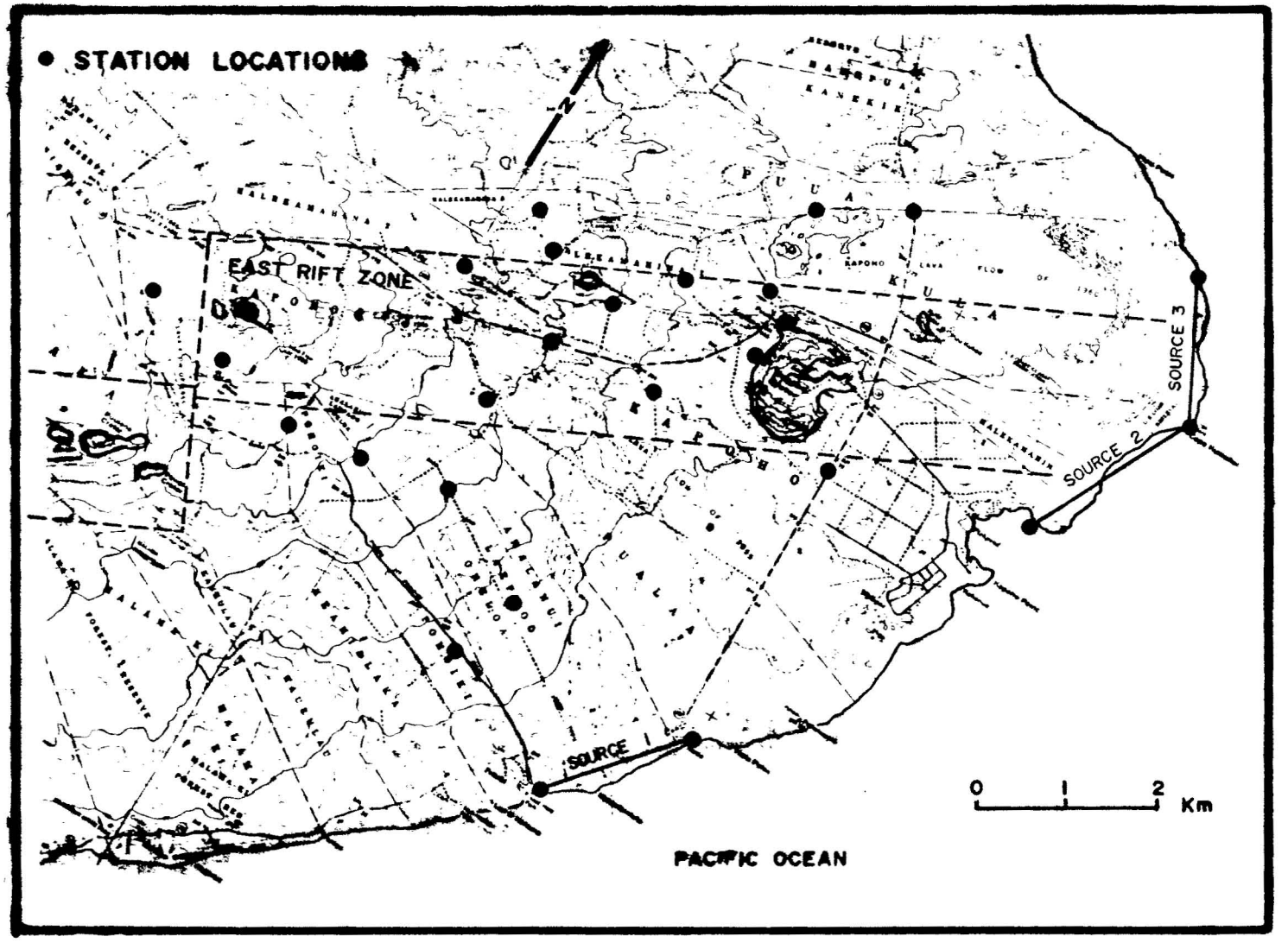

Figure 13. Station locations for the 1972 part of the time-domain electromagnetic survey.

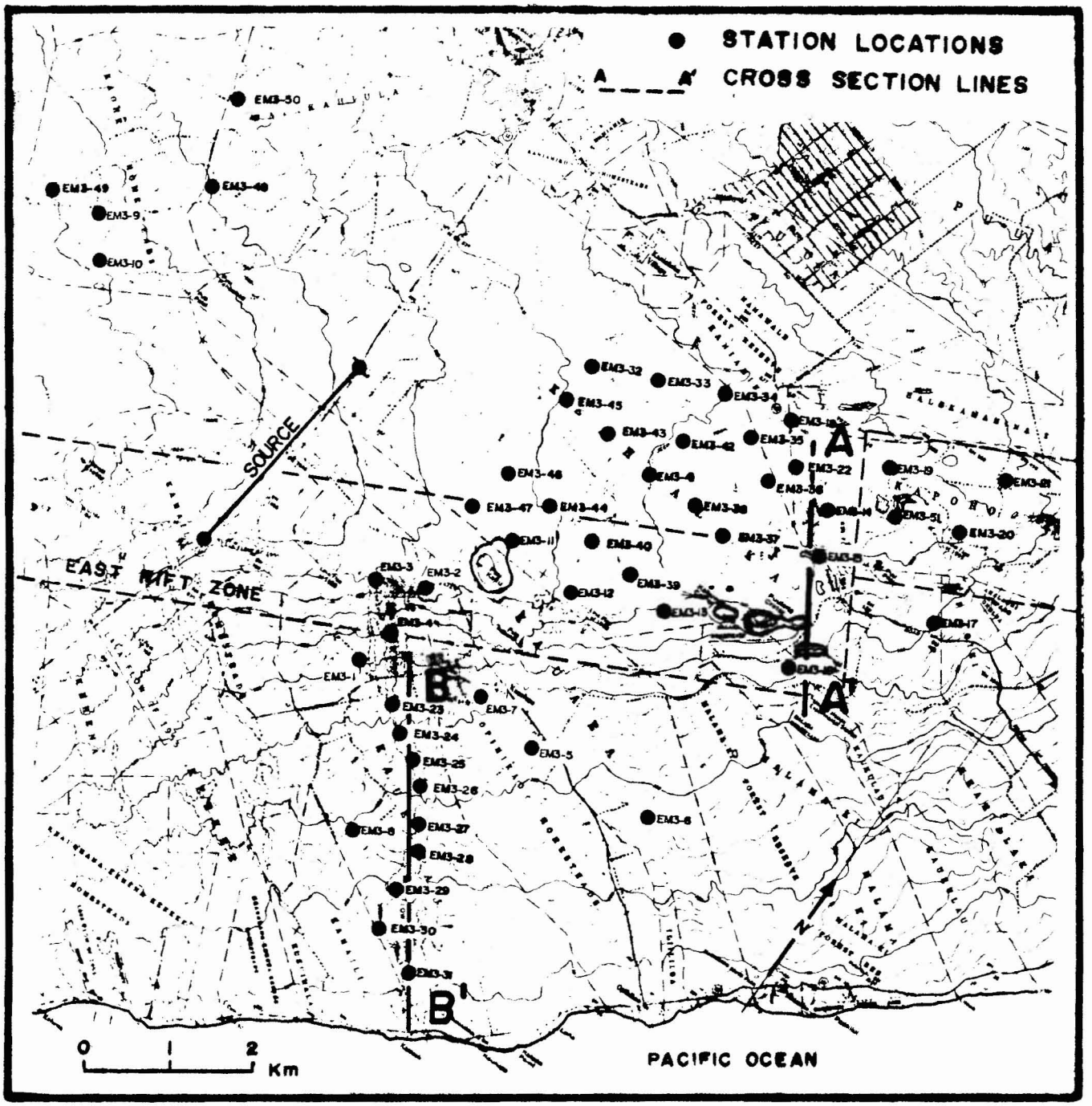

Figure 14 . Station locations for the 1973 part of the time-domain electromagnetic survey. Locations for two cross sections are indicated.

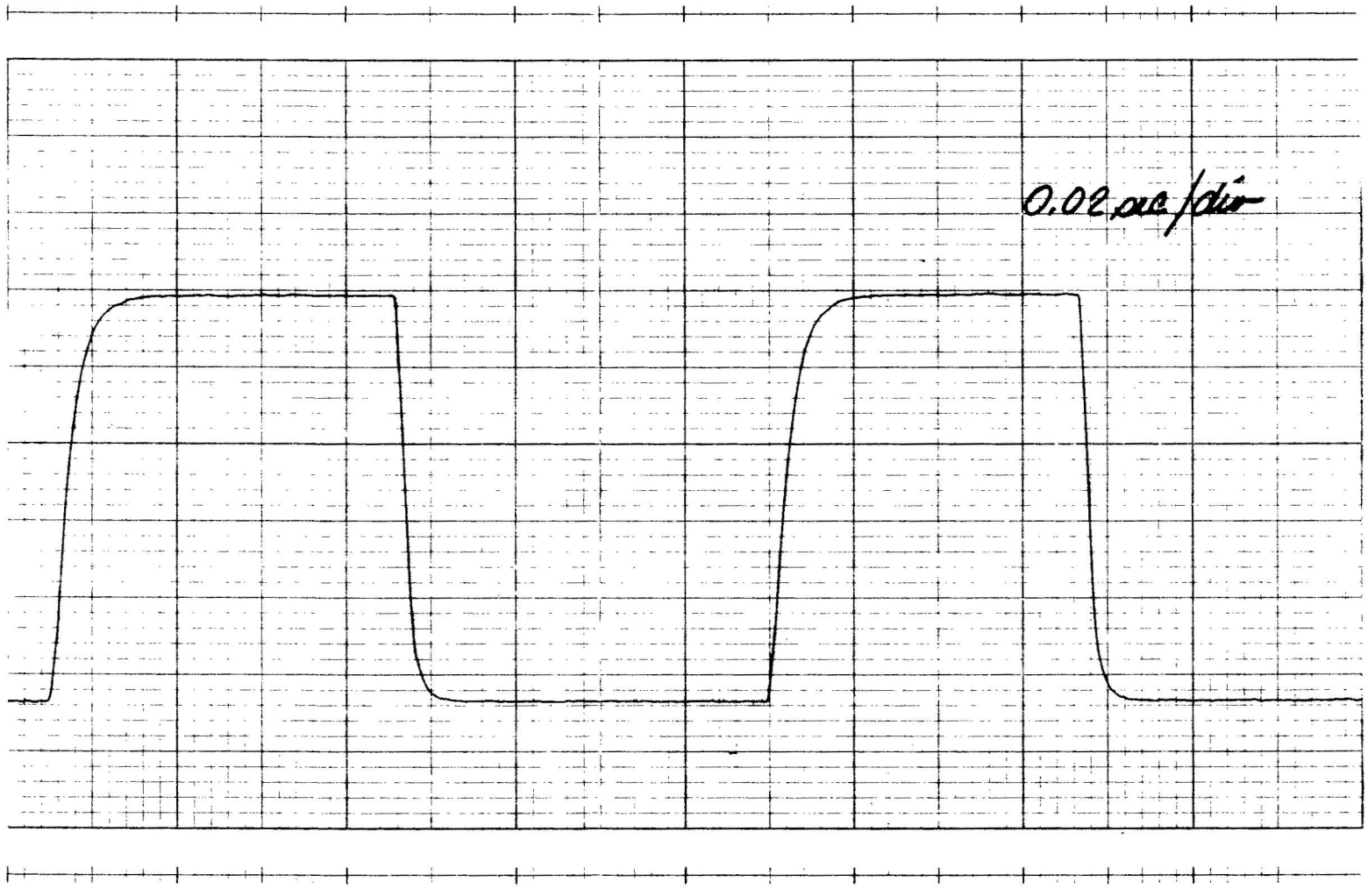

Figure 15. Sample step response of the recording equipment.

stacked 10-fold so that error in transient representation would be reduced. When the stacking procedure was required, a statistical test was applied to insure that each data point lay within a reasonable distance of the average signal. If the value were more than two standard deviations from the average, it was rejected. Statistically, for a large number (n) of stacked signals, the random the noise level is reduced by a factor $(n-1)^{\frac{1}{2}}$, which is a factor of three for n = 10. To illustrate the signal to noise ratio, Figure 16 lists the average maximum recorded voltage and the standard deviation for a few stacked signals.

A current step is introduced into the earth; the received signal is then passed through a recording system; thus the output is a function of the input step convolved with the earth response and the recorder response. To find the response of the earth to a step input, the step response of the recorder was removed through deconvolution. Figure 17 illustrates this process.

The output time function contained considerable noise at the Nyquist frequency which resulted from sampling and transforming. To reduce this noise, a non-linear filter was applied. Because the data are represented on a bi-logarithmic plot, the noise appears to have greater amplitude and to be higher in frequency in the later part. Therefore, a logarithmic smoothing technique was used. Linear times and voltages were converted to logarithmic times and voltages.

Station	(Vmax) Maximum Voltage (Volts)	(σ) Standard Deviation	$\frac{Vmax}{\sigma}$
5	046.9×10^{-5}	06.29×10^{-5}	7.47
7	$0120. \times 10^{-5}$	04.91×10^{-5}	24.4
8	0.322×10^{-3}	0.241×10^{-4}	13.3
14	0.795×10^{-3}	0.104×10^{-3}	7.65
15	0.127×10^{-2}	0.533×10^{-4}	23.8
16	06.66×10^{-4}	03.85×10^{-5}	17.3
25	084.7×10^{-5}	02.98×10^{-5}	28.4
26	0.449×10^{-3}	0.532×10^{-4}	8.48
27	0.372×10^{-3}	0.176×10^{-4}	21.1
28	0.161×10^{-3}	0.167×10^{-4}	9.65
29	0.103×10^{-3}	0.818×10^{-5}	12.6
30	0.837×10^{-4}	0.111×10^{-4}	7.54
34	0.292×10^{-3}	0.312×10^{-4}	9.36
35	0.206×10^{-3}	0.996×10^{-5}	20.7
36	0.235×10^{-3}	0.228×10^{-4}	10.6
37	0.296×10^{-3}	0.185×10^{-4}	16.0

Figure 16. The average voltage and standard deviation for some stacked signals.

Figure 17.

STEP 1:

STEP 2:

STEP 3: FOURIER TRANSFORM EACH OUTPUT

$$OUT1(\omega) = E(\omega)\cdot R(\omega)\cdot D^{-1}(\omega)$$

$$OUT2(\omega) = R(\omega)\cdot D^{-1}(\omega)$$

$$E(\omega) = \frac{OUT1}{OUT2} \quad \frac{\text{(recorded transient)}}{\text{(recorded instrument step response)}}$$

STEP 4:

$$E(\omega)\cdot j\omega \Longrightarrow e(t)*\delta^{-1}(t)$$

This is the step response of the earth alone.

TIME DOMAIN

$\delta^{-1}(t)$ - step

$e(t)$ - earth function

$r(t)$ - recorder function

FREQUENCY DOMAIN

$D^{-1}(\omega)$ - step

$E(\omega)$ - earth function

$R(\omega)$ - recorder function

Values were then interpolated to provide equally spaced logarithmic data. These values were then smoothed by seven point averaging.

The resultant deconvolved voltage was converted to apparent resistivity using the equation: $\rho a = \frac{2\pi R^4 V(t)}{3 M A \cos\theta}$ (Vanyan, 1967). The apparent resistivity and corresponding time value were then plotted on log-log paper for interpretation. Appendix B contains the plotted deconvolved data from the 1973 part of the survey.

Appendix C contains flow diagrams and complete listings for the computer programs used to process the data. SYSTEM.F4 computes the Fourier transform of the step response and STACK2.F4 carries out the deconvolution process, smooths the data, and converts voltages to apparent resistivities.

After deconvolution, the quality of some of the data was not good enough for the curve matching. Stations EM3-1, EM3-5, EM3-7, EM3-8, EM3-14 through EM3-16, EM3-22 through EM3-30, and EM 3-35 provided excellent transients. On the other hand, stations EM3-2 through EM3-4, EM3-9 through EM3-11, EM3-33, EM3-45 through EM3-48, and EM3-50 were taken so close to the source that the early part of the transient was lost in deconvolution. This resulted from the rise time of the signal being more rapid than the rise time of the recording apparatus. Another problem occurred with Stations EM3-6 and EM3-17 through EM3-21. To reduce the high noise level, a 30 μf capacitor was placed across the loop. The result

was to lengthen the rise time of the recorded signal. Figure 18 illustrates the result of excess filtering for station EM3-6. Because of the slow response of the recorder, the high frequency components were lost, the signal was distorted, and the front end of the deconvolved signal drooped. The remaining soundings were not of the quality as the first set mentioned, but they were interpretable.

Figure 18. A sample of the effect of excess filtering.

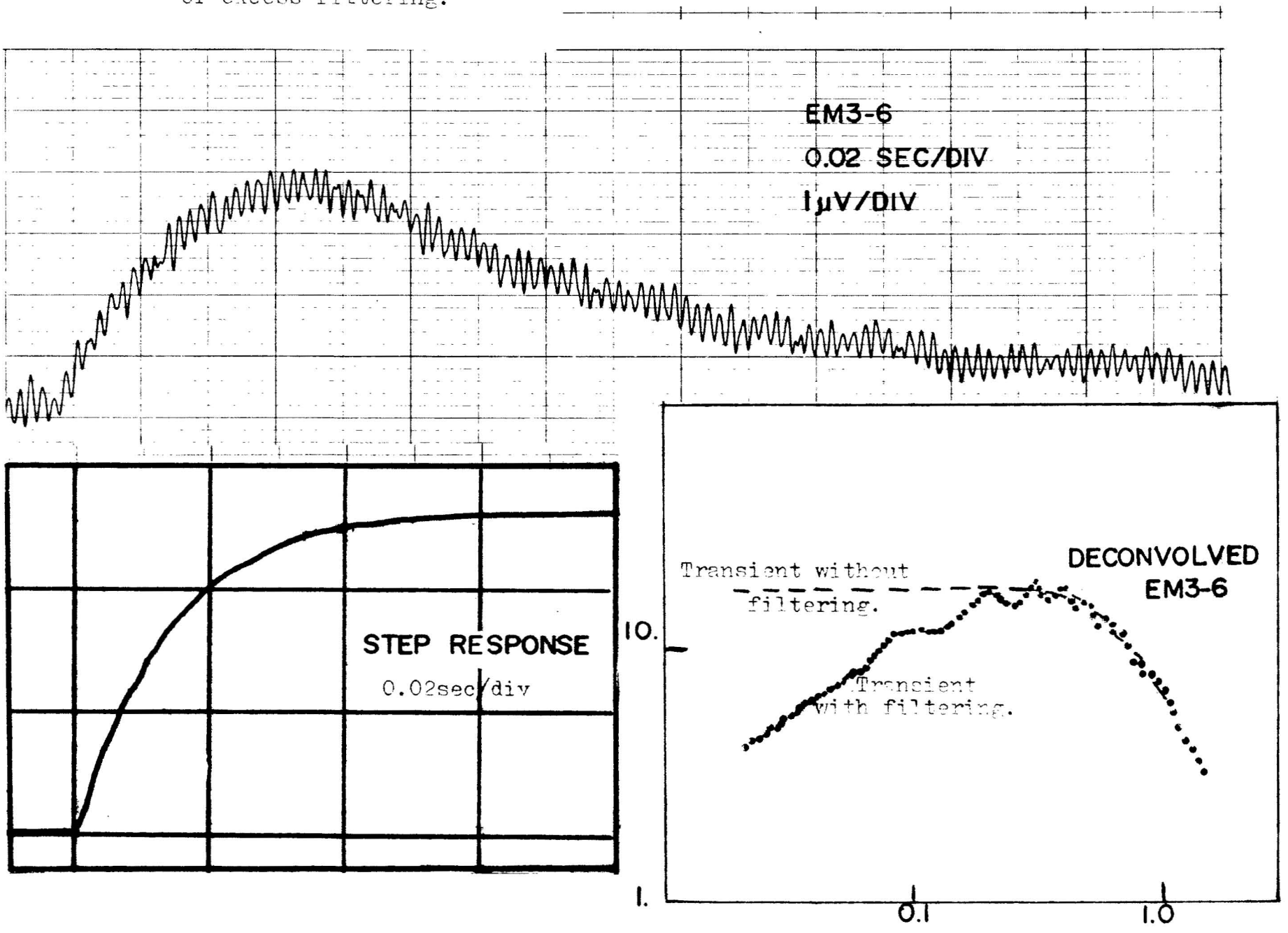

INTERPRETATION TECHNIQUES

Early-Time Maximum-Voltage Method

Through manipulation of Maxwell's equations, Vanyan (1967) has derived an equation for apparent resistivity for early-time coupling between a line source and a vertical-axis loop receiver:

$$\rho_a = \frac{2\pi R^4 V(t)}{3 M A \cos\theta}$$

ρ_a is apparent resistivity,

R is distance from source to receiver,

V is voltage received,

M is the source moment (current x length),

A is the area of the receiver loop, and

θ is an angle measured from source to receiver.

The following assumptions were used to arrive at this equation:

1. Displacement currents were considered small enough to be ignored.

2. μ was a constant ($4\pi \times 10^{-7}$) for all media.
3. The air layer above the surface of the earth was neglected.
4. The system displayed cylindrical symmetry.
5. $\lim R \rightarrow \infty$ while $\lim t \rightarrow 0$ or kt/R^2 is small.

This equation is valid for early time:

$$\tau = 2\, t/\mu\sigma R^2 < 1/4\pi \quad \text{(Vanyan, p. 49).}$$

Here: τ is normalized time

t is recorded time,

μ is $4\pi \times 10^{-7}$ Henrys/m, and

σ is conductivity (inverse of resistivity).

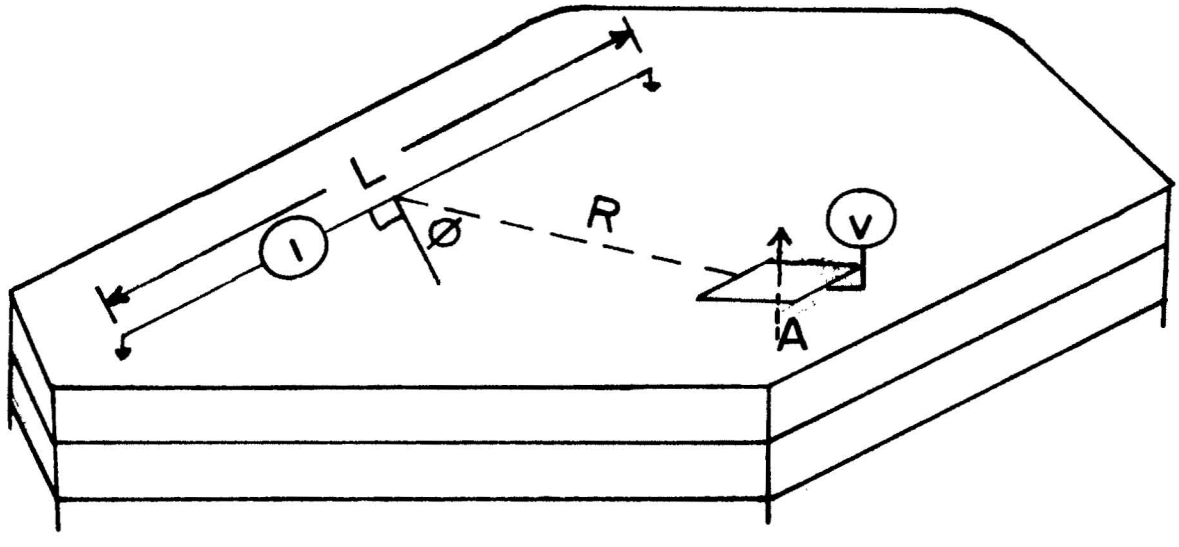

Figure 19. The measuring configuration for a time-domain electromagnetic survey.

Figure 19 illustrates the measuring configuration for line-loop time-domain electromagnetic surveys. Figures 20a and 20b are the mapped results of applying the early-time equation to the maximum voltage of the received transient signal. Because the 1972 sources are on the ocean and the 1973 source is on land, the level of resistivities is different but trends are continuous. When a source is located on a large conductor, such as the ocean, much is the current spreads seaward instead of landward thus causing the resistivities to appear lower.

If there is a conductor below the first layer, the maximum voltage resistivity is equal to the first layer resistivity. With a resistive second layer, there is a slight increase in resistivity with time before the transient drops off. Therefore, when a resistor is present, the maximum voltage resistivity is slightly greater than, but close to, the first layer resistivity. The distortion depends upon the resistivity contrast from first to second layer and layer thickness. Because a conductive second layer was present in the East Rift Zone, the maximum voltage resistivity map is a representation of the first-layer resistivities. But the first-layer resistivity observed with a time-domain electromagnetic survey may not be the surface layer resistivity. Because the transient is sampled at a finite time after transmission, very shallow information is lost. Figure 21 illustrates

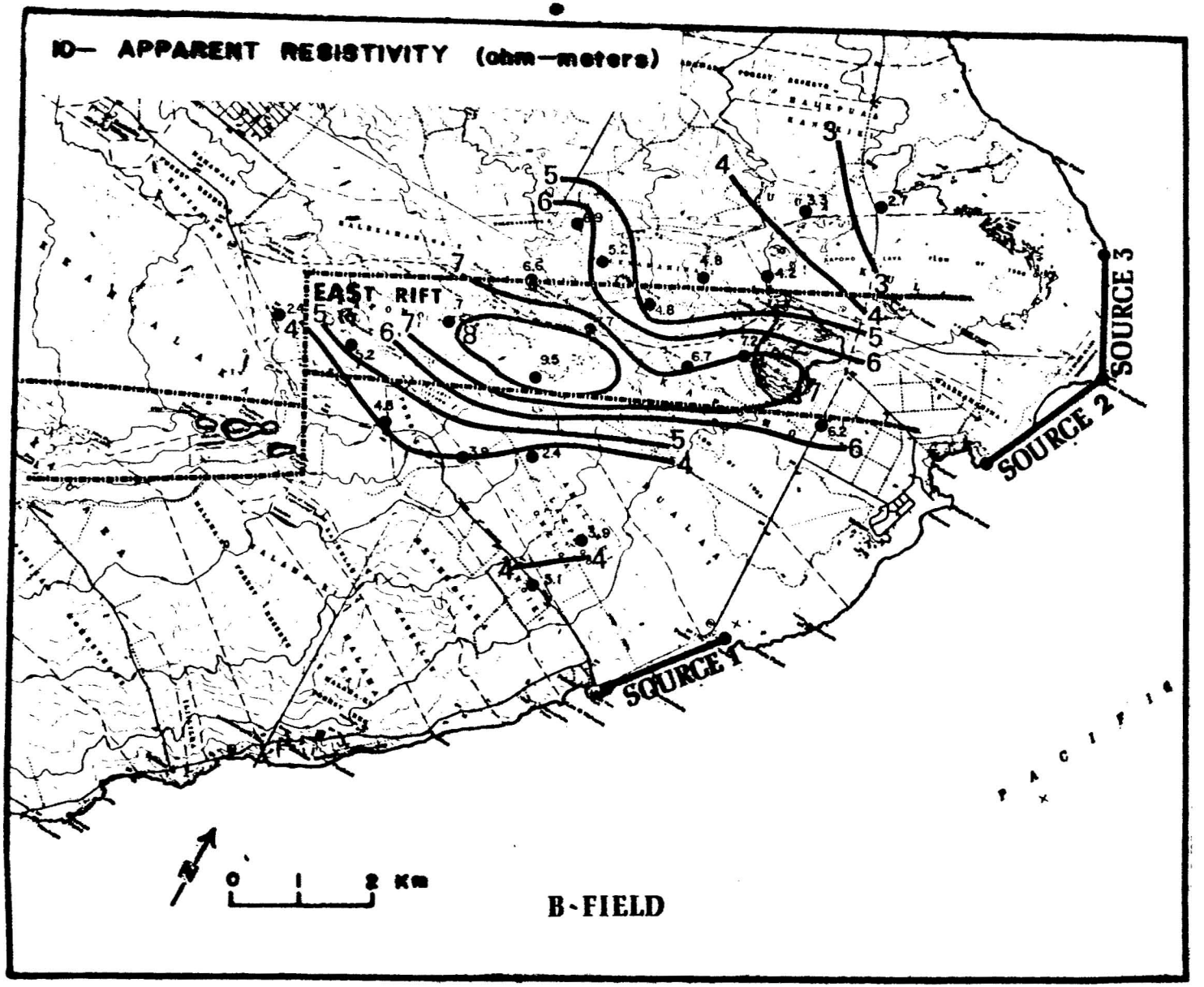

Figure 20a. Maximum-voltage resistivity map from the 1972 survey.

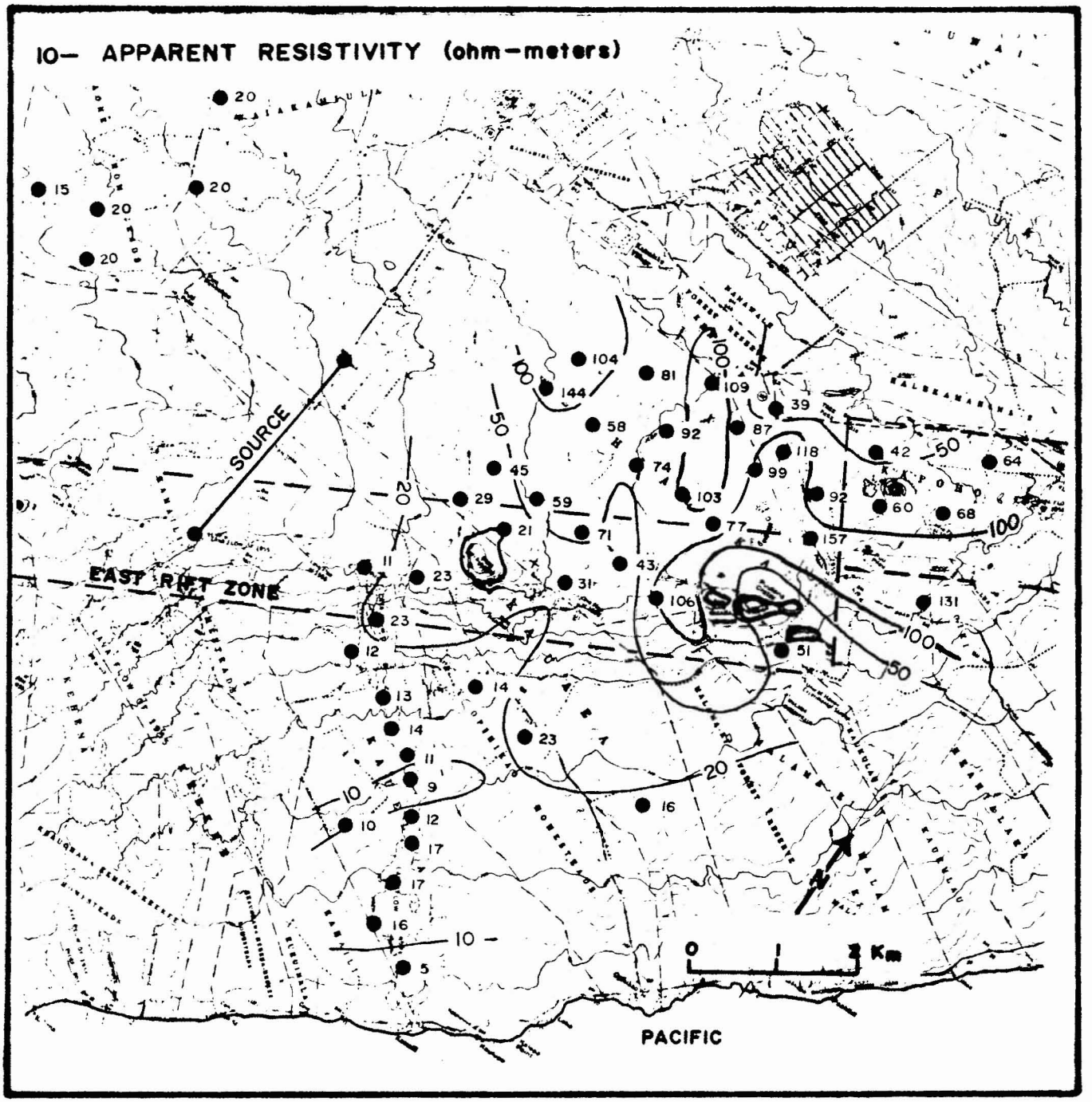

Figure 20b. Maximum-voltage resistivity map from the 1973 survey.

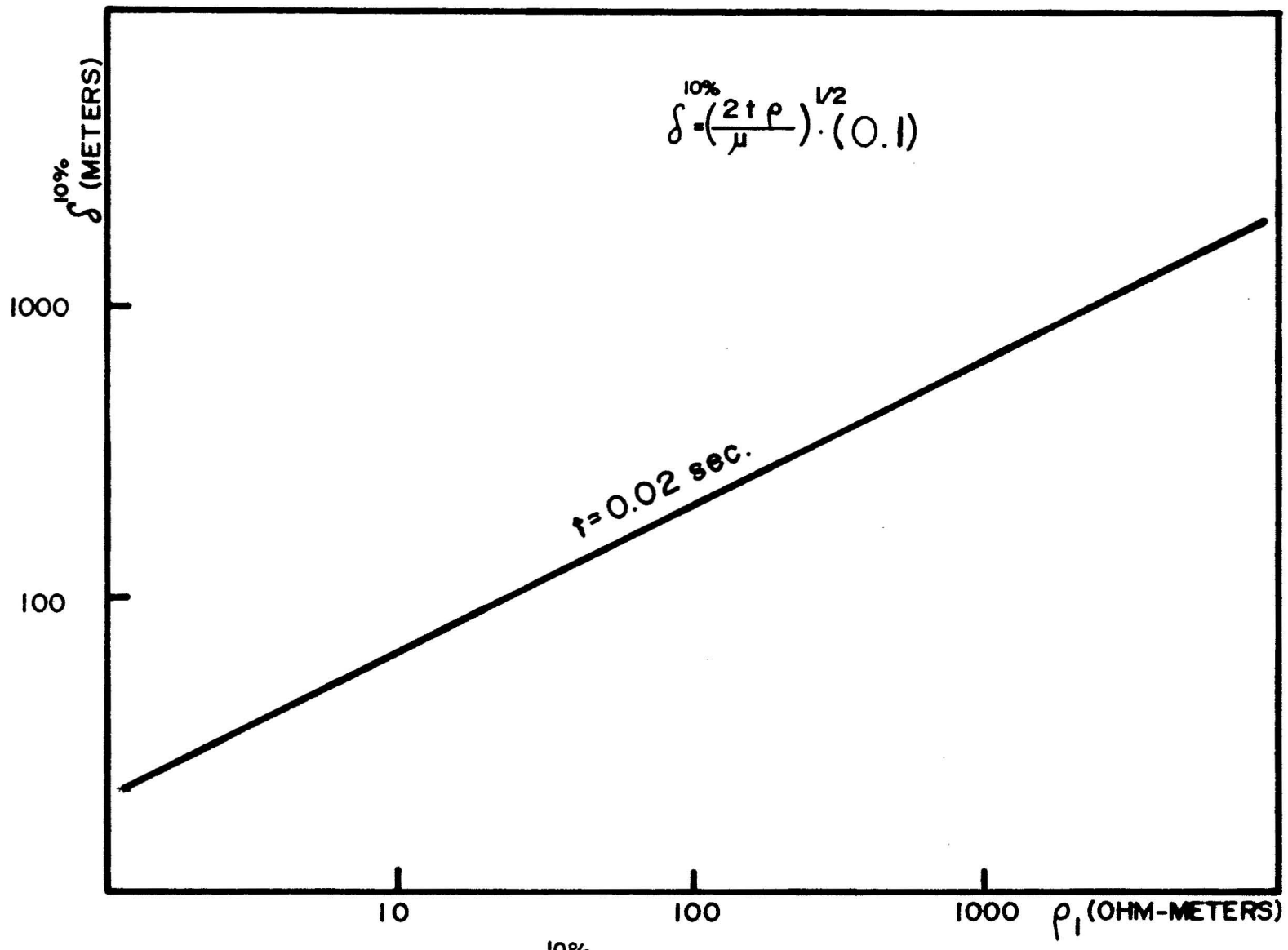

Figure 21. The thickness, $\delta^{10\%}$, of a layer that would not affect the transient after the time 0.02 seconds by more than 10% as a function of resistivity.

the thickness of a layer that would not affect the transient by more than 10% after the smallest sampling time as a function of resistivity. This shows a characteristic of time-domain soundings; the surface layer is not seen. Discussion of the results is presented in the interpretation section.

Asymptotic Curve Matching Method

It has been shown that the early-time asymptote for electromagnetic coupling may be computed from the magnetotelluric Q^2 function (King, 1971). In the magnetotelluric method, natural electric and magnetic fields in the earth are measured. Apparent resistivity is defined as $1/\mu\omega(E_x/H_y)^2$ (Cagniard, 1953). The ratio of first layer resistivity to apparent resistivity is the function Q^2. $\underline{E}_x$ is the electric field, $\underline{H}_y$ is the magnetic field, and $\underline{\omega}$ is angular frequency.

To calculate the asymptotes, first the Q^2 function was computed in the frequency-domain. This was then transformed into the time-domain using a polygonal-approximation transform method. Appendix A contains the resultant time-domain Q^2 curves for a step input. The Q^2 curves were calculated for three-layer cases assigning the basement (third layer) resistivity a value of zero (a perfect conductor). For each set of curves, H2/H1 was varied while $\rho 2/\rho 1$ was held constant. The following Figure displays the layered earth model used for these curves.

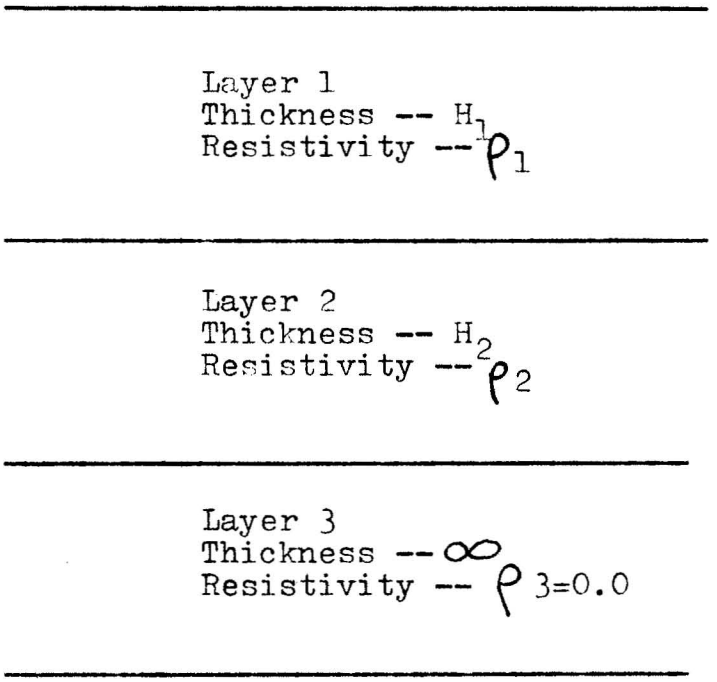

Figure 22. The layered-earth model.

To analyze the field data, the deconvolved curves (apparent resistivity vs. time) must be compared with the theoretical curves (ρ_a/ρ_1 vs τ) using a curve matching technique. Both curves are plotted on log-log paper. Keeping the axes parallel, the deconvolved curve is moved along the theoretical curves until a favorable match is found. However, because ρ_1 (abcissa) must equal ρ_1 (ordinate), there is only one degree of freedom in shifting the curves, a line with a slope of -45°. This insures that ρ_1 from $\tau (= t\ \rho_1/\mu R^2)$ must be the same as the value of resistivity obtained from the ρ_a/ρ_1 axis. The limiting match line is indicated on the samples which follow. The result of curve matching is to find values for the ratios ρ_2/ρ_1 and H_2/H_1.

These asymptotic curves are appropriate only for environments where the basement is a conductor, or where a conductive layer is so thick that the sounding does not penetrate completely through it. Such was the case in the East Rift Zone of the Island of Hawaii.

The next few pages show samples of processed field data matched with asymptotic curves. After a first estimate is obtained from the asymptotic curves, a more accurate interpretation may be made using theoretical coupling curves as presented in the next section.

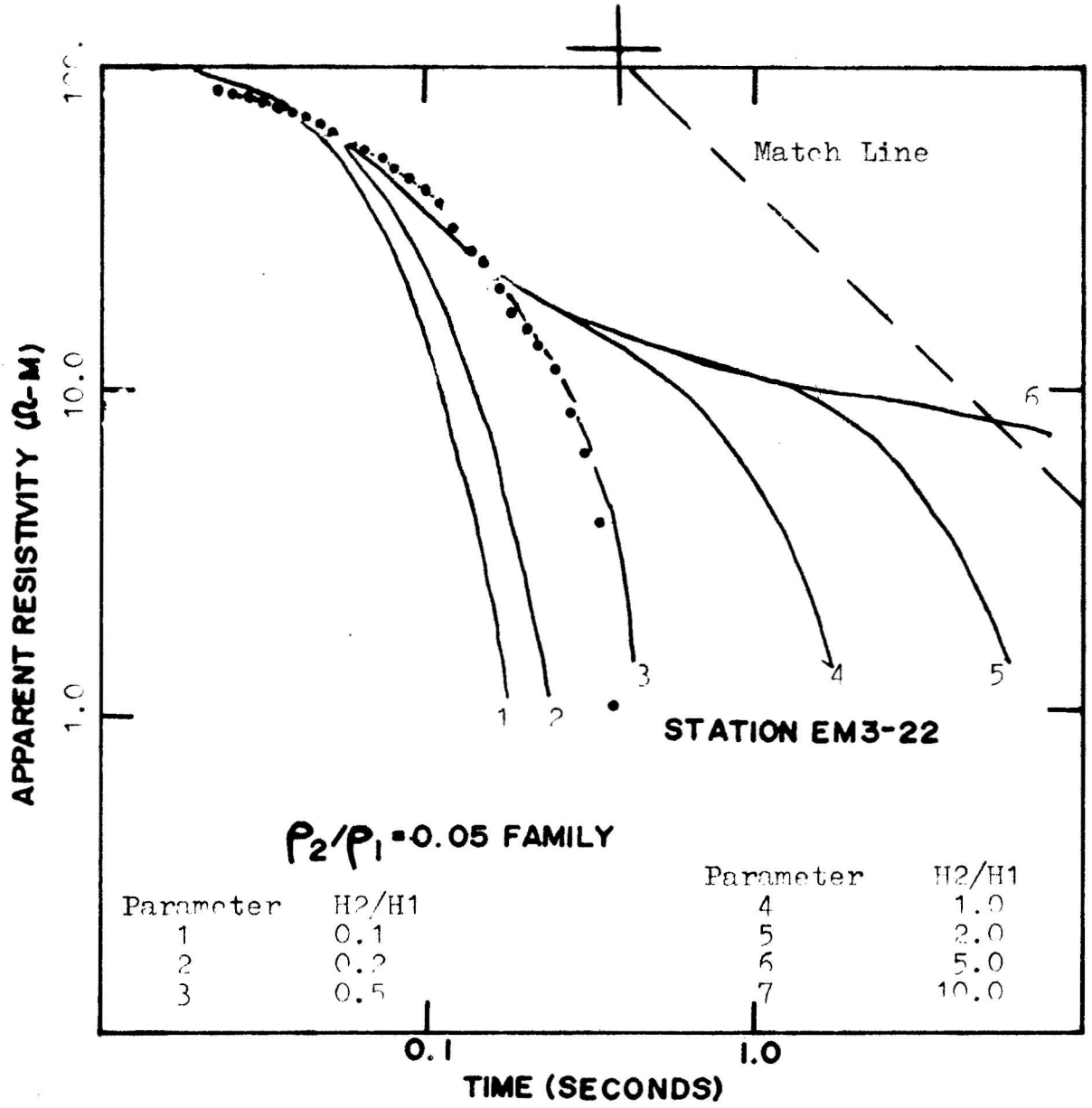

Figure 23a. Sample asymptotic curve match for Station EM3-22. The point set is the field curve; the solid lines are the asymptotes. The theoretical intercept is the point (1.0, 1.0).

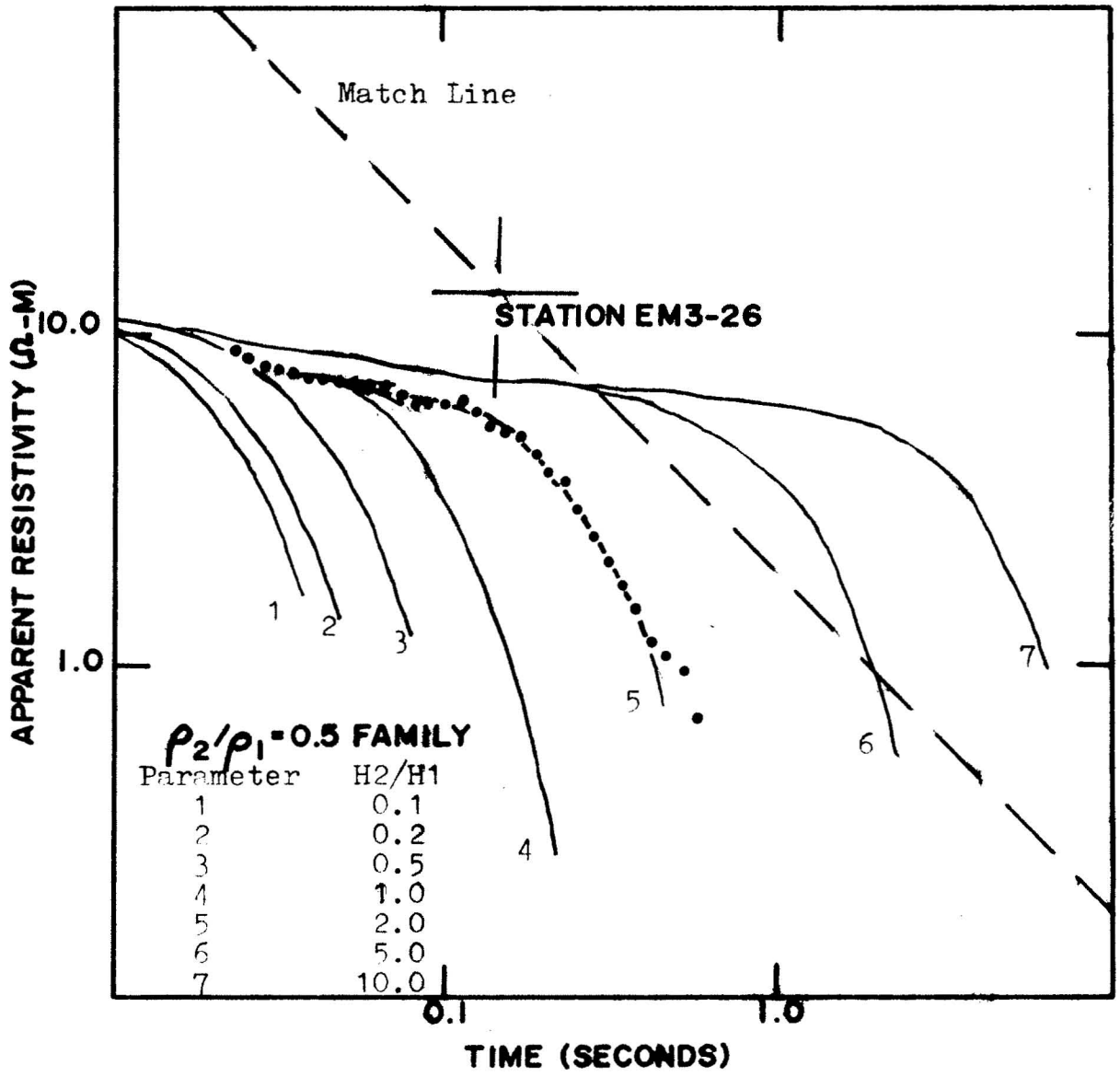

Figure 23b. Sample asymptotic curve match for Station EM3-26. The point set is the field curve; the solid lines are the asymptotes. The theoretical intercept is the point (1.0,1.0).

Theoretical Layered-Earth-Model Curve Matching Method

Daniels (1974) developed a pair of computer programs for electromagnetic interpretation. The first program utilized linear filter theory to numerically evaluate an electromagnetic field for a dipole source over a layered earth. Because of its speed and accuracy, a convolution technique was used to calculate theoretical frequency-domain curves. The second program uses a least-squares curve-fitting procedure (Marquardt's method) to interpret frequency-domain electromagnetic sounding data. First, a theoretical model is chosen. The resistivity and thickness parameters estimated for a field curve are chosen and a theoretical curve is calculated. Next, the theoretical curve and field curve are compared and an error is calculated. Adjustments are made to the estimated parameters, and another comparison is made. This process continues until the error is small. The output is a sequence of layer resistivities and thicknesses and an error value. This error (ϕ) is calculated as (Yobserved-Ymodel).^{2} This definition of error is not very useful in analyzing the closeness of two curves on a bi-logarthmic plot. Therefore, when discussing error, an RMS value will

be calculated:

$$\left(\frac{\sum (\log Y \text{ observed} - \log Y \text{ calculated})^2}{N} \right)^{1/2}$$

Because the Hawaii field data were recorded in the time-domain, Daniels' model program for curve matching was not directly applicable. The first approach to this problem was to convert the deconvolved field data into the frequency-domain. A polygonal-approximation transform method (Papoulis, 1962, p. 56-59) produced frequency-domain data from the original time-domain curves. Because the time-domain curves resulted from a step input, the step must be deconvolved, so that the impulse response, alone, is transformed into the frequency-domain. A curve-matching technique could now proceed in the frequency-domain.

Next, the same polygonal-approximation method was applied to the computer-generated frequency-domain curves. These curves were calculated on the basis of first approximations made with asymptotic curves. These model curves were converted to the time-domain and the step-response was calculated. The time-domain field data was then matched to the resultant time-domain mathematically-modeled curves.

Figures 24a and b illustrate a few of the field transients converted to the frequency-domain and the theoretical coupling curves used for matching. The next two illustrations

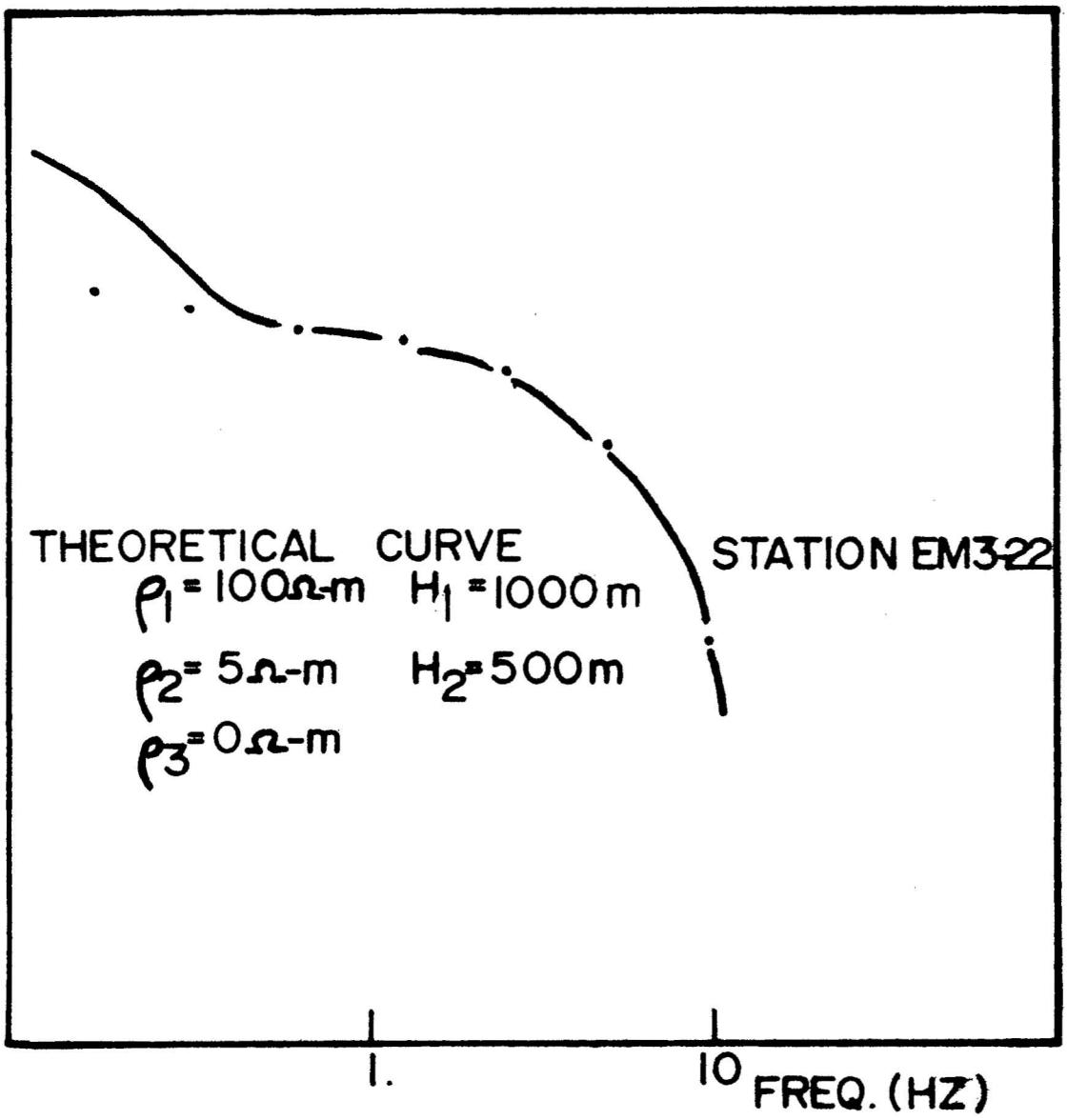

Figure 24a. Sample frequency-domain curve match for Station EM3-22. The point set is the transformed field curve, the solid line is the theoretically calculated curve.

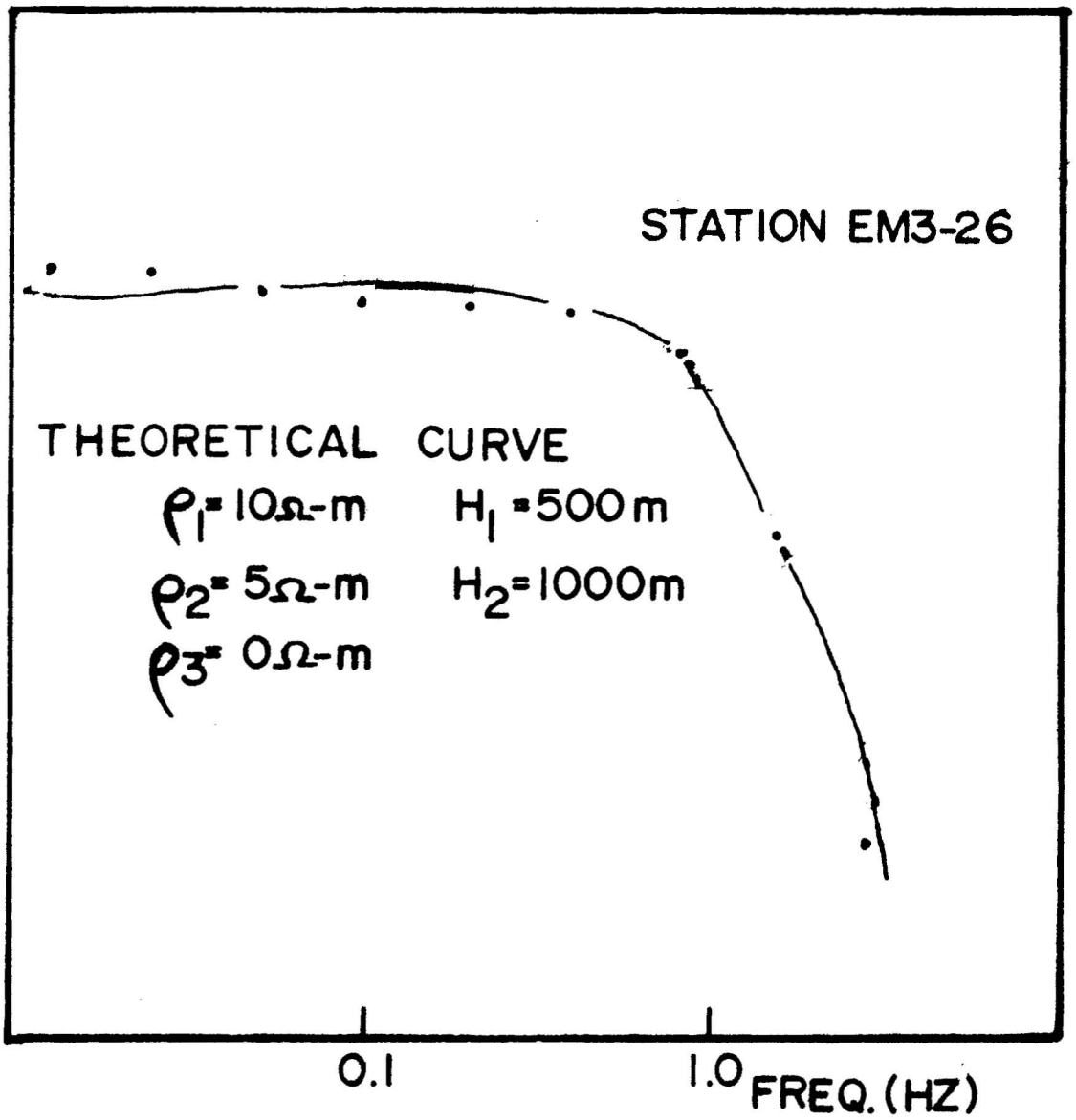

Figure 24b. Sample frequency-domain curve match for Station EM3-26. The point set is the transformed field curve, the solid line is the theorectically calculated curve.

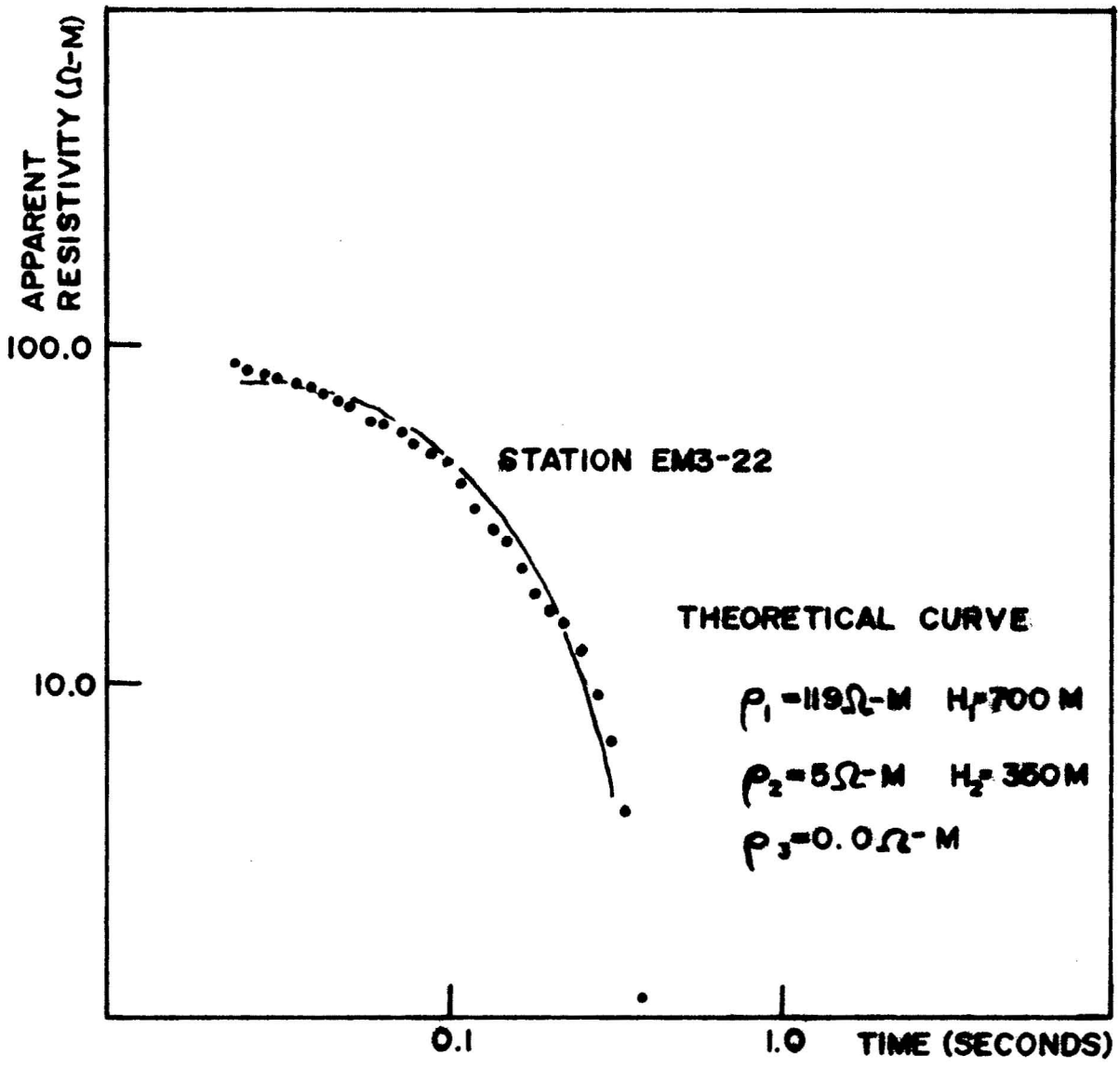

Figure 25a. Sample time-domain curve match for Station EM3-22. The point set is the transformed field curve, the solid line is the theoretically calculated curve.

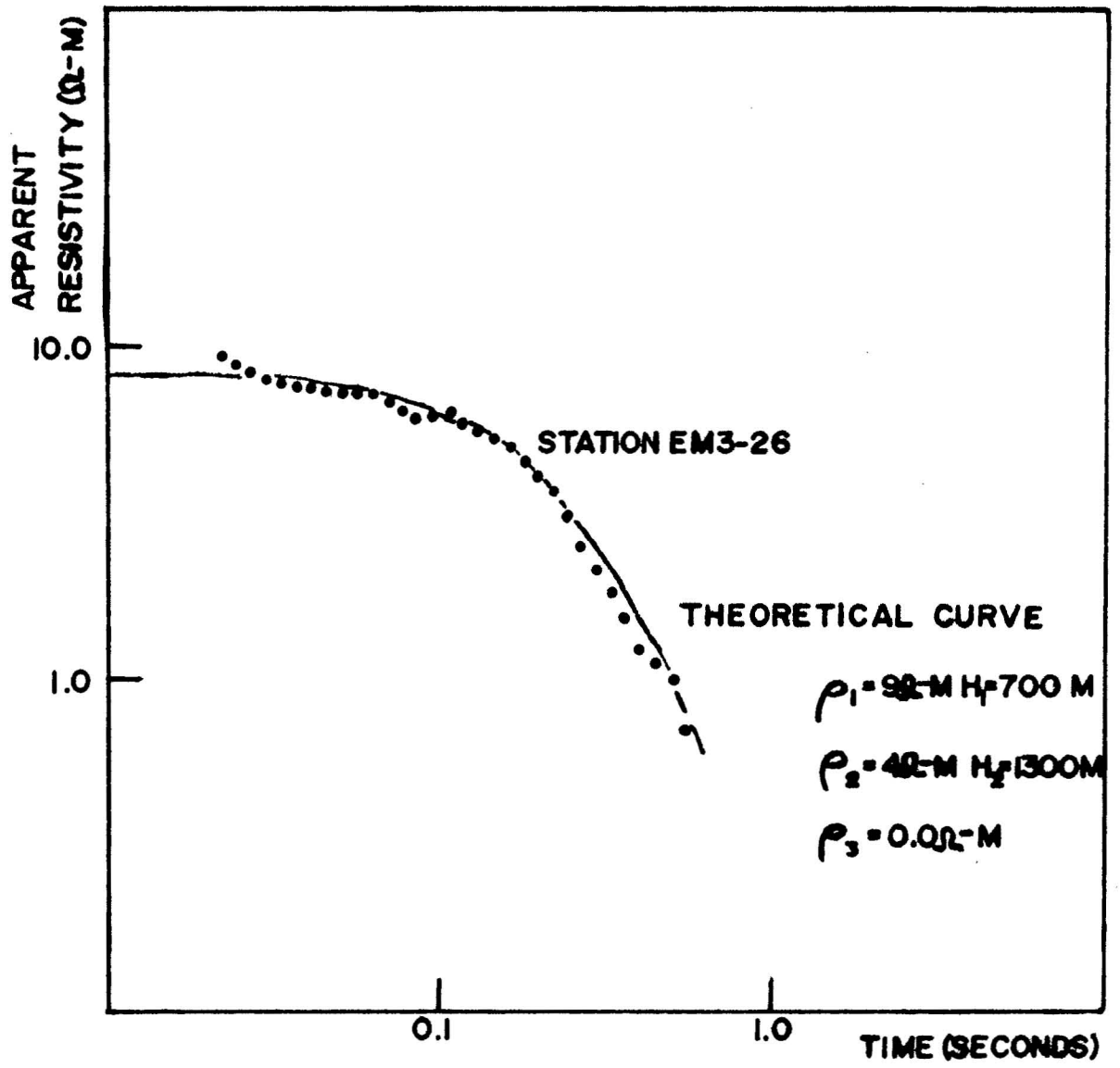

Figure 25b. Sample time-domain curve match for Station EM3-26. The point set is the transformed field curve, the solid line is the theoretically calculated curve.

(Figures 25a & 25b) show the same curves compared in the time-domain.

Truncation and sampling caused the major problems in the transformation process. Because of these digital procedures, there was ripple in the transformed curves (see Figure 26).

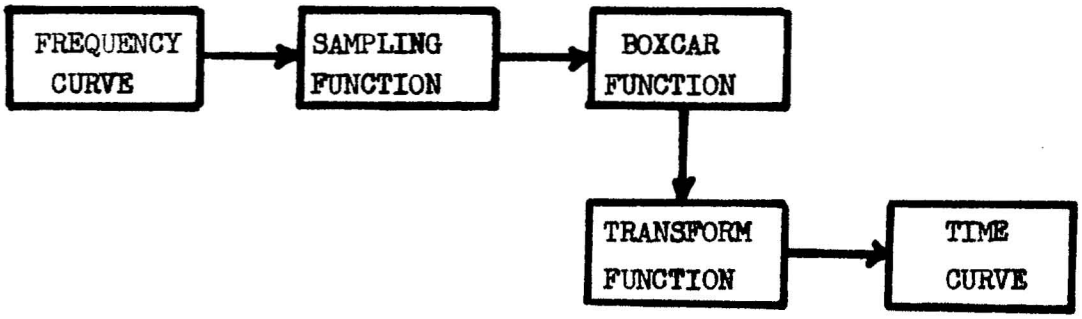

$$F(\omega) * S(\omega) * B(\omega) \Longrightarrow f(t) \cdot s(t) \cdot b(t)$$

Figure 26. The digital transform process.

The boxcar function from truncation has no effect if the function which was transformed was zero for all values not sampled. However, if the function is not bounded by zeros, such as the case of the electromagnetic curves, a ripple is superimposed on the transformed function. The ripple may be reduced by increasing the length of the function to be sampled. By sampling over a 6 decade range, the oscillations due to trunction were reduced to a tolreable level. A more noticeable ripple resulted from sampling. The problem here is similar to the problem discussed in the data processing section under computer deconvolution. The difference is the previous sampling procedure used equally spaced data. For the polygonal-approximation transform method, the sampling procedure used non-equally spaced data. But the data were equally spaced on a logarithmic scale so an analogy may be made. The Nyquist frequency is one half of the logarithmic sampling frequency. The resultant ripple in the transformed curve is constant in frequency when plotted on a log-log graph but, as before, the ripple amplitude appears greater as the transformed curve decreases in amplitude. Due to the symmetry principle, the above discussion is valid for transformation in both the time and frequency-domains.

Finally, some of the best curves were interpreted using Daniels' Marquardt least-squares-fit program to provide better interpretations.

A listing and flow diagram for Daniels' program which have been modified to calculate only the real part of line-loop coupling are included in Appendix C.

The following graph (Figure 27) illustrates the reduction in error that may be expected when using the least-squares-fit computer program. The diagonal lines divide areas of similar error improvement. As would be expected, the better the first estimate, the better the final output. This generalization is not true, however, if the first estimate is too close. When this happens, the program is unable to make an improvement. Figure 28 shows the reduction of error with each iteration for some sample runs of the least-squares-fit program.

To test the reliability of the fitting program, a theoretical curve was used as the observed curve. The parameters were:

$\rho_1 = 10\,\Omega\text{-m}$ $\quad h_1 = 500$ m

$\rho_2 = 5\,\Omega\text{-m}$ $\quad h_2 = 1000$ m

$\rho_3 = 0\,\Omega\text{-m}$ $\quad R = 5000$ m

The program was run seven times with the estimated parameters:

$\rho_1 = 10\,\Omega\text{-m}$ $\quad h_1 = 500$ m

$\rho_2 = .1, .2, 1, 3, 4, 7,$ and $20\,\Omega\text{-m}$ $\quad h_2 = 1000$ m

$\rho_3 = 0\,\Omega\text{-m}$ $\quad R = 5000$ m

Figure 29. Initial versus final error for curves processed in the least-squares-fitting program.

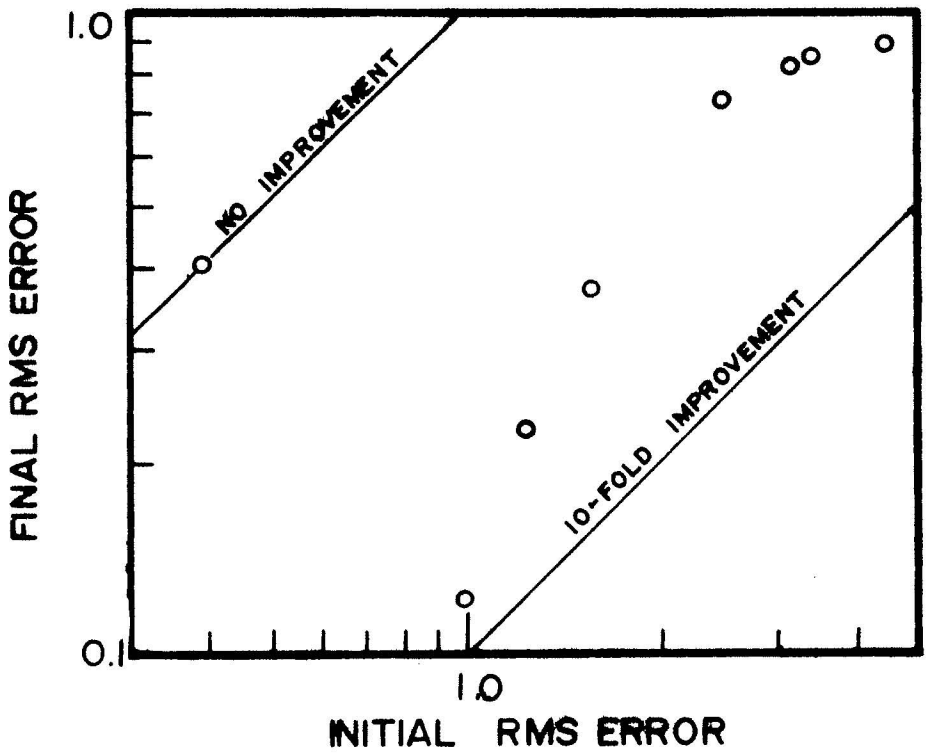

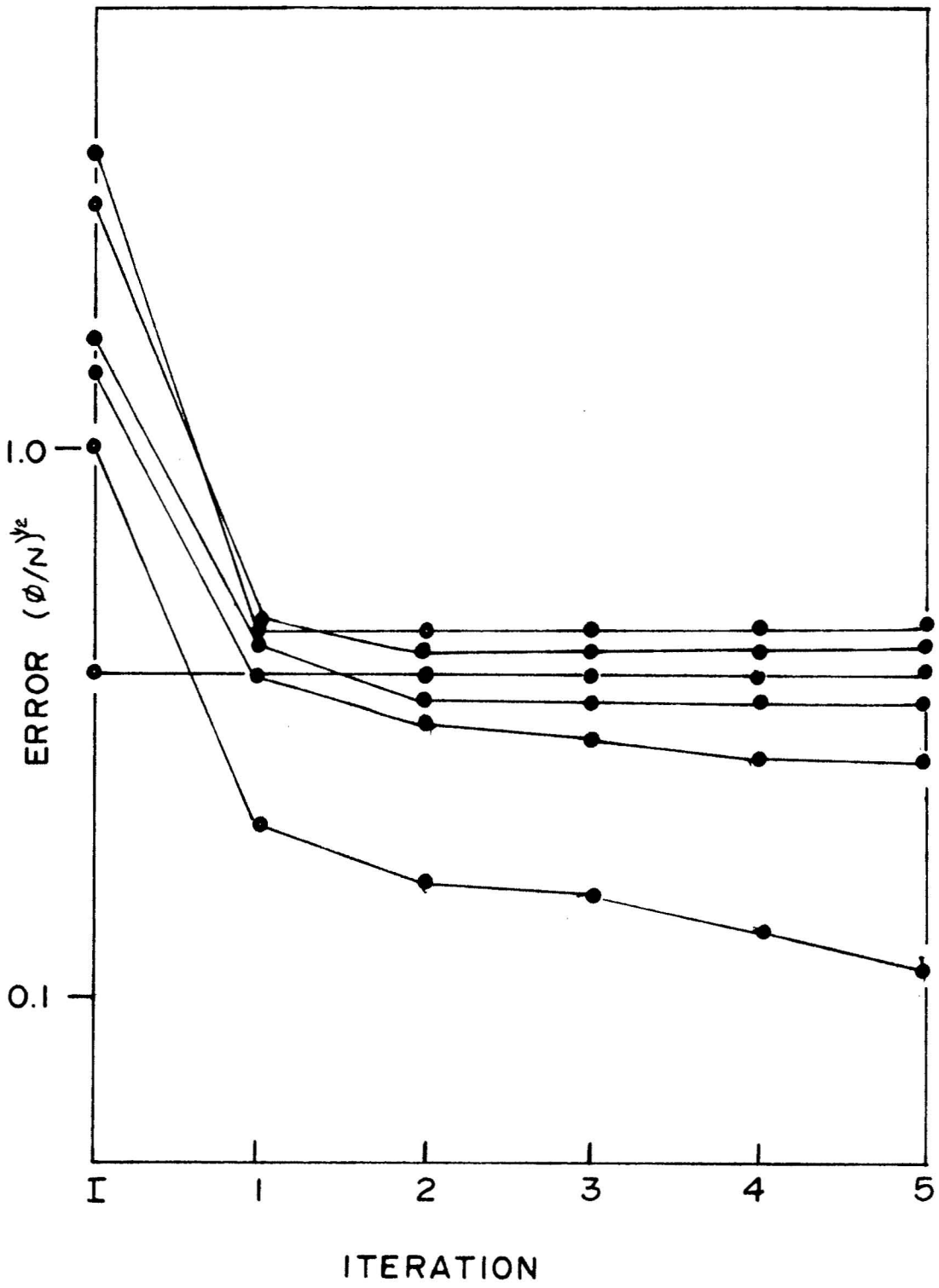

Figure 28. The reduction of error with each iteration.

When the parameter ρ_2 was far from its' true value (.1 to 3, 7, and 20), the fitting program tended to reduce h_2 to approximately 150 meters and did not adjust ρ_2 to its correct value of 5 Ω-m. Only when the estimated ρ_2 parameter was close to the true value did the program converge towards the theoretical solution. Daniels (1974) stated, and this test confirmed, that the input parameter should be within 20% of their true values for a good fit. Otherwise, a false fit may occur.

It should be emphasized that a final RMS error of 2% does not imply that the resistivities which result are $\pm$ 2%. The RMS error only indicates how close the observed curve is to the calculated curve.

INTERPRETATION OF GEOPHYSICAL STUDIES OF THE PUNA RIFT ZONE

DC Resistivity Data

Variations in resistivity may be mapped using the dipole-mapping method. Current is introduced into the ground through a line source and voltage is measured with perpendicular short-line receivers. In the summer of 1973, a detailed dipole-mapping survey of the Puna and Kau districts was sponsored by the University of Hawaii under a grant from the National Science Foundation.

Figure 29a is a map of the dipole survey around source 2 which is identical to the source used for the 1973 time-domain electromagnetic survey. The resistivity distributions from the EM and DC data are very similar. It is felt that a geothermal reservior would be characterized by a relatively high porosity and temperature in excess of 180° C. Both factors would cause a rock to have a lower resistivity. Thus, in prospecting for a geothermal reservior, we search for a region with diagnostically low values of resistivity. Approximately 2 km south of the source is a region of lower resistivity. In both the DC and EM data, this region is enclosed in a 10Ω-m contour with higher contours surrounding. This area of interest will be examined more closely in the

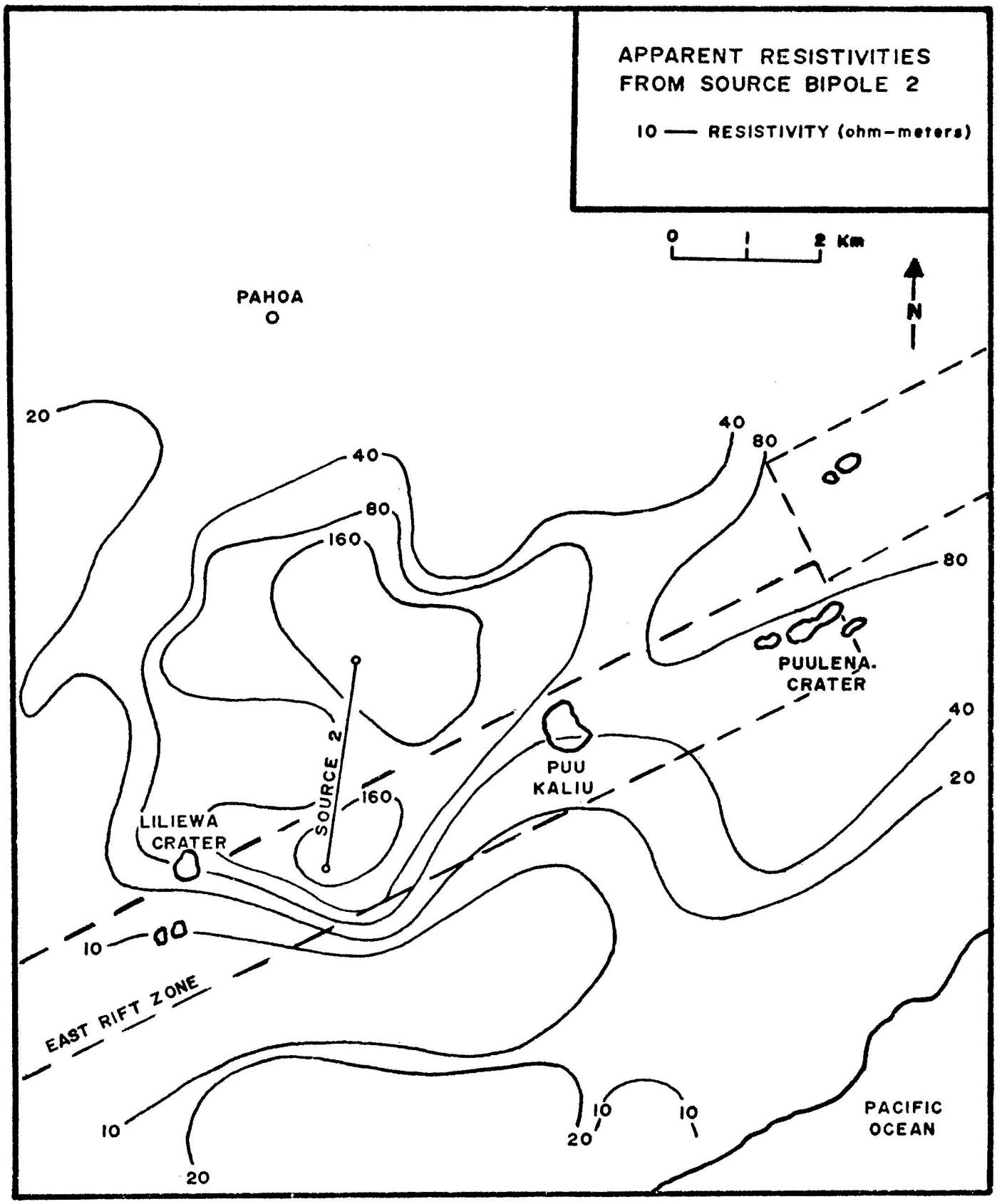

Figure 29a. Apparent resistivity map about bipole source 2, located along the road from Pahoa to Kaimu, in Puna. (Shupe, written communication, 1973).

following section. Generally, the remaining resistivities decrease toward the ocean because the salt-water/fresh-water interface is closer to the surface.

Figures 29b, c, and d are the results of dipole mapping measurements from additional sources. These are used to confirm the results from source 2 and to expand the coverage to the 1972 survey area. As with the electromagnetic data in Figures 13 and 14, the shoreline source 10 data and inland source 2, data can not be directly compared but trends can be compared. Source 10 confirms the low resistivity zone that was apparent from source 2.

Time-Domain Electromagnetic Data

The results of the interpretation of the 1973 part of the electromagnetic survey are summarized in tabular form in Figure 30. A layered-earth interpretation was not possible for all curves. For stations too close to the source, only a first-layer resistivity could be calculated from the maximum-received voltage. For the stations very far from the source where extreme filtering was used, the transients were too distorted for a curve-matching interpretation. Only a maximum-voltage resistivity is listed for these soundings.

The contoured maximum resistivity map reflects the geology. The Kilauea dike system is expressed by a high resistivity

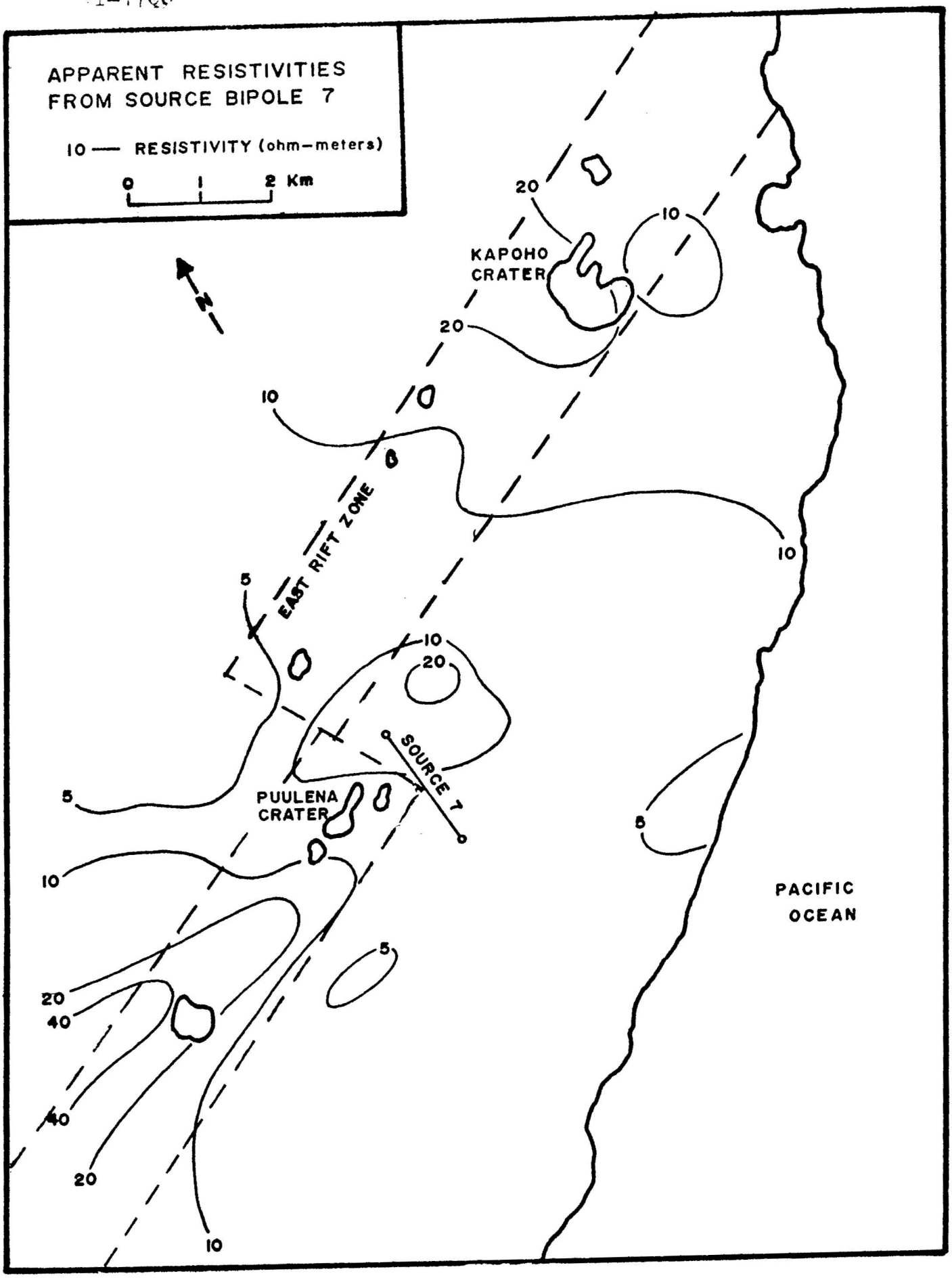

Figure 29b. Apparent resistivity map about bipole source 7. (Shupe, written communication, 1973)

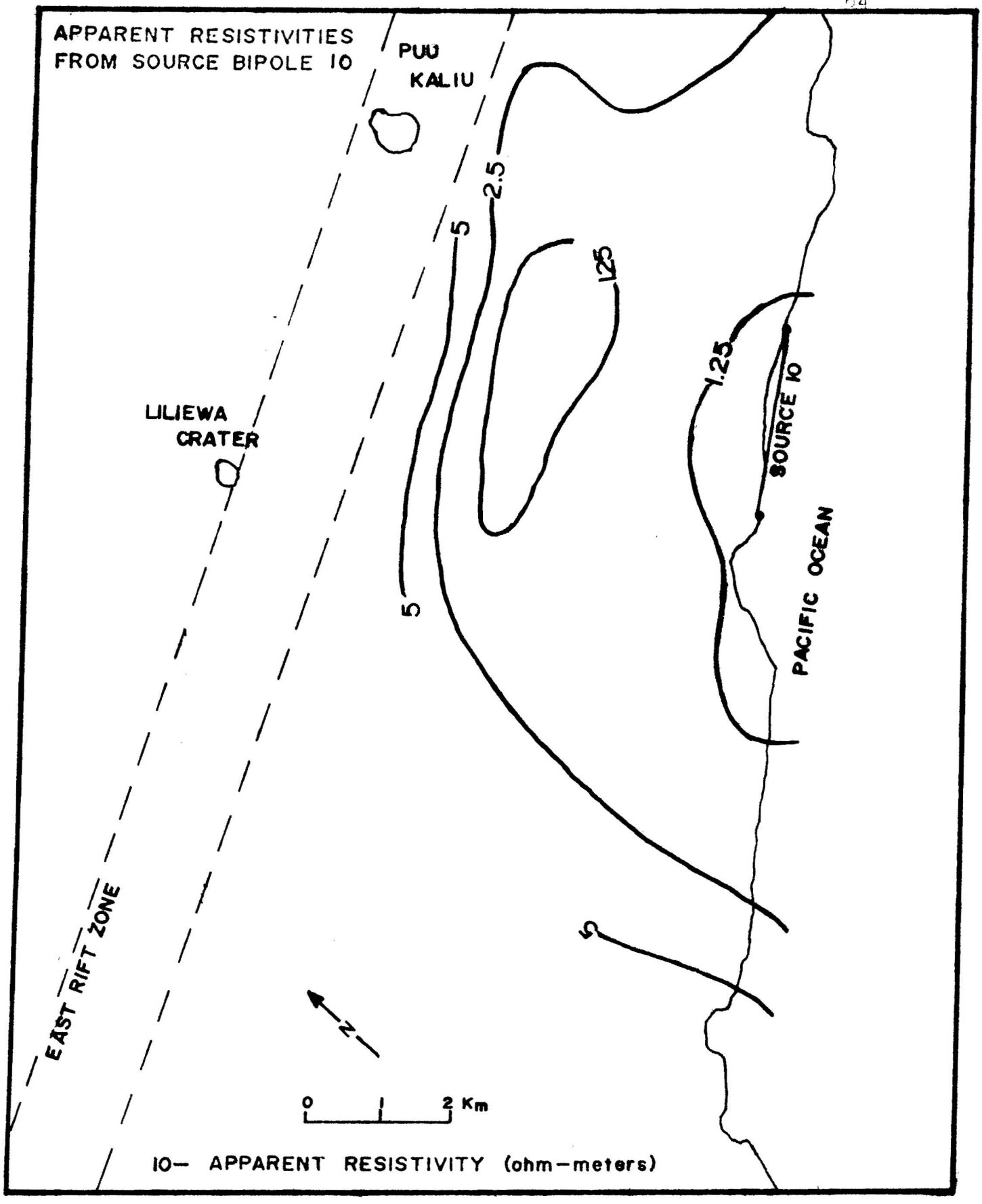

Figure 29c. Apparent resistivity map about bipole source 10 along the Kaimu-Pahoiki coastal road. The low resistivity zone from source 2 is verified. (Shupe, written communication, 1973).

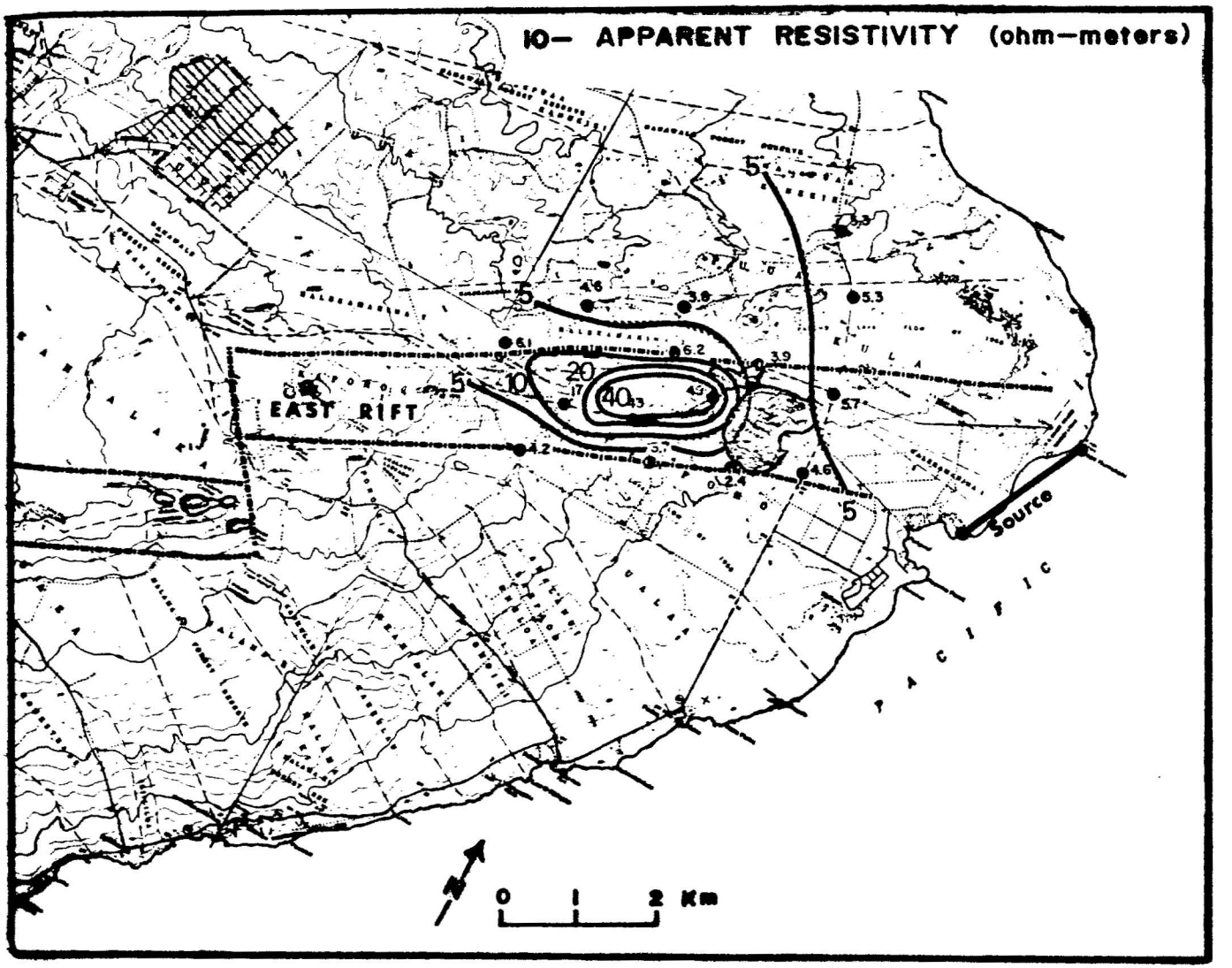

Figure 29d. Apparent resistivity map about a bipole source (1972).

Figure 30. Table of Interpretation Results.
(Resistivity -- ohm-m; Thickness -- m)

Station	ρ_1	H_1	ρ_2	H_2	ρ_3
1	12	500	24		
2	23				
3	11	(93)			
4	23				
5	23	800	10	1400	1
6	16	(EXCESSIVE FILTERING)			
7	14	700	5	1300	1
8	10	700	5	1000	1
9	20	(320)			
10	20	(280)			
11	21	(260)			
12	31	(580)			
13	106	440	5	440	2
14	92	800	18		
15	157	500	31		
16	51	(BEST MATCH - UNIFORM EARTH)			
17	131	(EXCESSIVE FILTERING)			
18	39	(EXCESSIVE FILTERING)			
19	42	(EXCESSIVE FILTERING)			
20	68	(EXCESSIVE FILTERING)			
21	64	(EXCESSIVE FILTERING)			
22	119	700	5	350	2

Figure 30 (cont.).

Station	ρ_1	H_1	ρ_2	H_2	ρ_3
23	13	600	4	600	1
24	14	600	5	600	1
25	11	600	4	1200	1
26	9	700	4	1300	1
27	12	820	6	1000	
28	17	1400	12		
29	17	1340	11		
30	16	800	5	950	1
31	~ 5	(SIGNAL BELOW NOISE LEVEL)			
32	104	(595)			
33	81	(720)			
34	109	950	5		
35	87	1400	17		
36	99	1050	5		
37	77	1050	5		
38	103	440	68	440	5
39	43	440	67	440	5
40	71	1020	5		
41	74	1080	5		
42	92	1050	6		
43	58	945	5		
44	59	900	5		
45	144	775	6		

Figure 30 (cont.).

Station	ρ_1	H_1	ρ_2	H_2	ρ_3
46	45	(41)			
47	29	(41)			
48	20	(295)			
49	15	940	1		
50	20	(272)			
51	60	(RECORDER PEN BROKE DURING MEASUREMENT)			

zone which is particularly noticeable on the 1972 resistivity map. The displacement on the rift is characterized by a resistivity high on the 1973 map. As discussed in the hydrology section, it is thought that the East Rift dike system forms a barrier to ground water movement from the heavy rainfall area to the north. The higher resistivities to the north could result from saturation with fresh water instead of more saline sea water which produces lower resistivities toward the ocean.

Two cross sections were drawn to summarize the electromagnetic interpretation results. The cross sections were selected to two very different regions of the survey. Cross section A-A' (Figure 31) illustrates a dike complex in the rift area. This type of structure is characterized by higher resistivities. Cross section B-B' (Figure 32) shows the low resistivity zone which begins at the surface and becomes more conductive at a depth of about 700 m. It is presumed that this resistivity low is a result of both salt in solution in ground water and heat. Surrounding resistivity zones are also influenced by salt water underground.

Comparison of DC and TDEM Methods

A comparison was made of the apparent resistivities from the dipole resistivity (DC) data and the maximum-voltage resistivities from the time-domain electromagnetic

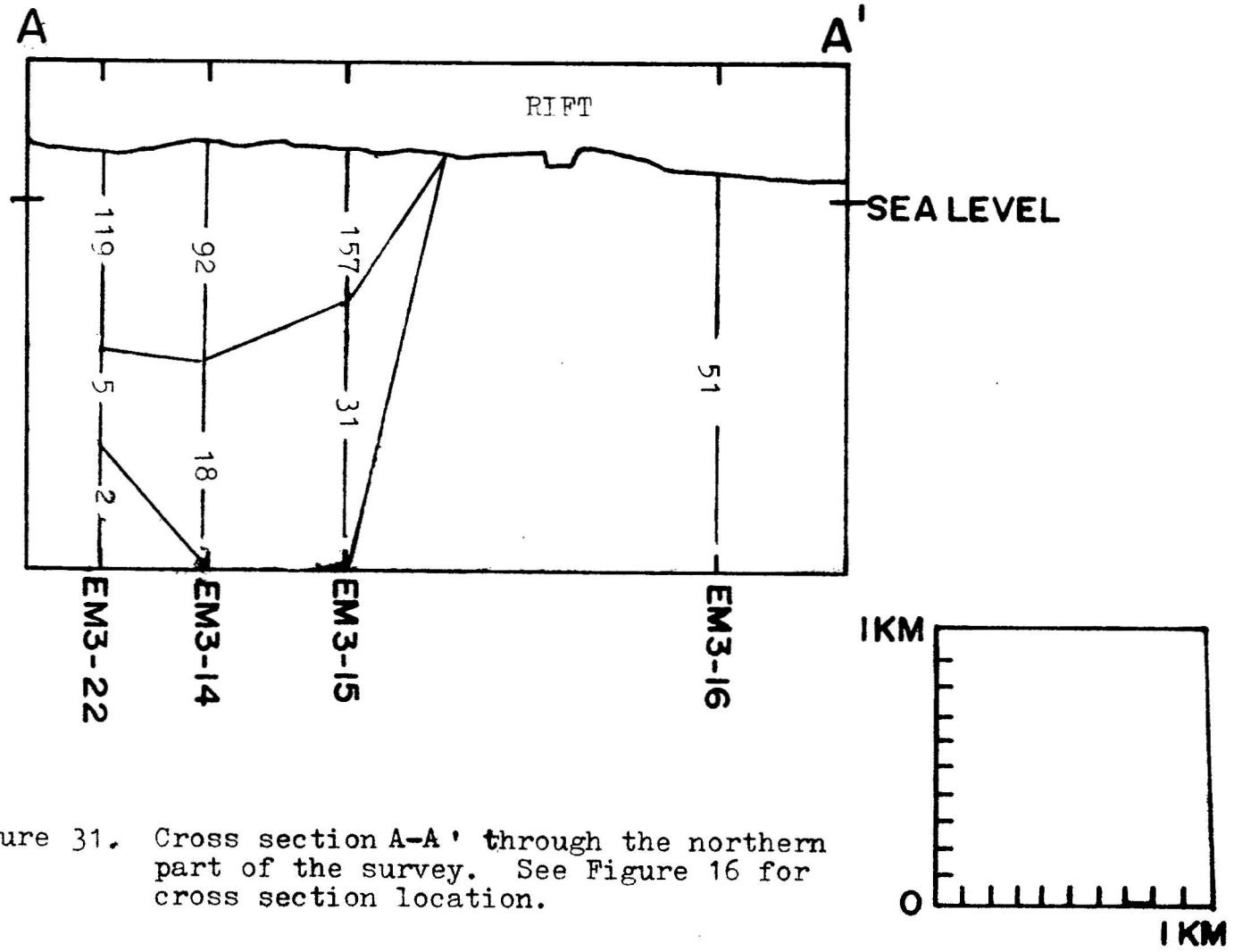

Figure 31. Cross section A-A' through the northern part of the survey. See Figure 16 for cross section location.

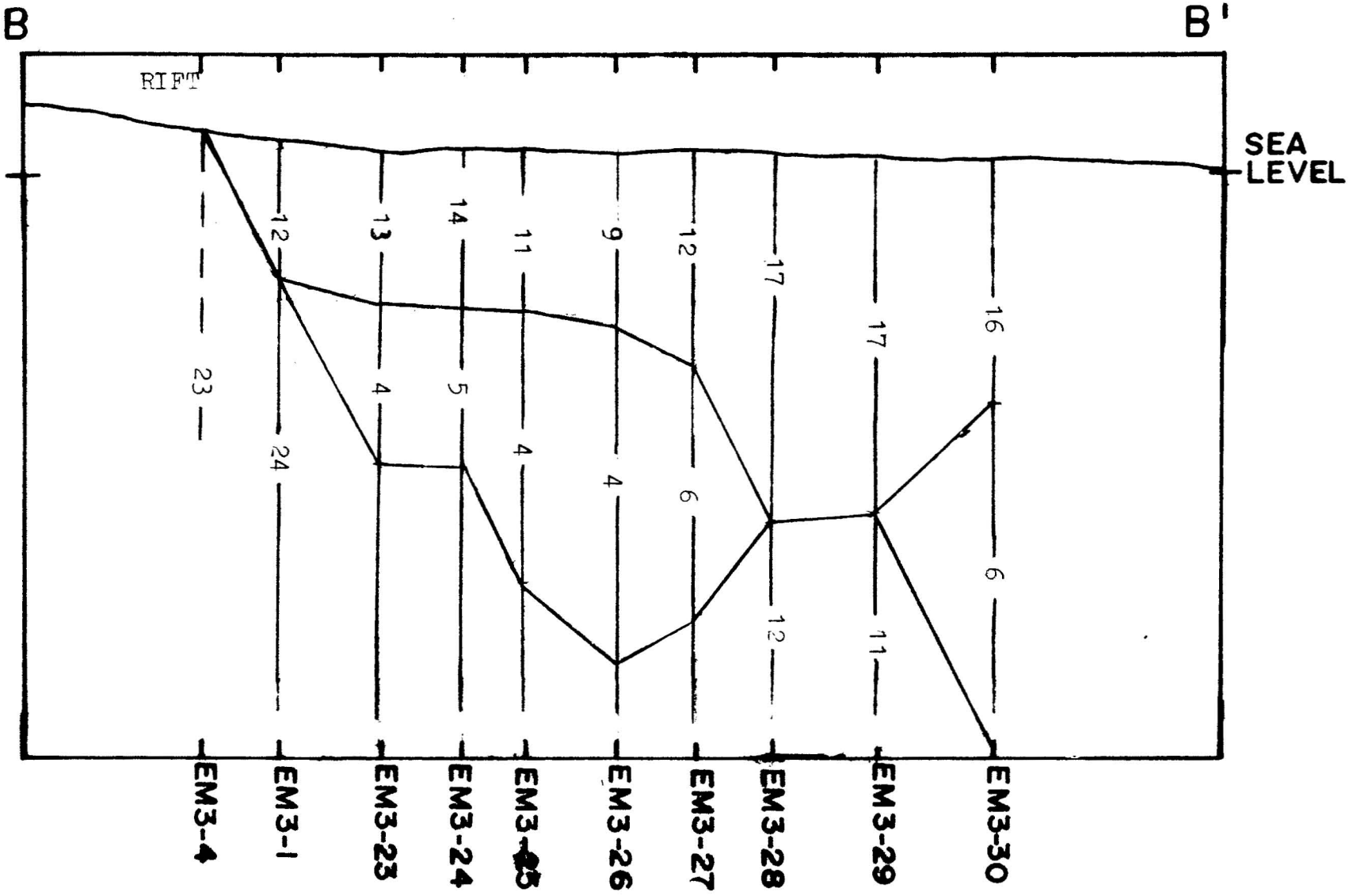

Figure 32. Cross section B-B' through the southern part of the survey. See figure 16 for cross section location. See figure 36 for horizontal and vertical scale.

(TDEM) data. First the survey area was broken into one-square-kilometer cells (see Figure 33a) DC resistivities from four sources which covered the area were averaged for each cell. The same was done for the two TDEM surveys. Figure 33b summarizes the results of this comparison. The dashed line is the $\rho_{DC} = \rho_{TDEM}$ line. Resistivities from the two methods are very much alike. However, with the TDEM method ρ versus depth information is gained at each station, while with the DC method, only a ρ_a value is obtained at each station. Therefore, TDEM is a better exploration tool.

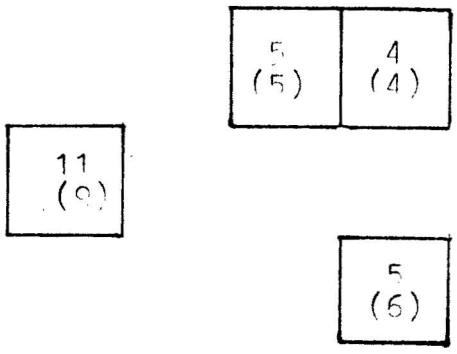

One-kilometer square cells for which there were DC and TDEM data available for averaging around the 1972 bipole source. See Figure 29d for location.

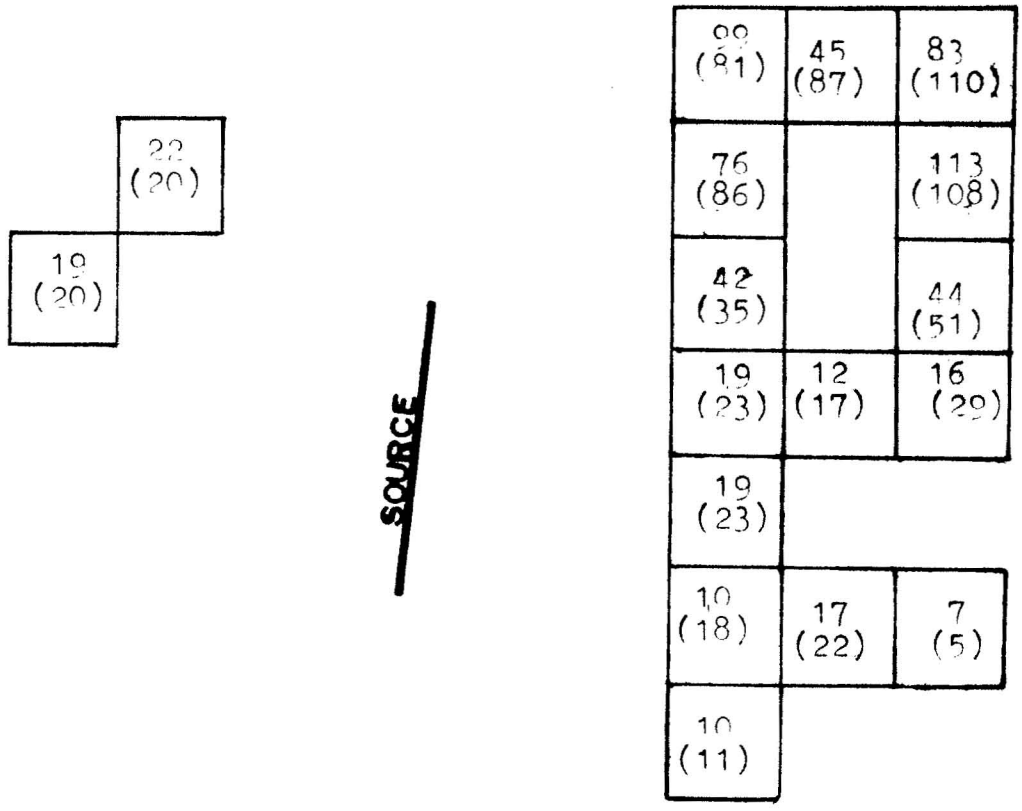

One-kilometer square cells for which there were DC and TDEM data available for averaging around source bipole 2. See Figure 29a for location. Data from source 7 was included for averaging as well.

Figure 33a. Sketch maps of averaging "cells". Plain numbers are DC averages; parenthetical numbers are TDEM averages.

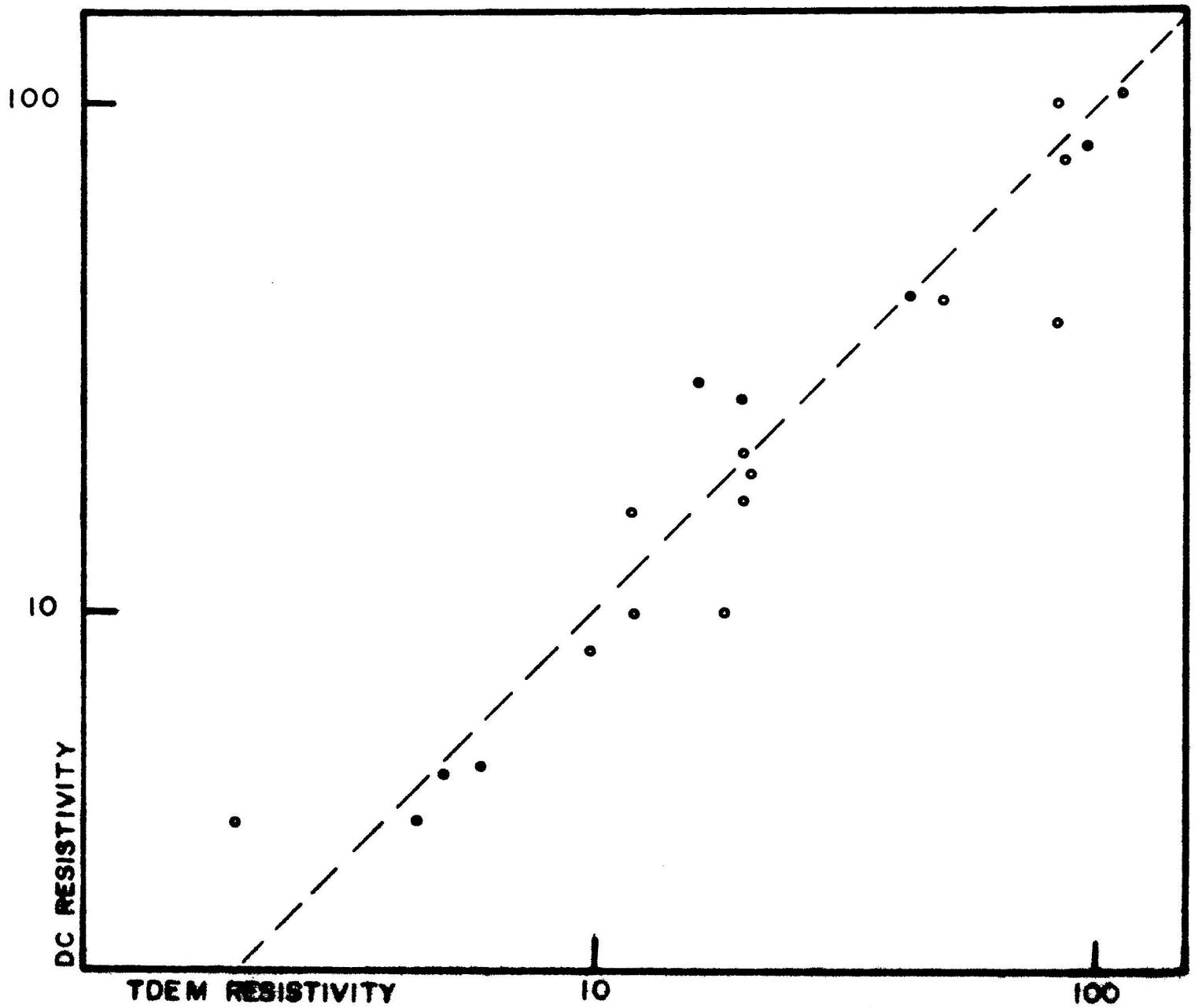

Figure 33b. Average apparent resistivities from 1 km^2 areas compared with average maximum-voltage resistivities from the same areas.

CONCLUSIONS

Interpretation Techniques

Field data from a time-domain electromagnetic survey in the East Rift Zone of Kilauea were interpreted using a layered-earth model. First, the maximum voltage of the transient signal is multiplied by a geometric factor to give a value for apparent resistivity. This calculation is simple and can be quickly plotted and contoured in the field. Geologic interpretations may be gained from this preliminary technique. With computer assistance, a more sophisticated interpretation of the data is possible. After the step response of the recording equipment is removed through deconvolution, the data are compared with a set of asymptotic three-layer curves. From a first estimate obtained from the asymptotic match, theoretical three-layer curves are computed in both frequency and time domains for a more exact matching. Both methods give comparable results. Finally, a least-squares-fit computer program is used to improve the match. The asymptotic interpretation procedure works well for conductive-basement curves but for resistive-basement

curves, another first-estimate approach must be employed. Silva (1969) has published a two-layer catalog and Daniels' work (1974) contains a few sample two- and three-layer curves. Both of these references may be employed to begin the interpretation process. The least-squares-fitting technique should be considered a refinement procedure. If the input parameters are within 20% of their true values, the fitting program can reduce the RMS error to less than one. However, if the initial estimate is not good, a false match will result. Reasonable results require good judgement; the interpretation should be geologically meaningful.

Geologic Interpretation

The electromagnetic data and the DC data were combined for geologic interpretations (See Figure 34). It was found that the resistivities calculated with both DC and EM methods were generally the same. Moreover, the EM data provided information on resistivity versus depth at each station. This added dimension makes the electromagnetic method a superior exploration tool.

A magnetic high and gravity high are characteristic of dense near-surface material. The DC and EM data revealed a resistivity high in the same region. All of these data indicate a shallow dike complex along the surface expression of the East Rift Zone.

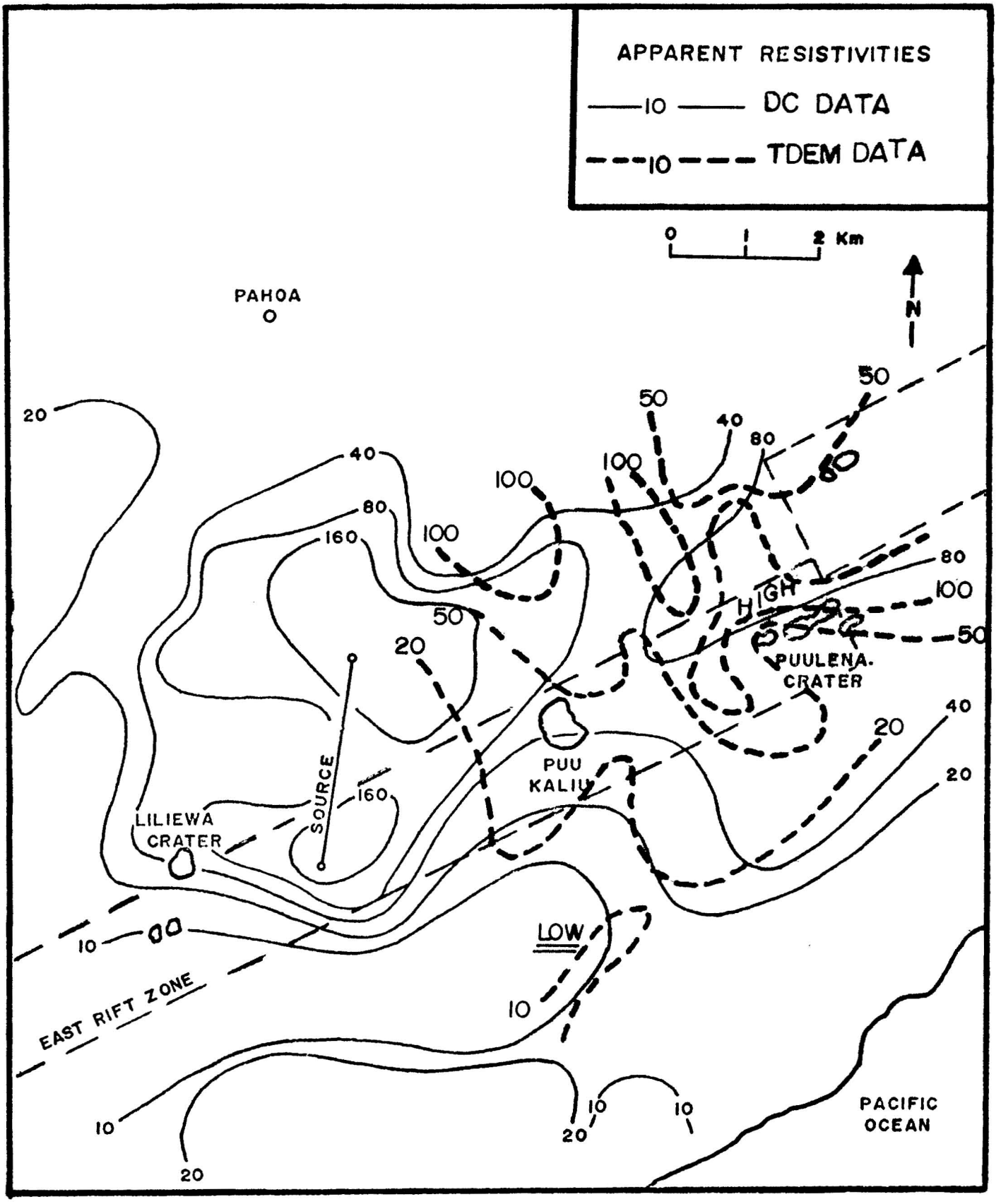

Figure 34. Summary map of DC and TDEM data.

Of geothermal interest was a low-resistivity zone approximately two kilometers south of the rift which appeared in both the DC and EM data. A cross section shows this zone becoming more conductive at a depth of about 700 m. The only way to completely evaluate the geothermal potential of this zone would be to drill a test hole.

APPENDIX A

Three-Layer Time-Domain Asymptotic Curves

Parameter	H2/H1
1	0.1
2	0.2
3	0.5
4	1.0
5	2.0
6	5.0
7	10.0

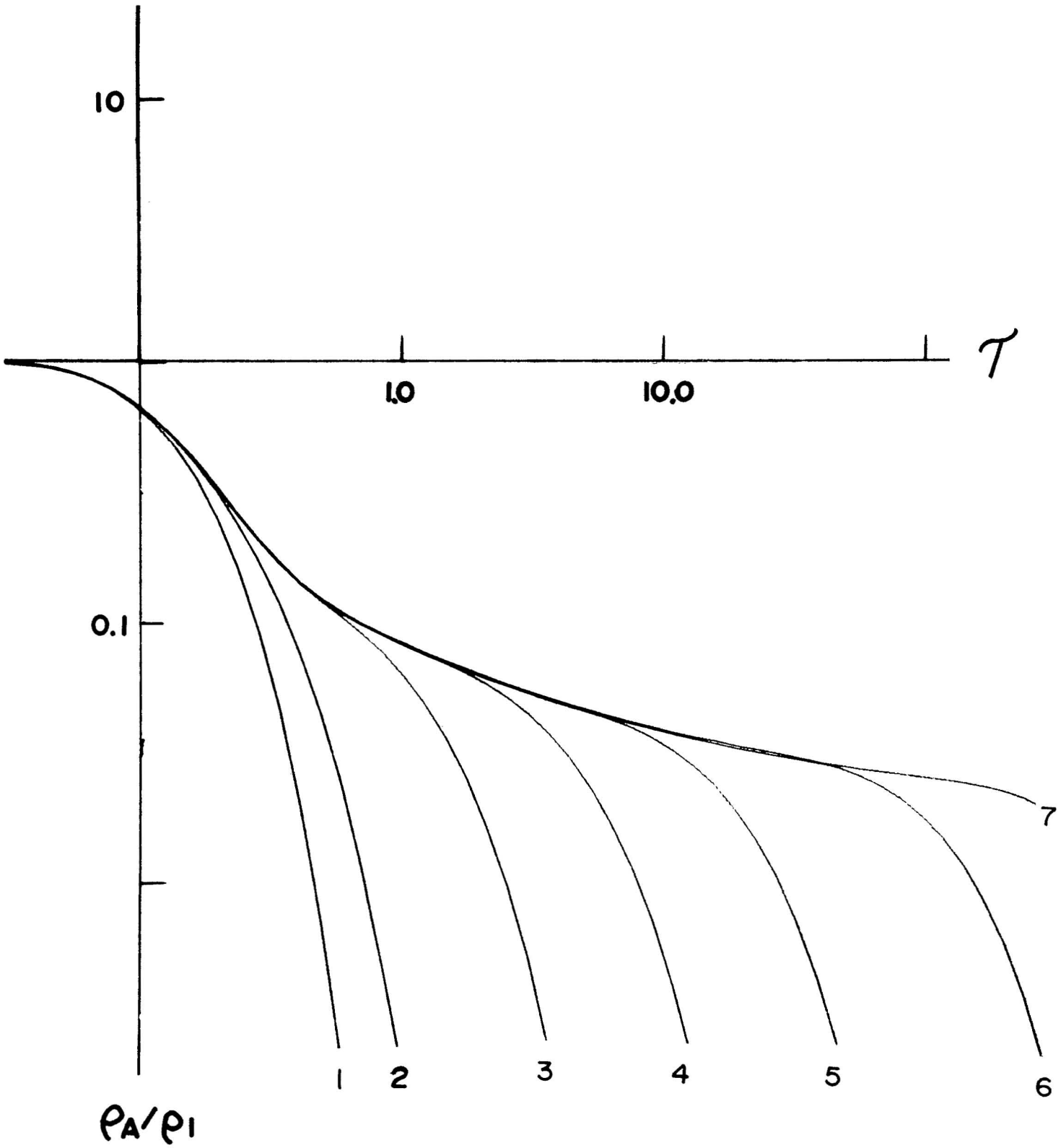

STEP RESPONSE (R3/R1=0) (R2/R1=.02)

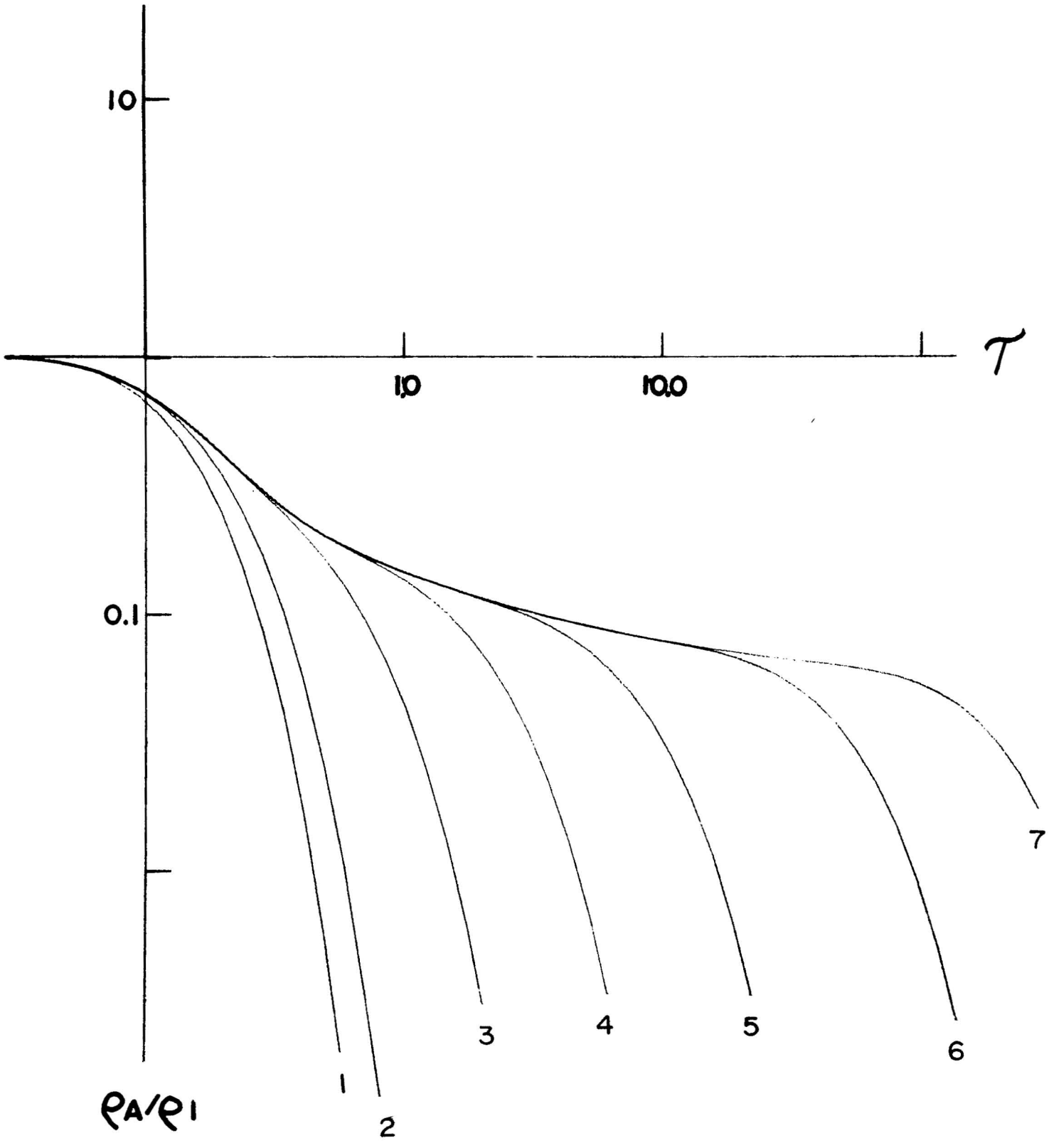

STEP RESPØNSE (R3/R1=0) (R2/R1=.05)

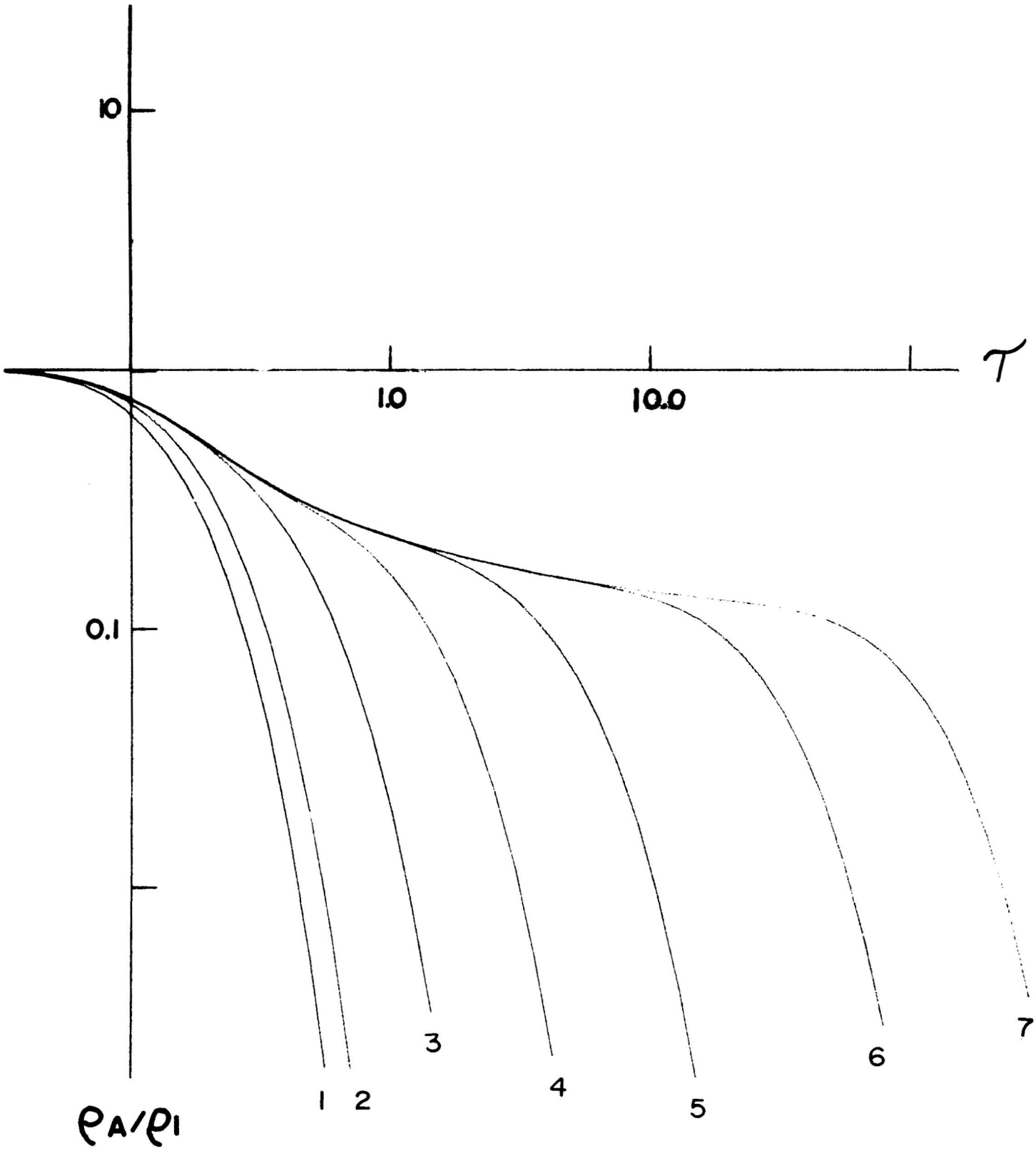

STEP RESPONSE (R3/R1=0) (R2/R1=0.1)

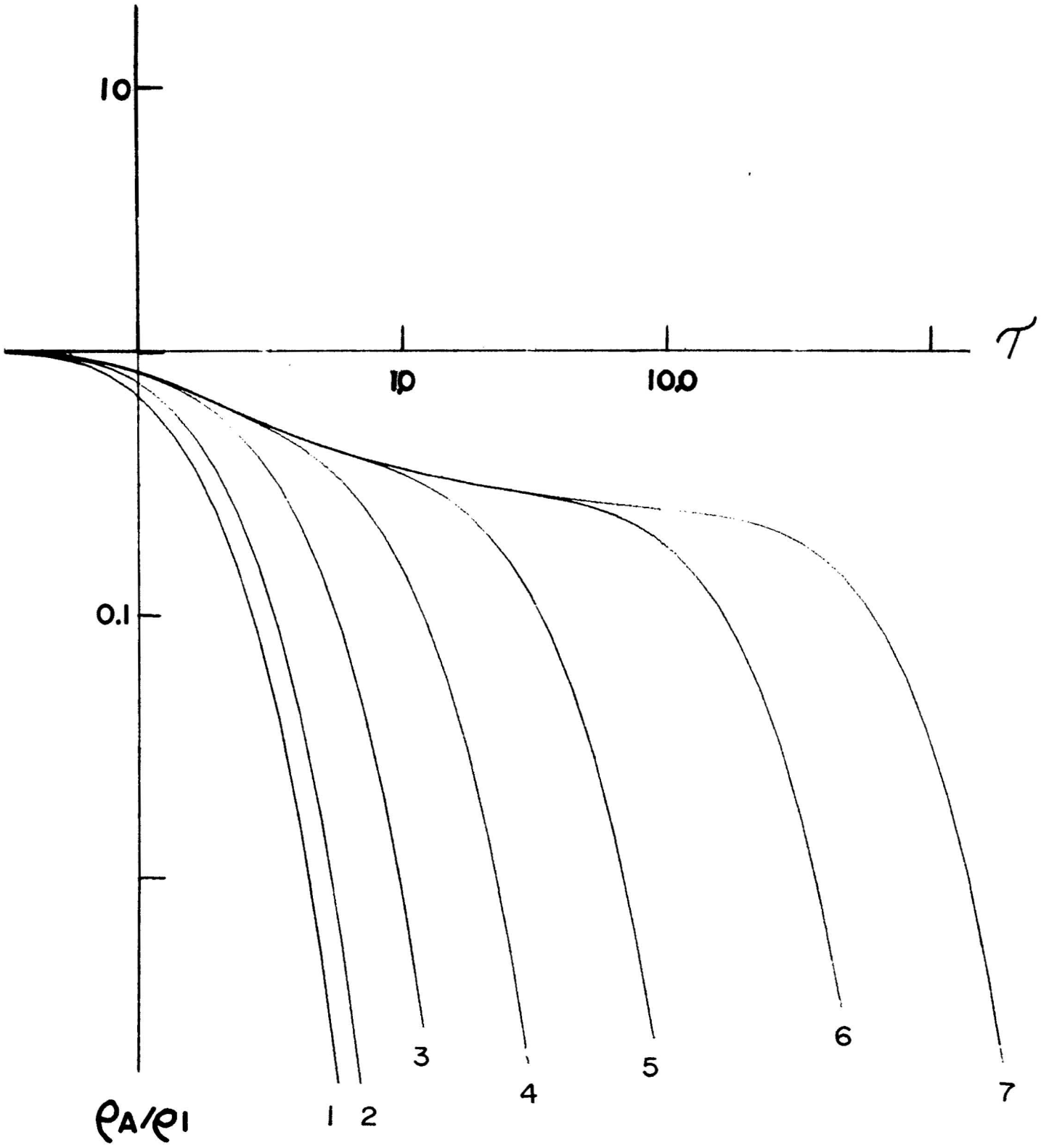

STEP RESPONSE (R3/R1=0) (R2/R1=0.2)

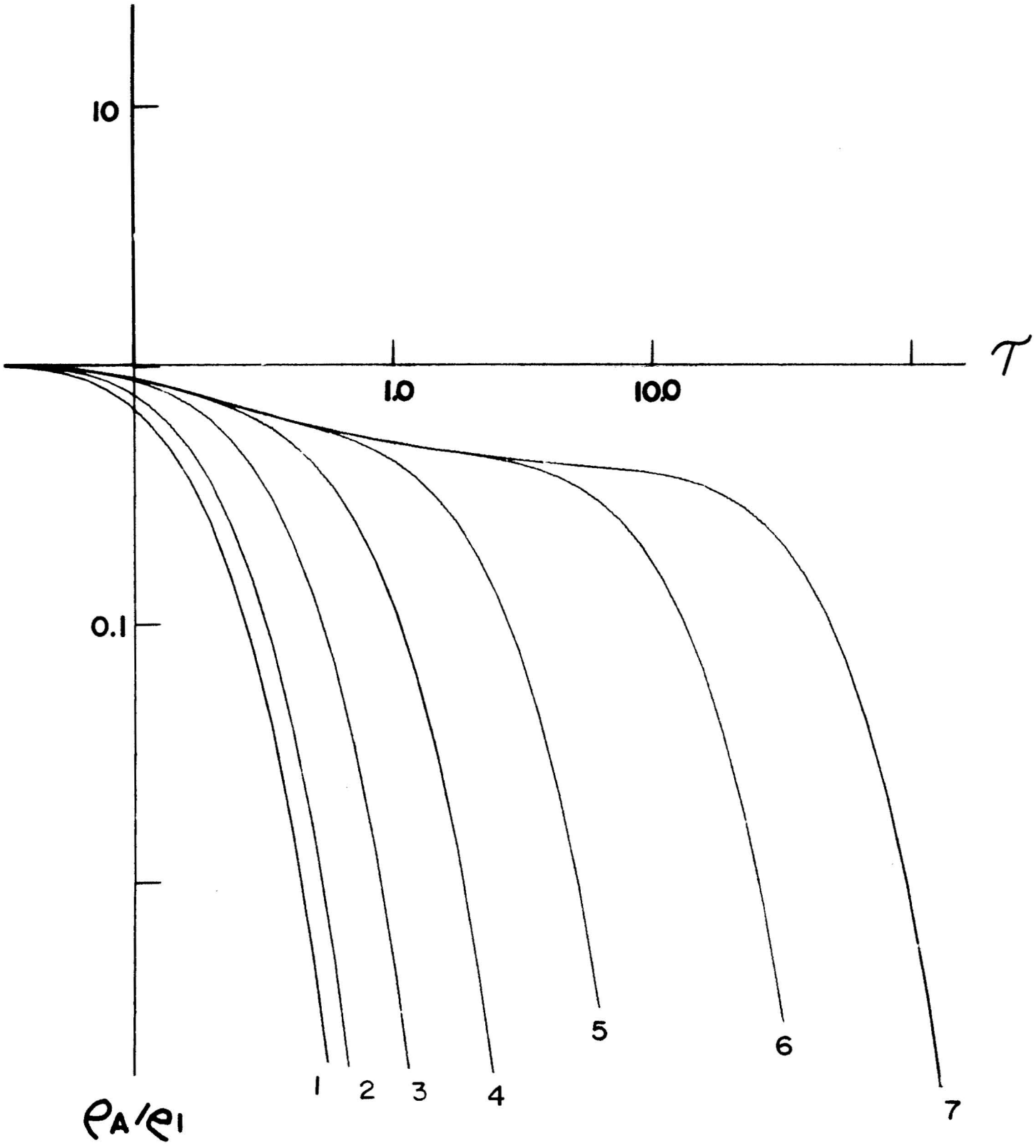

STEP RESPØNSE (R3/R1=0) (R2/R1=1/3)

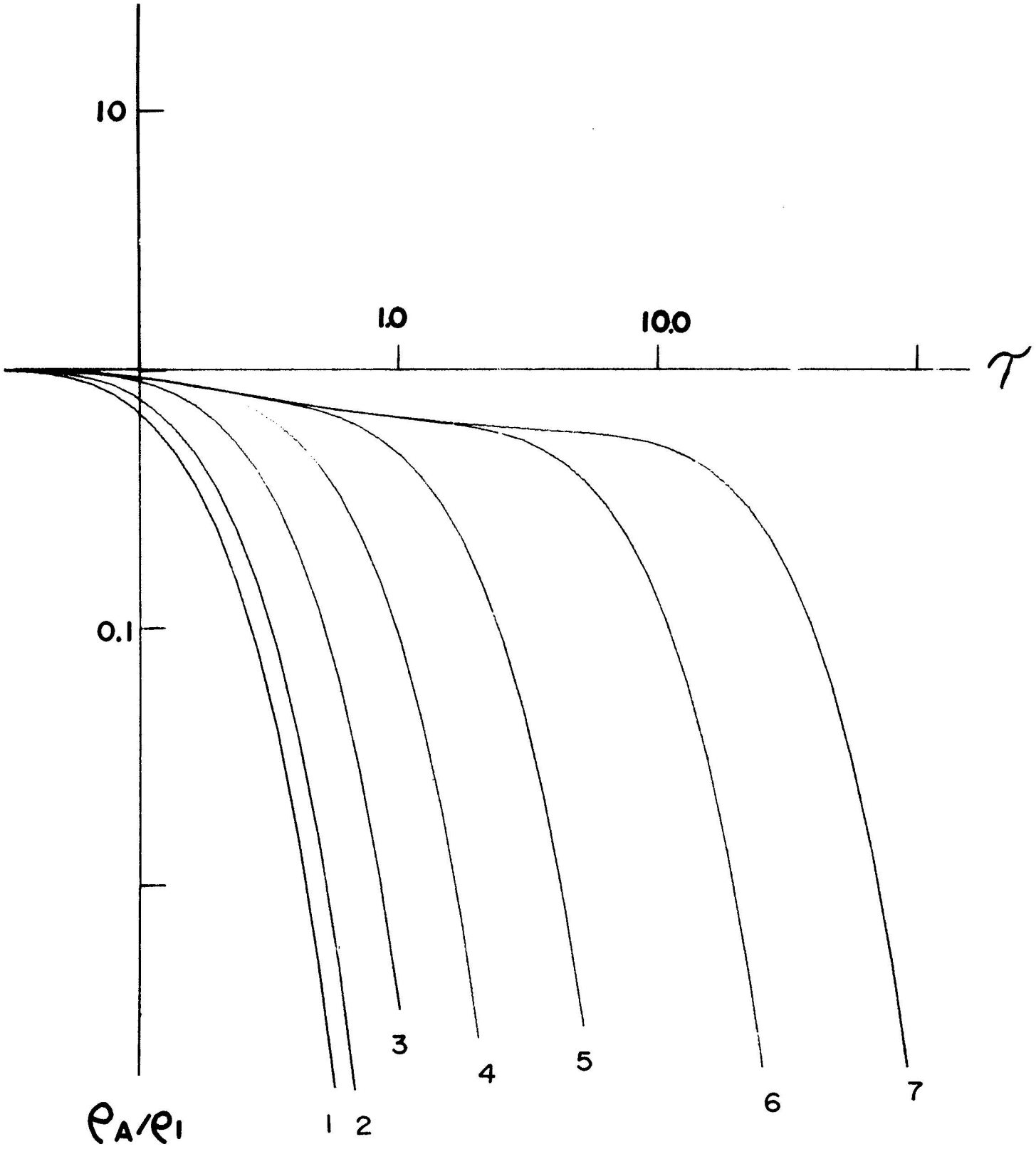

STEP RESPONSE (R3/R1=0) (R2/R1=0.5)

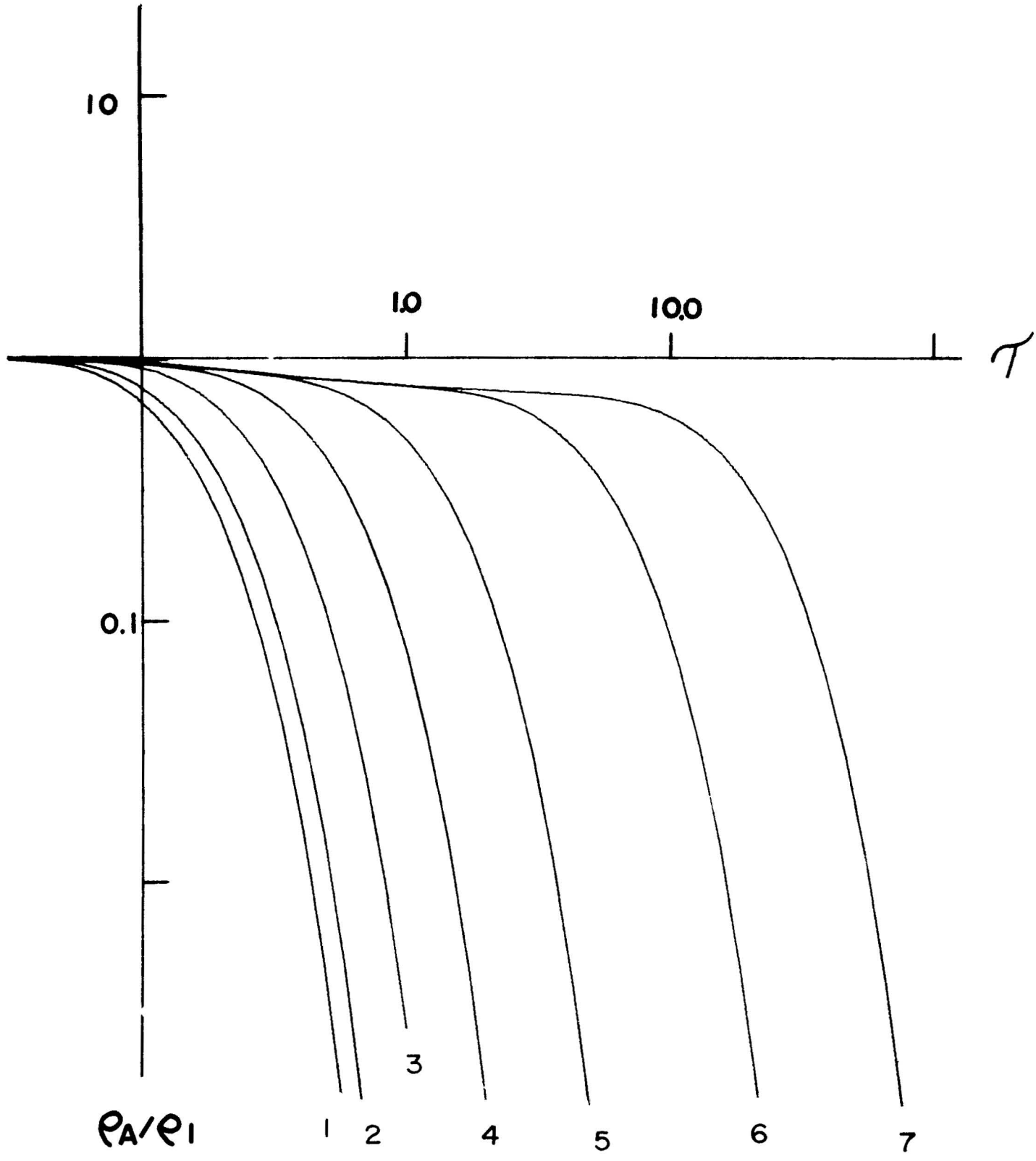

STEP RESPØNSE (R3/R1=0) (R2/R1=2/3)

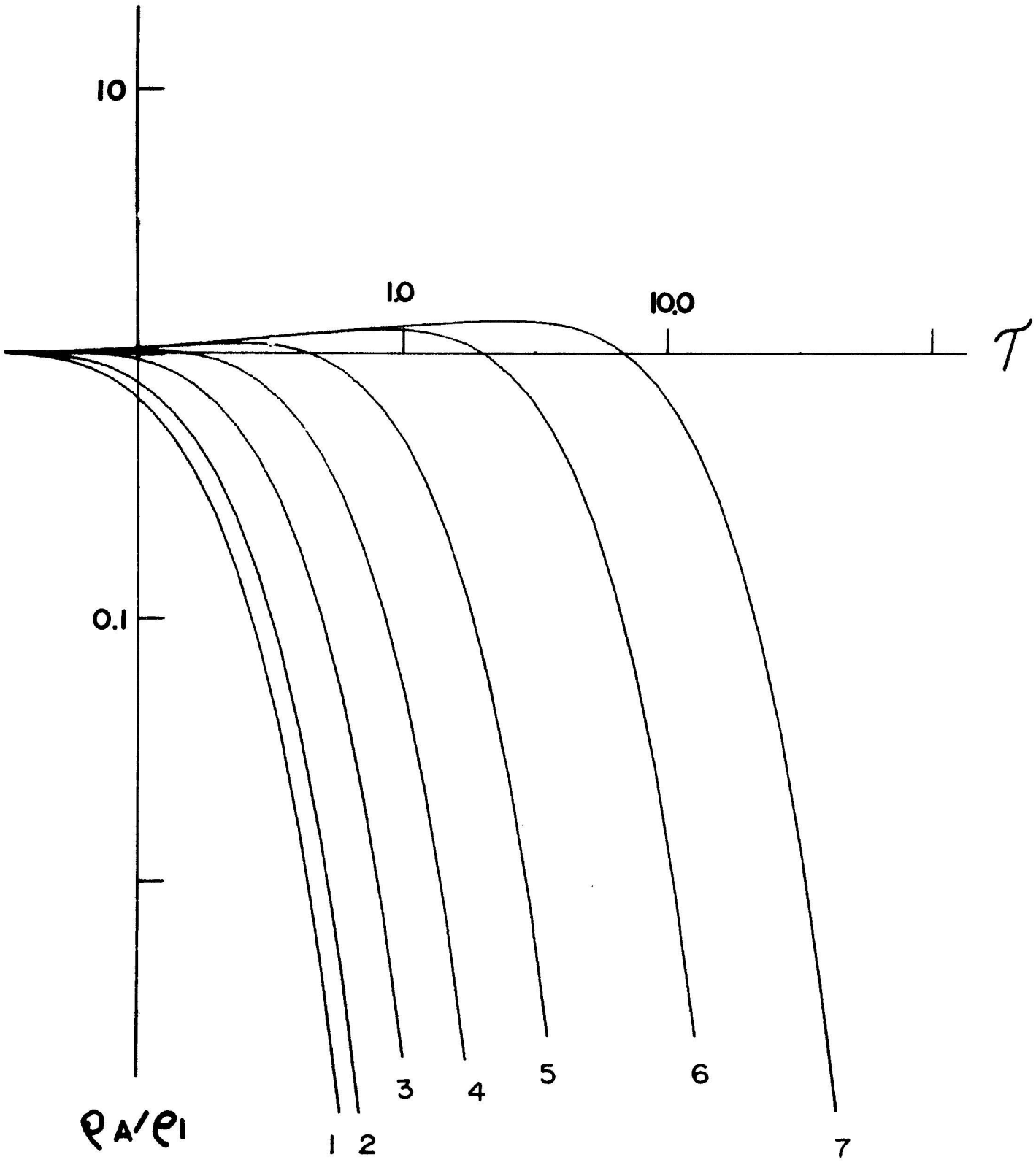

STEP RESPØNSE (R3/R1=0) (R2/R1=1.5)

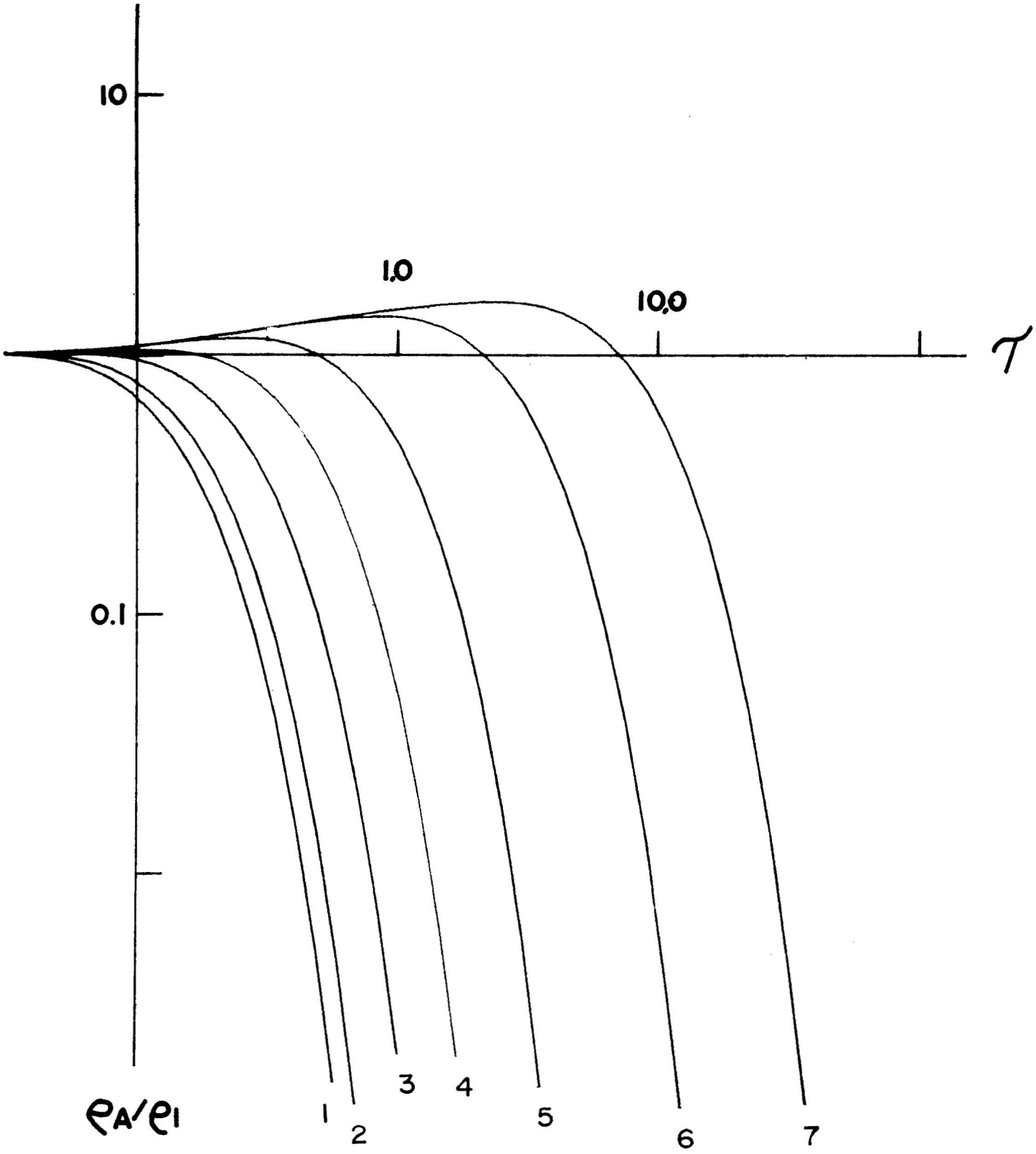

STEP RESPØNSE (R3/R1=0) (R2/R1=2.0)

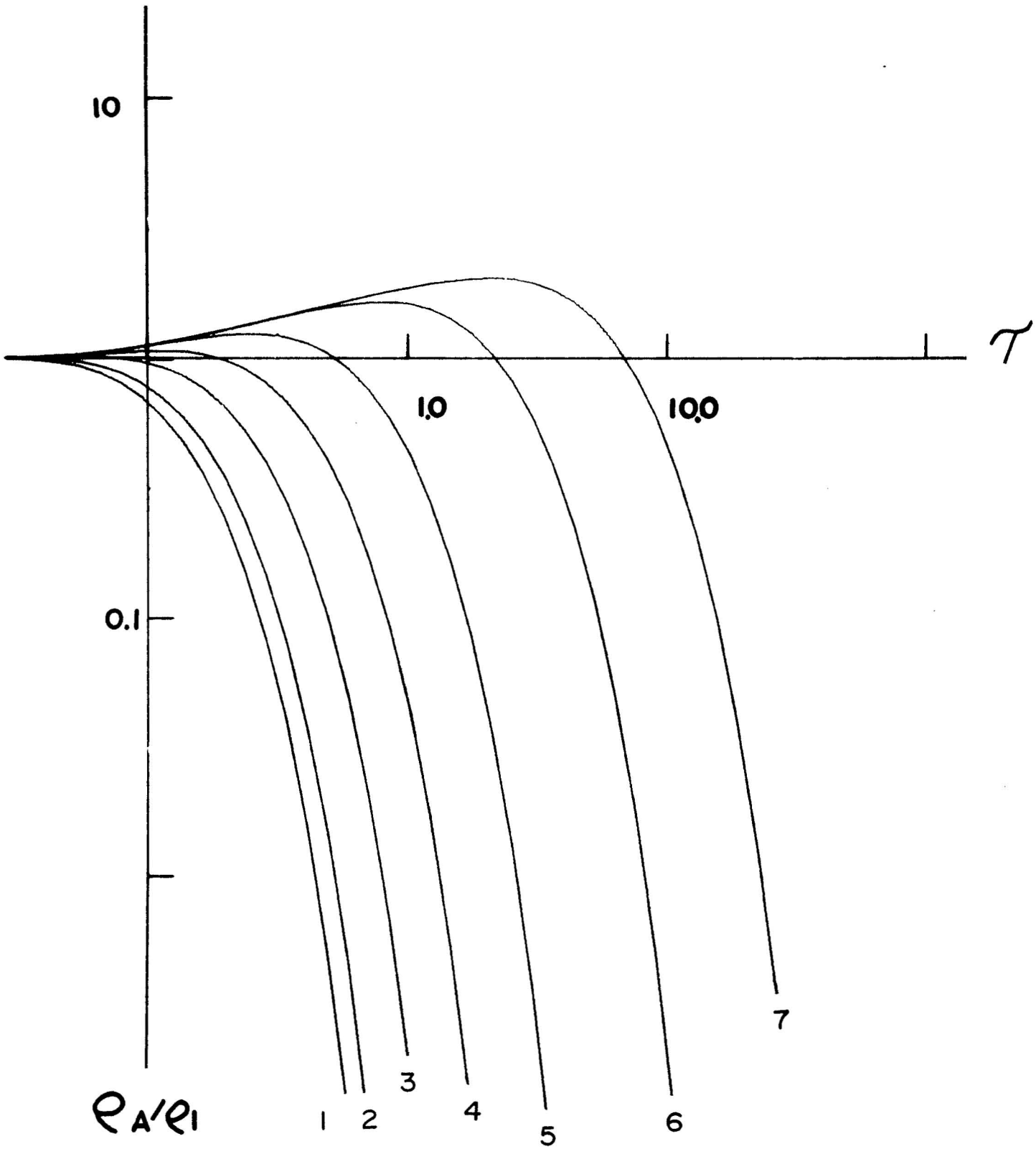

STEP RESPØNSE (R3/R1=0) (R2/R1=3.0)

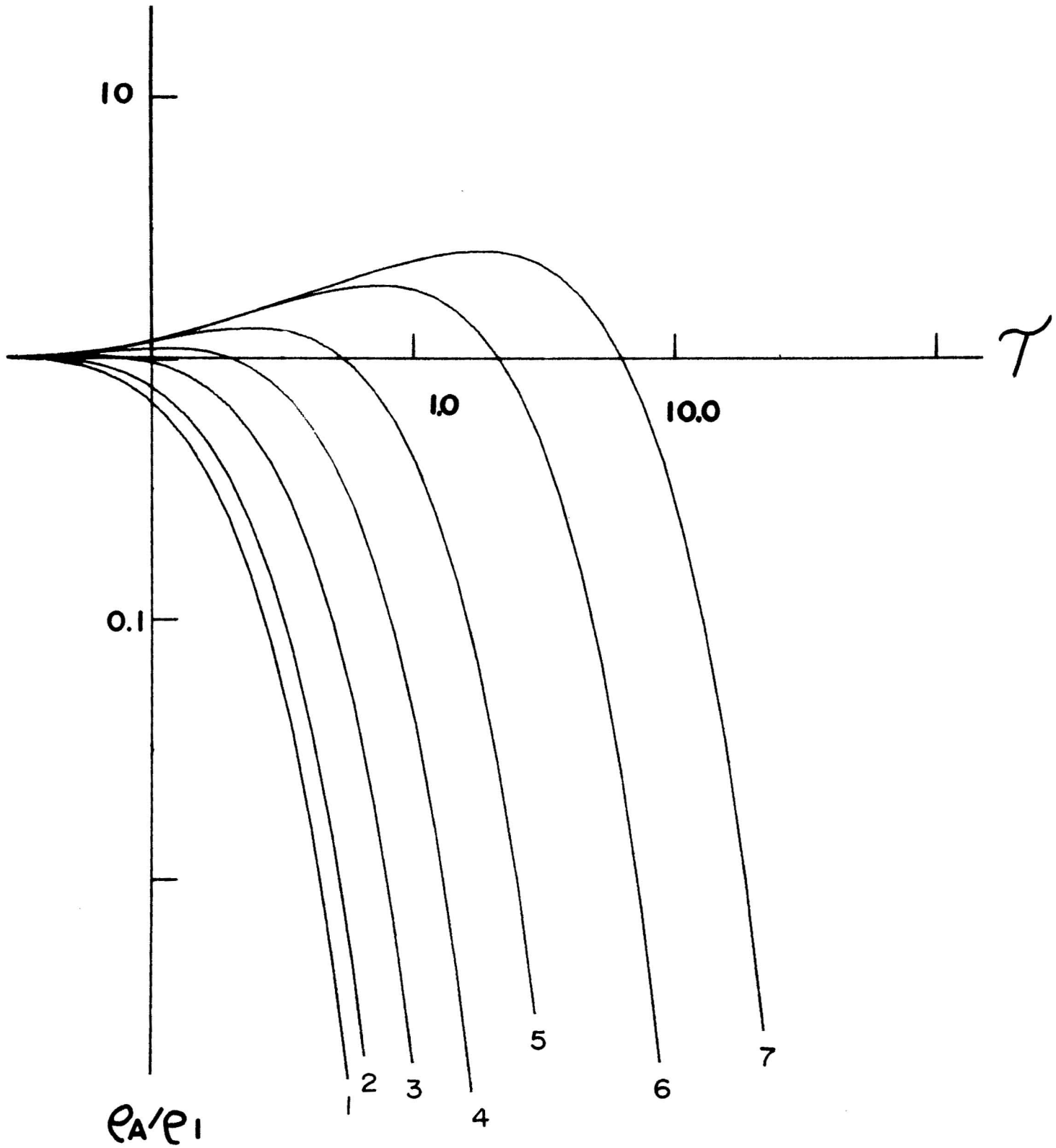

STEP RESPØNSE (R3/R1=0) (R2/R1=5.0)

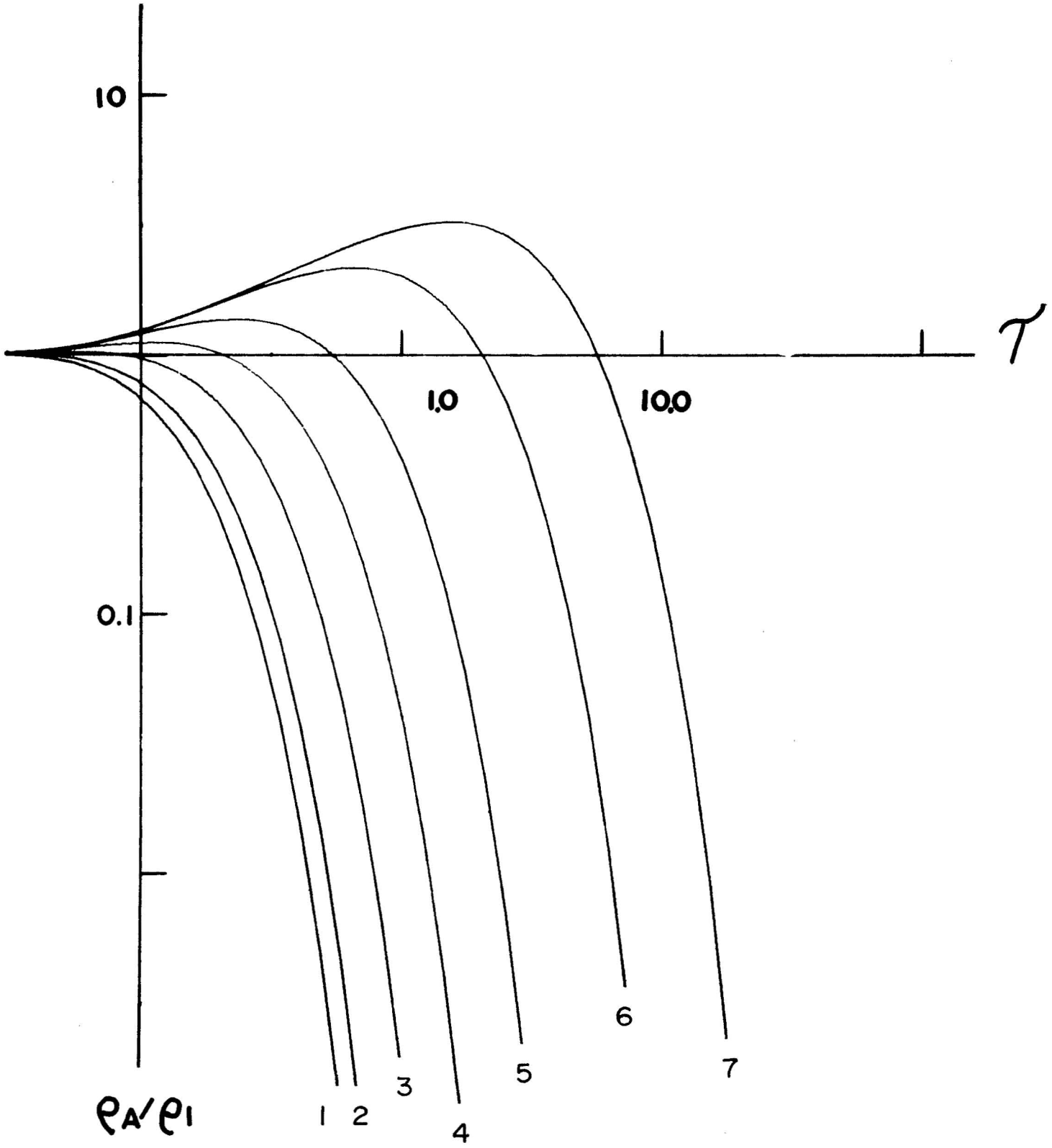

STEP RESPØNSE (R3/R1=0) (R2/R1=10.)

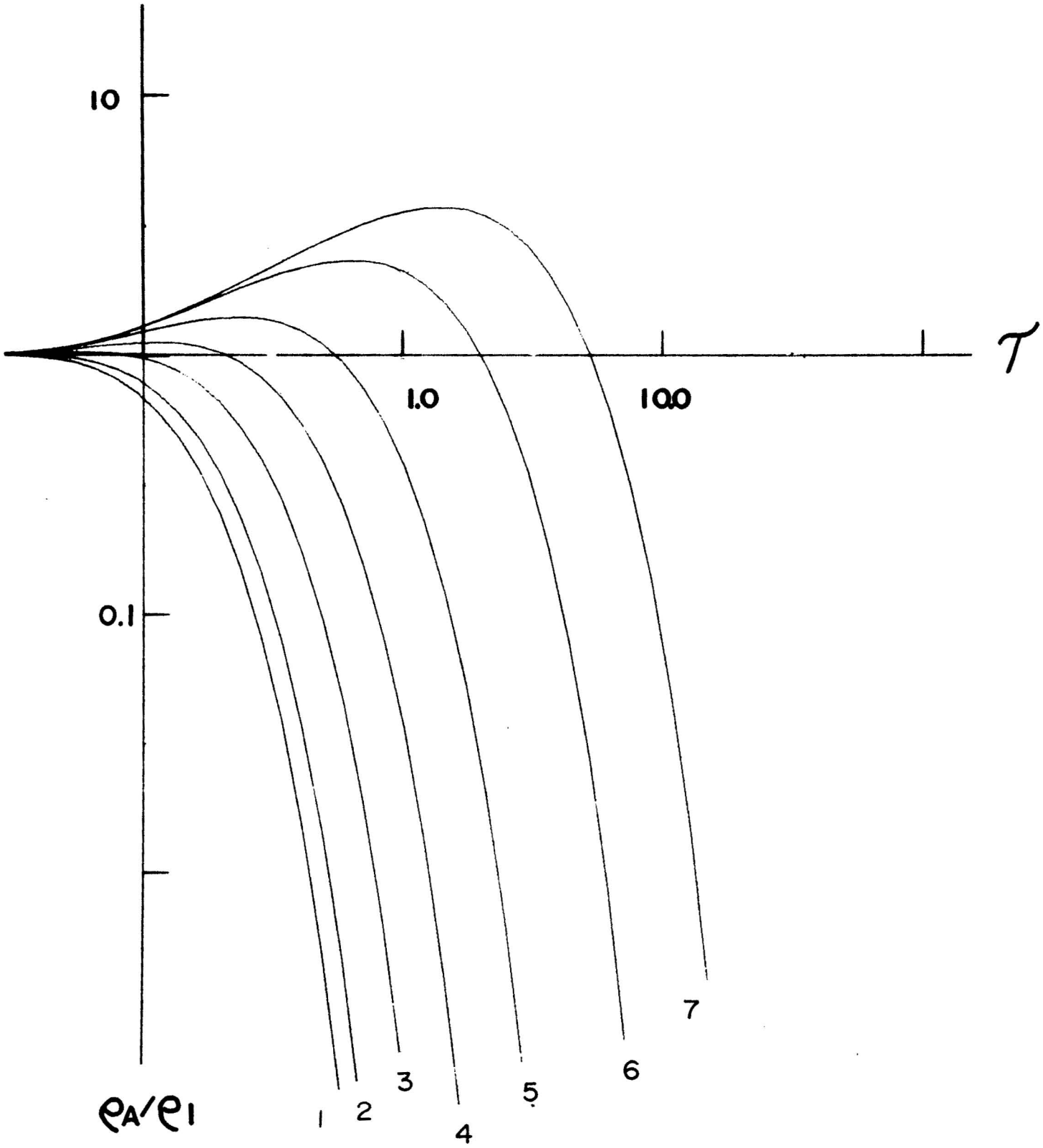

STEP RESPONSE (R3/R1=0) (R2/R1=20.)

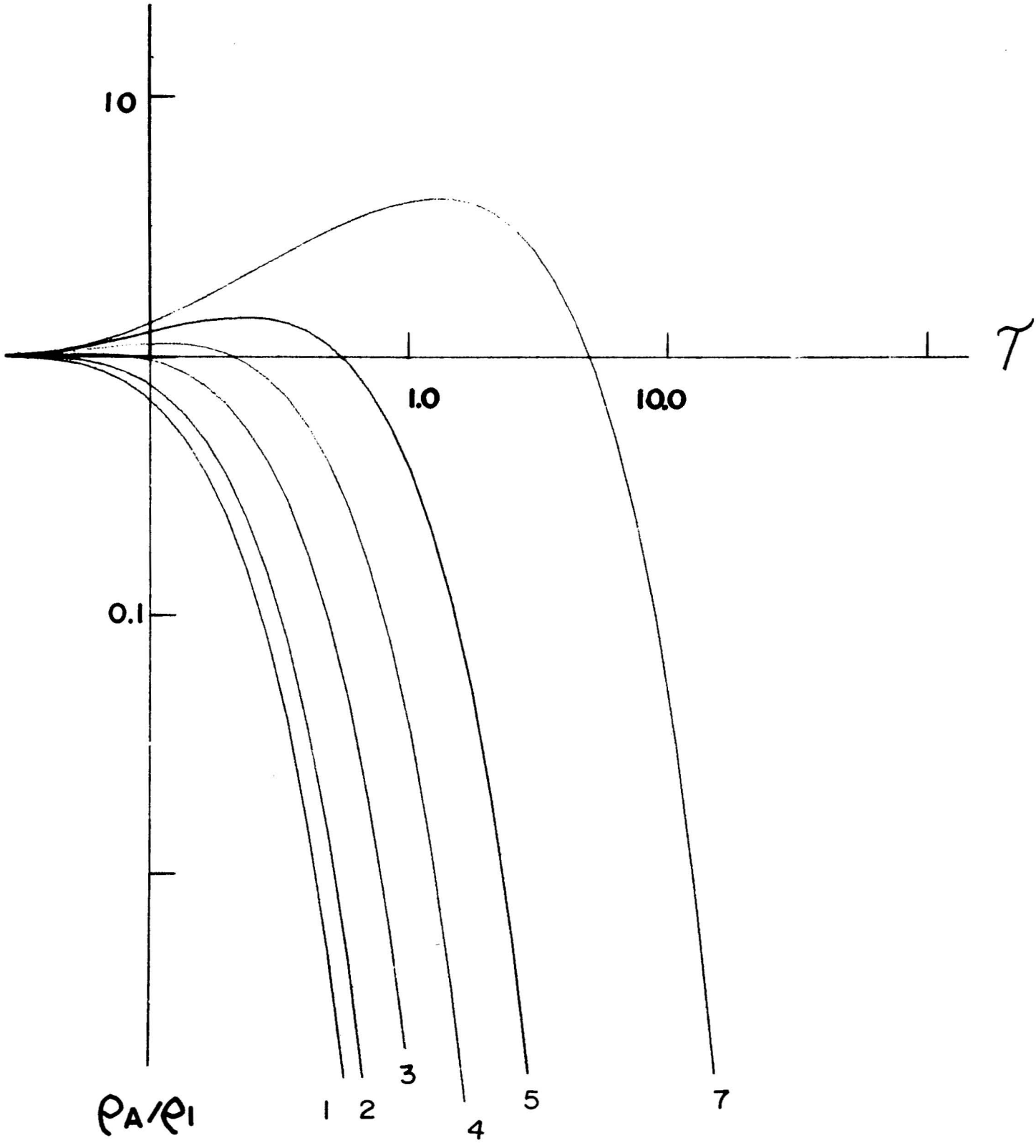

STEP RESPØNSE (R3/R1=0) (R2/R1=50.)

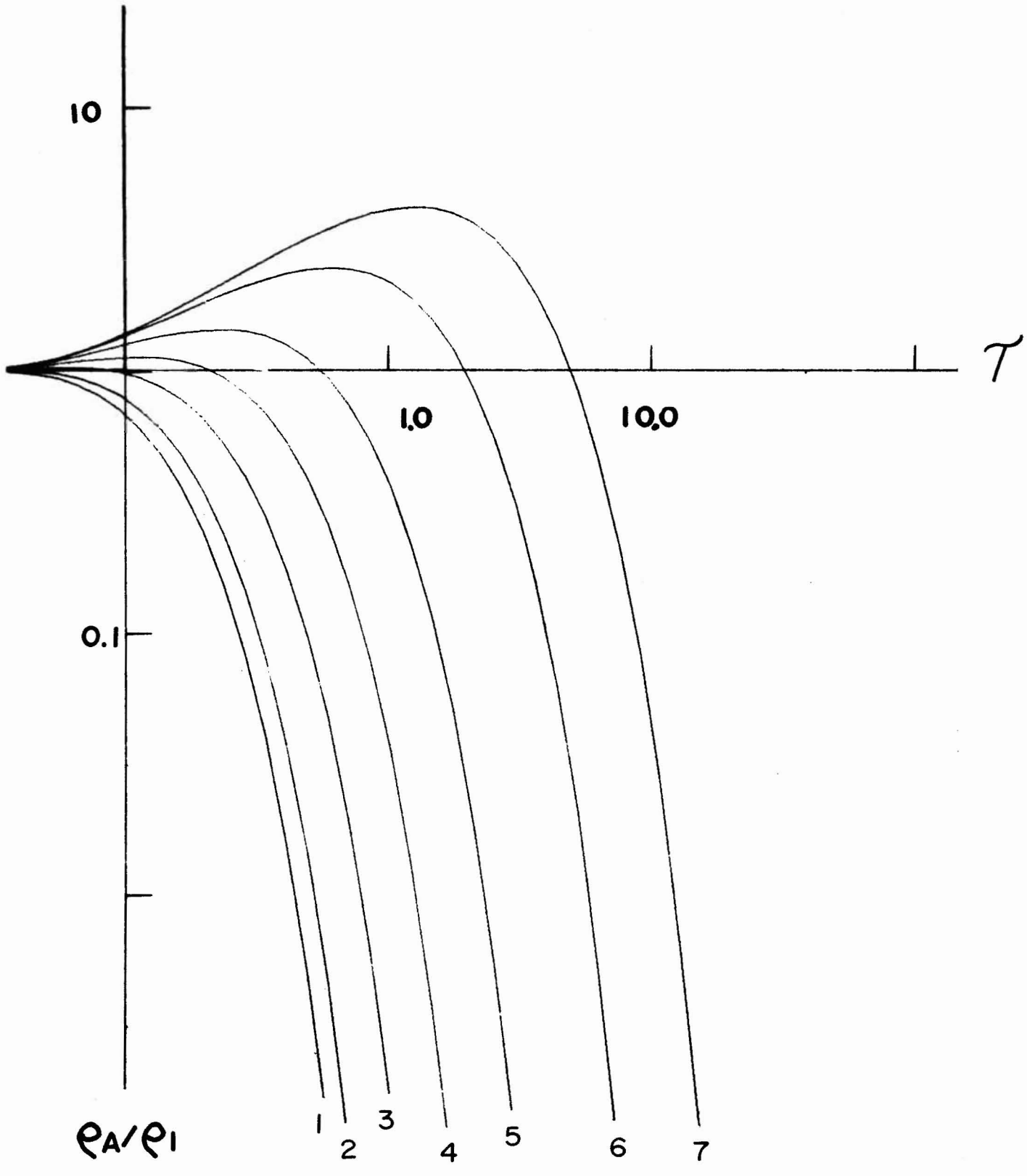

STEP RESPONSE (R3/R1=0) (R2/R1=100)

APPENDIX B

Deconvolved Field Data

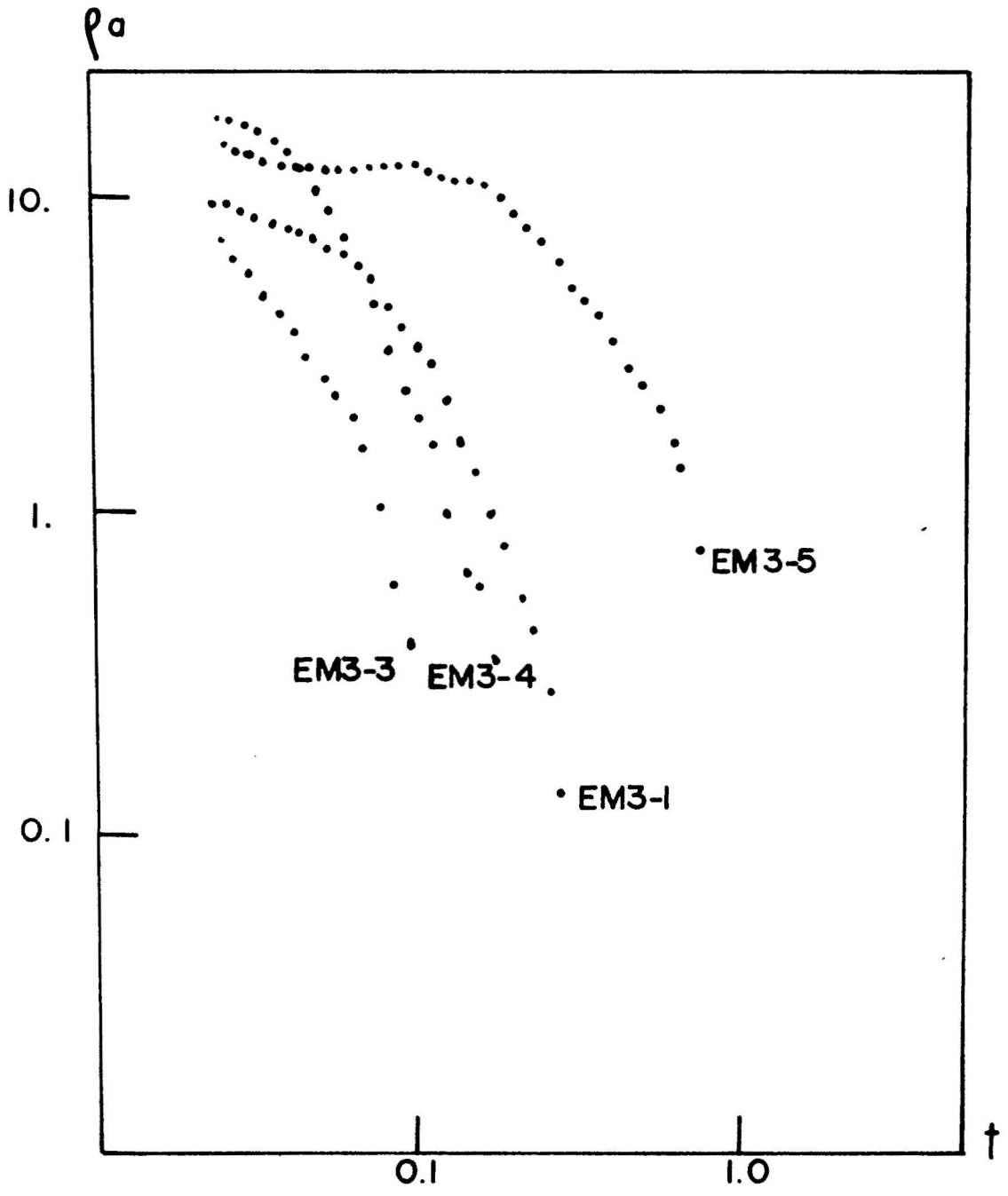
ρa
10.
1.
0.1
EM3-5
EM3-3
EM3-4
EM3-1
0.1
1.0
t

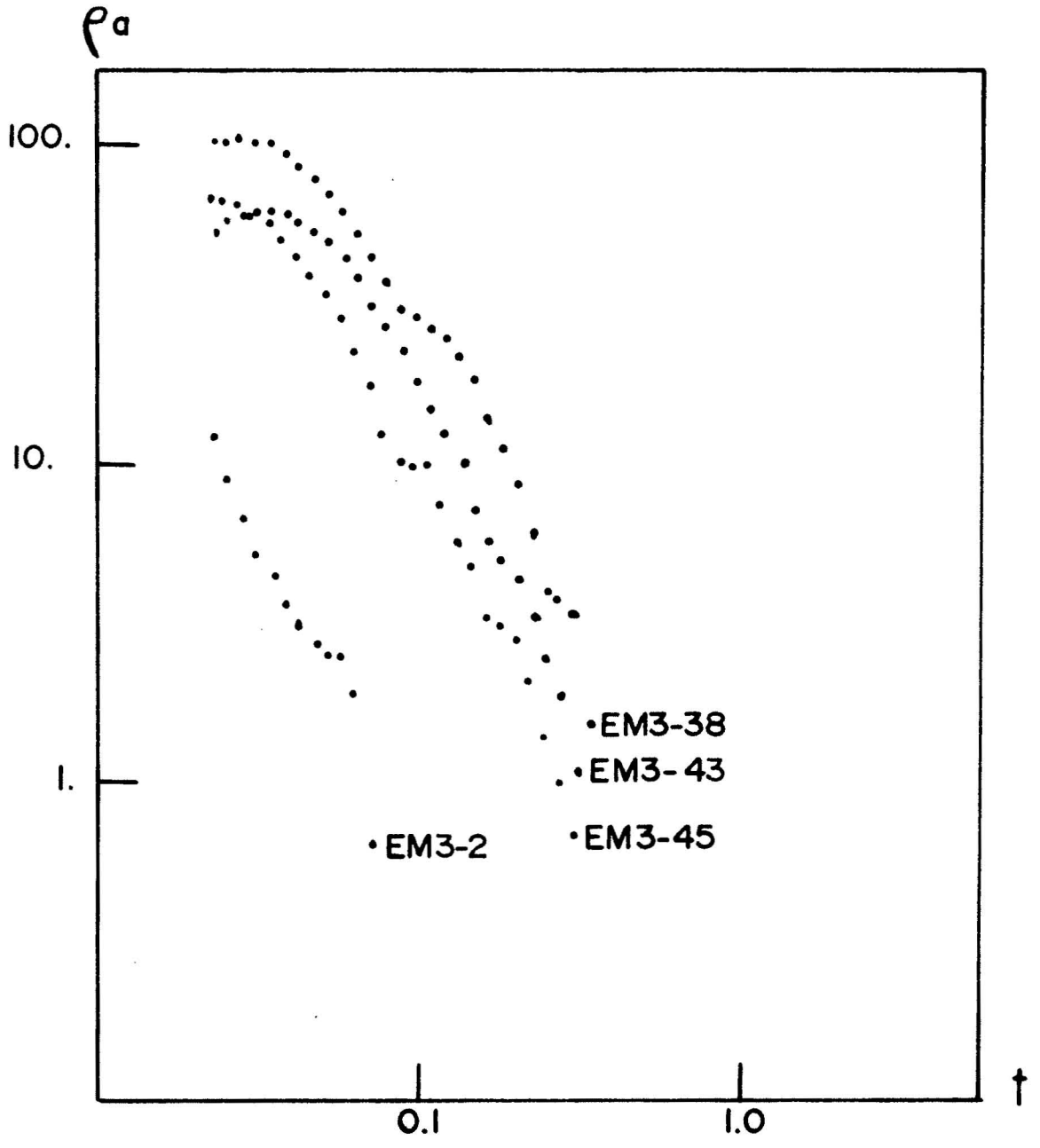
ρa
100.
10.
1.
EM3-38
EM3-43
EM3-45
EM3-2
0.1
1.0
t

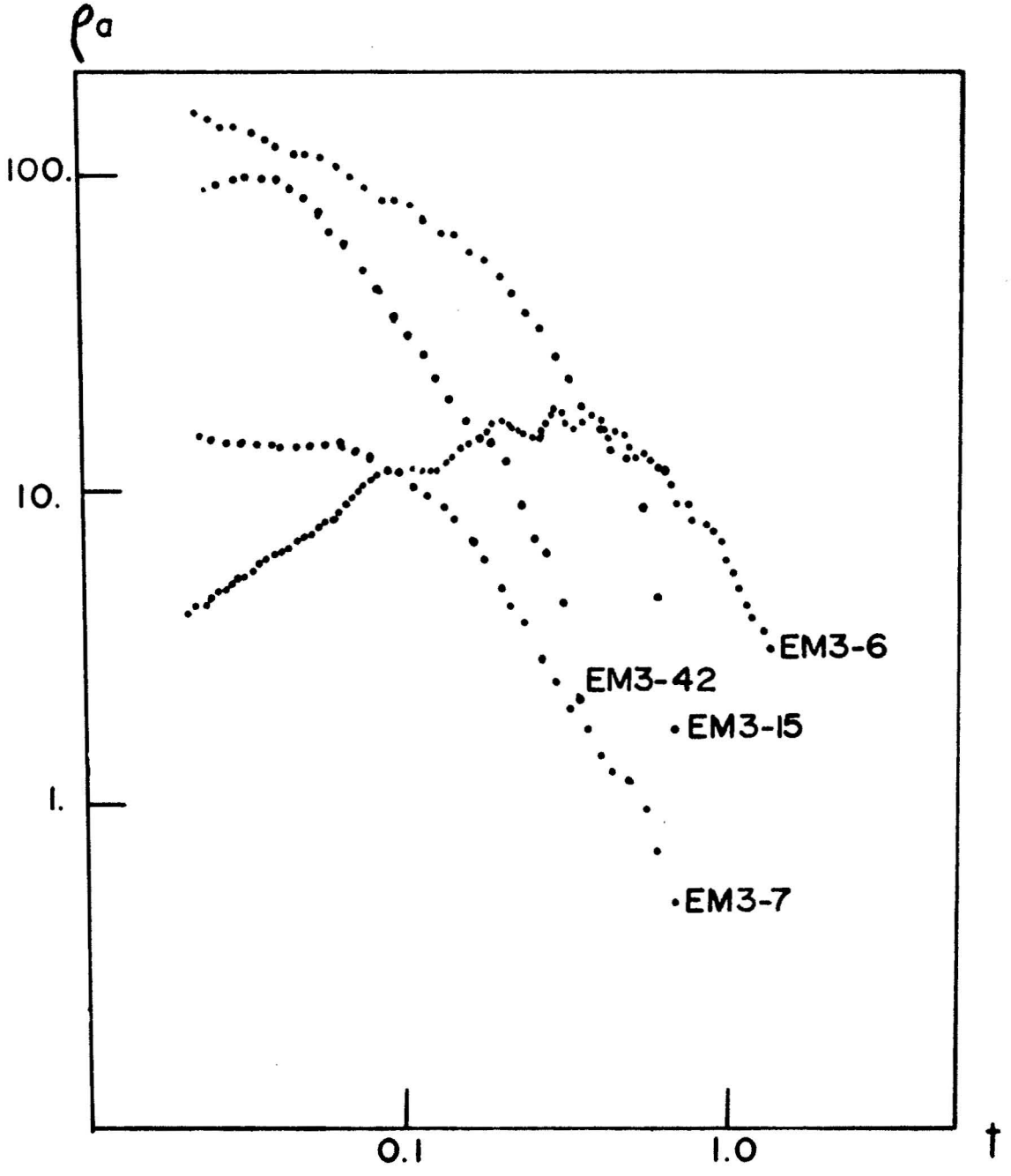
ρa
100.
10.
1.
EM3-6
EM3-42
EM3-15
EM3-7
0.1
1.0
t

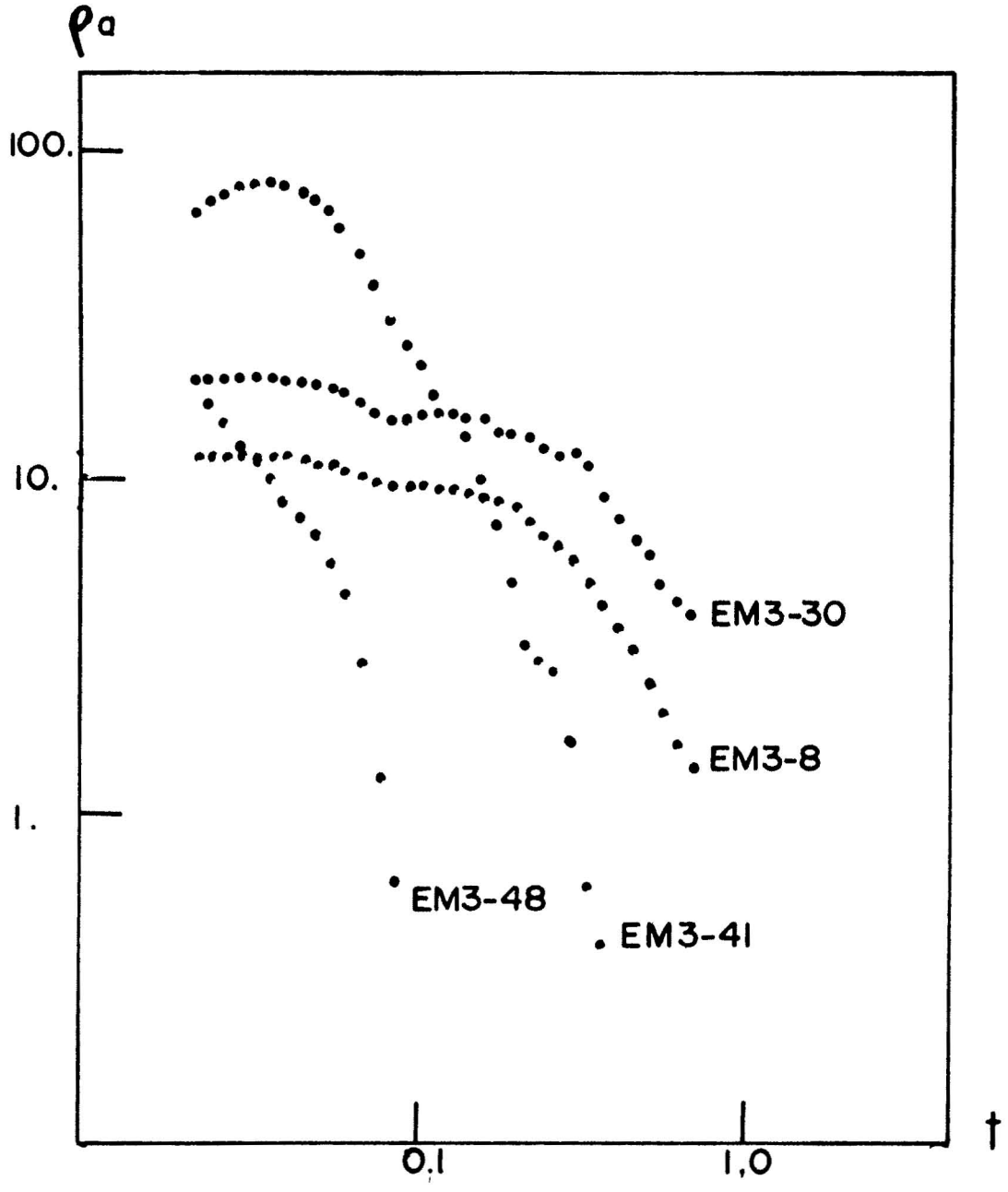
ρa
100.
10.
1.
EM3-30
EM3-8
EM3-48
EM3-41
0.1
1.0
t

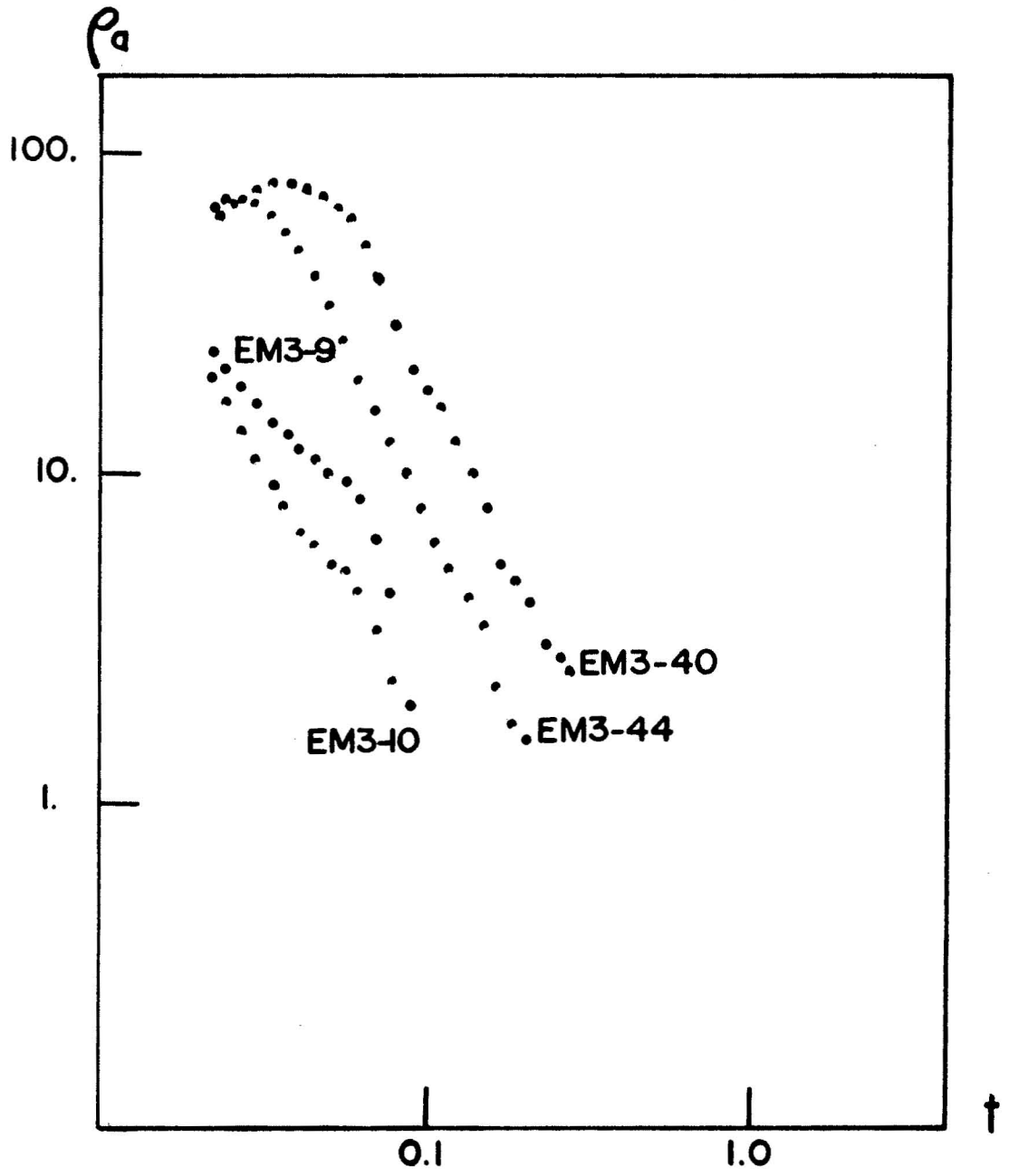
Pa
100.
10.
1.
EM3-9
EM3-40
EM3-10
EM3-44
0.1
1.0
t

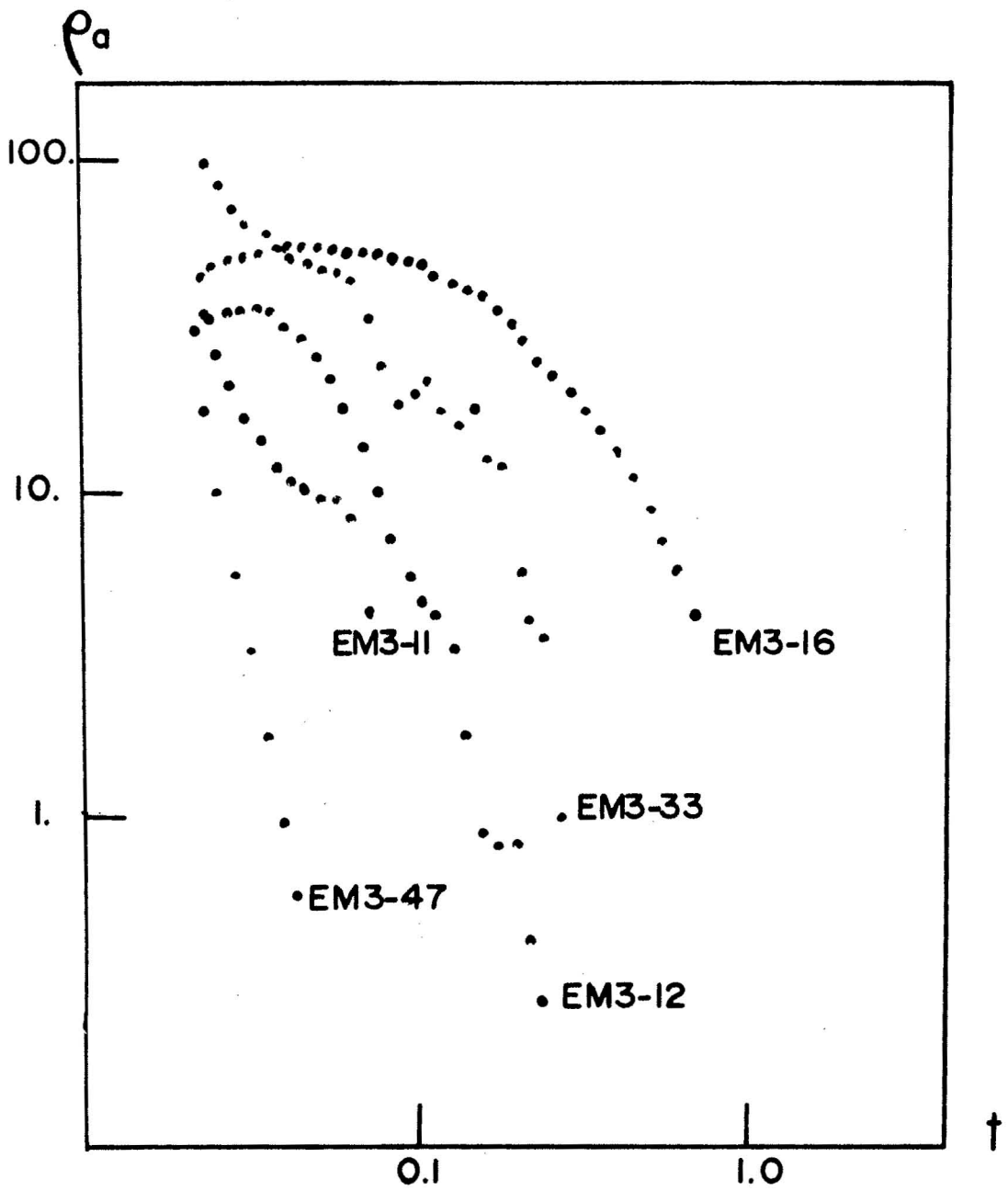
ρa
100.
10.
1.
EM3-11
EM3-16
EM3-33
EM3-47
EM3-12
0.1
1.0
t

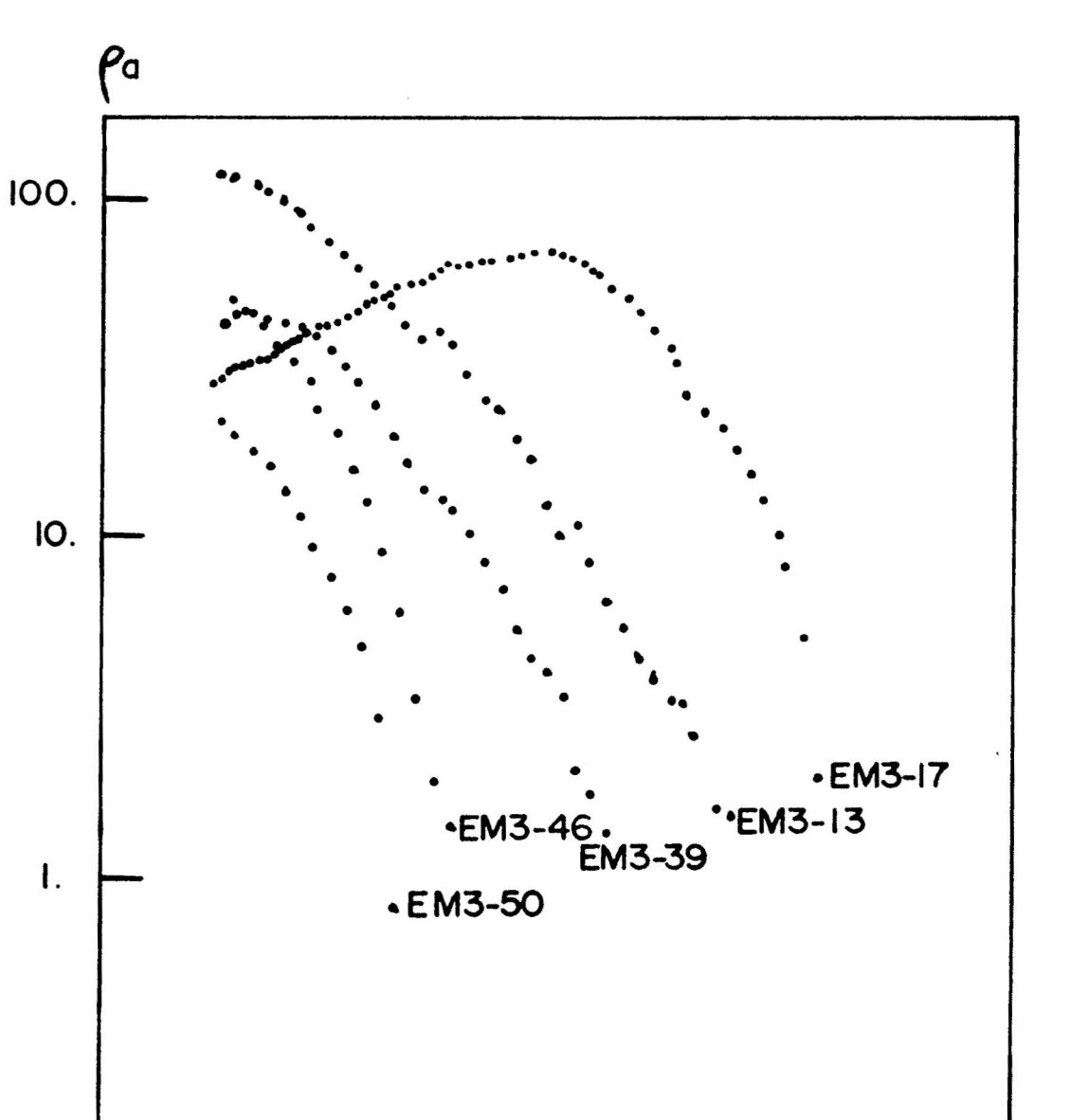
ρa
100.
10.
1.
EM3-17
EM3-13
EM3-46
EM3-39
EM3-50
0.1
1.0
t

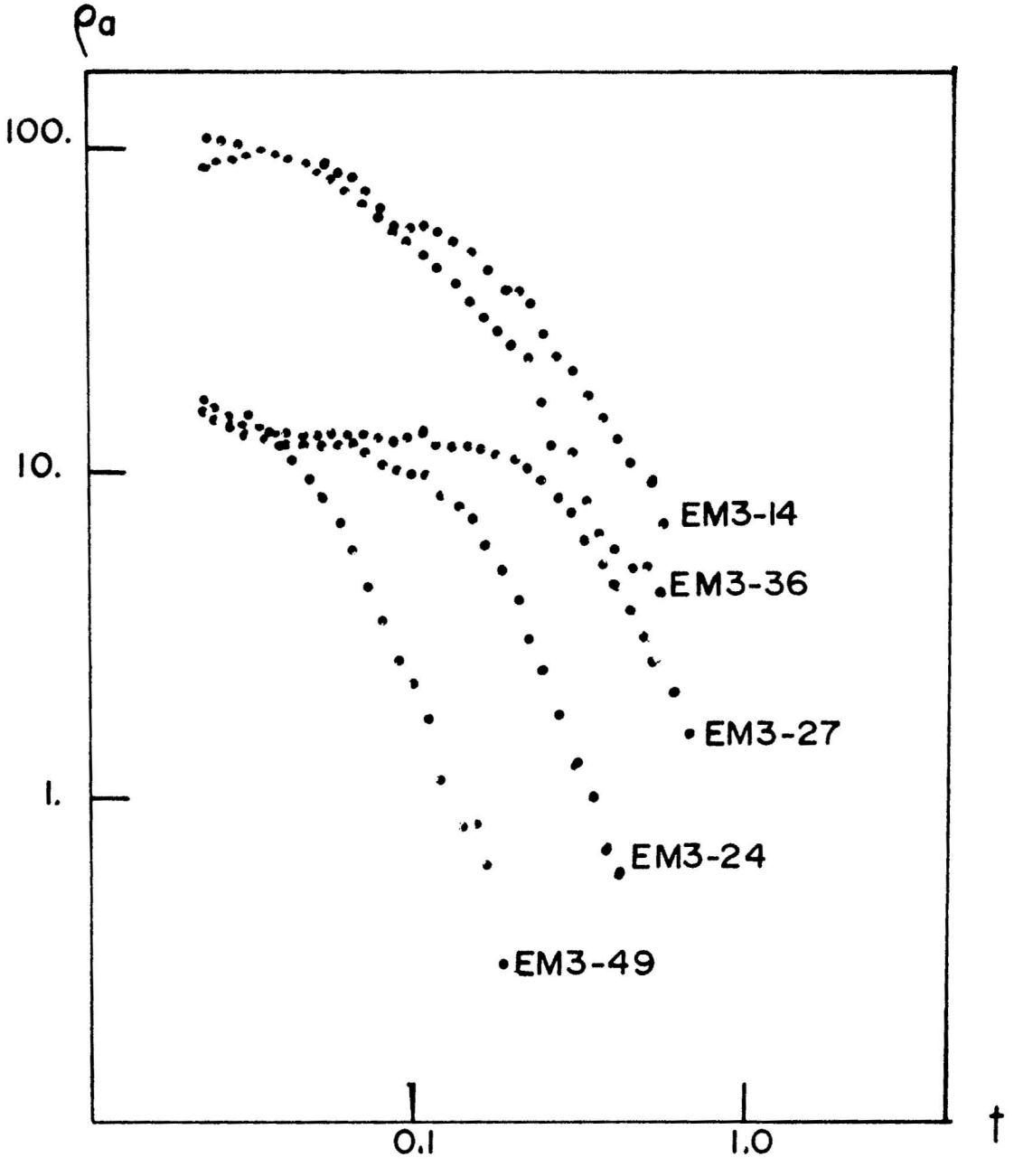
ρa
100.
10.
1.
EM3-14
EM3-36
EM3-27
EM3-24
EM3-49
0.1
1.0
t

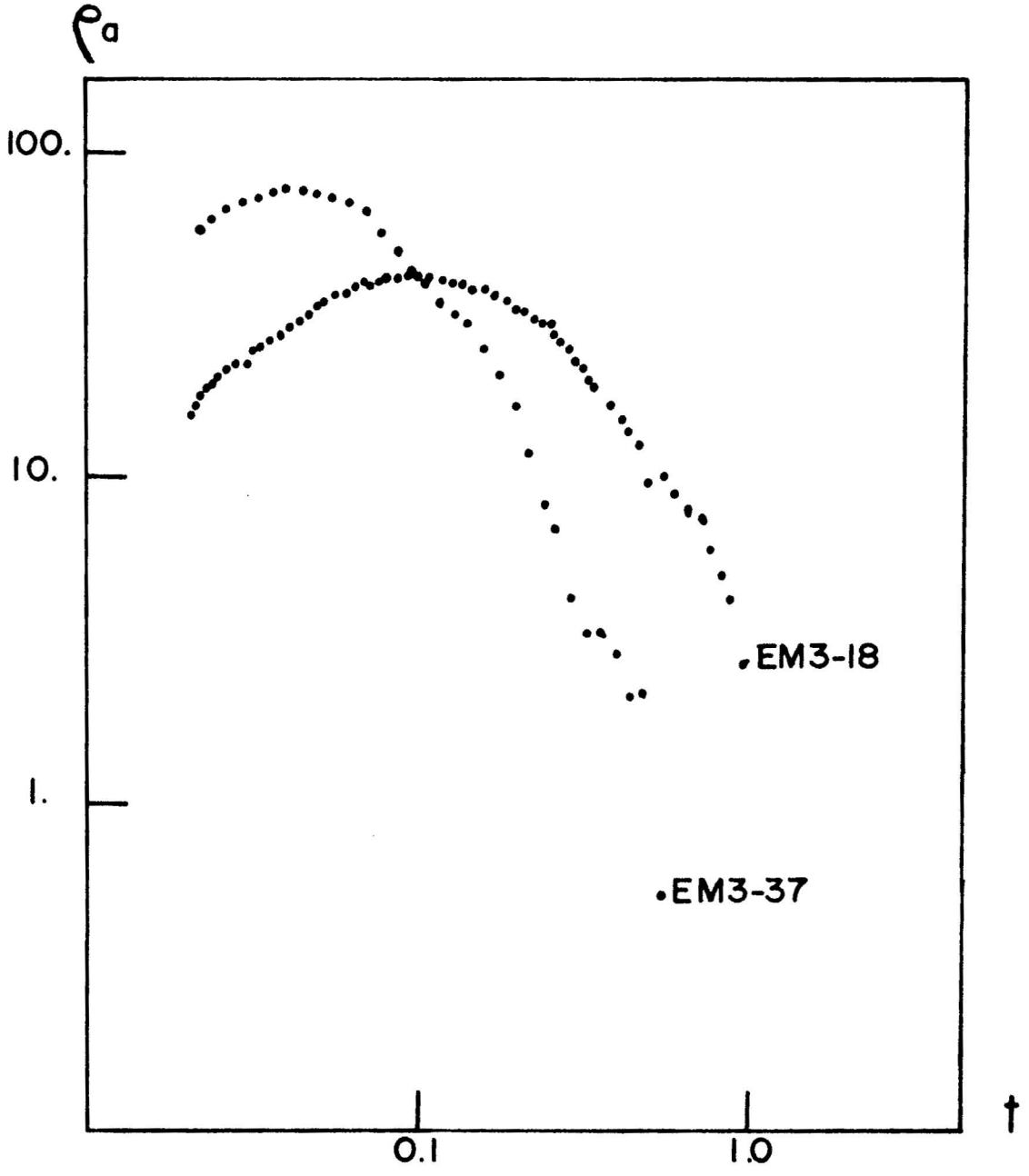
ρa
100.
10.
1.
EM3-18
EM3-37
0.1
1.0
t

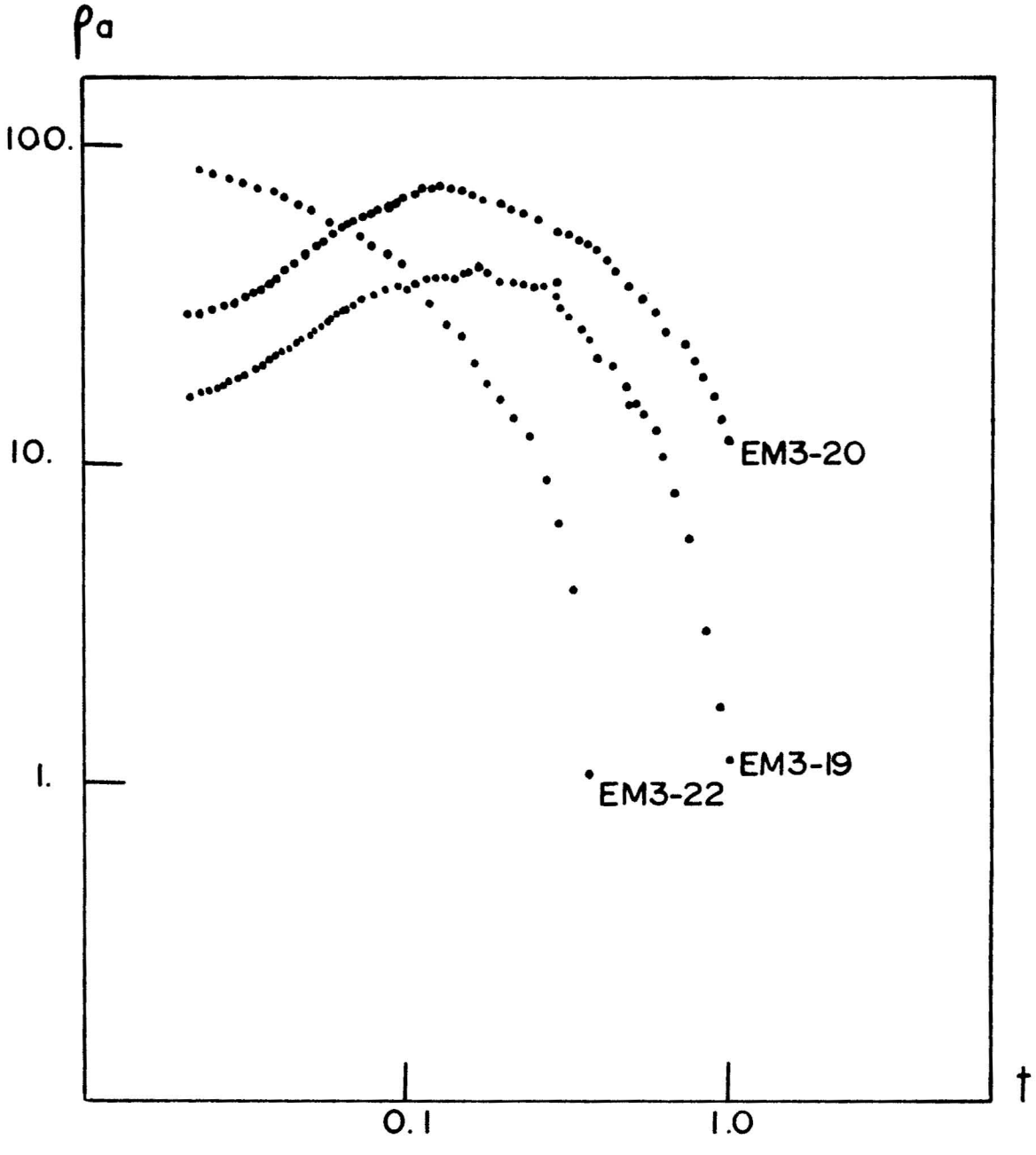
ρa
100.
10.
1.
EM3-20
EM3-19
EM3-22
0.1
1.0
t

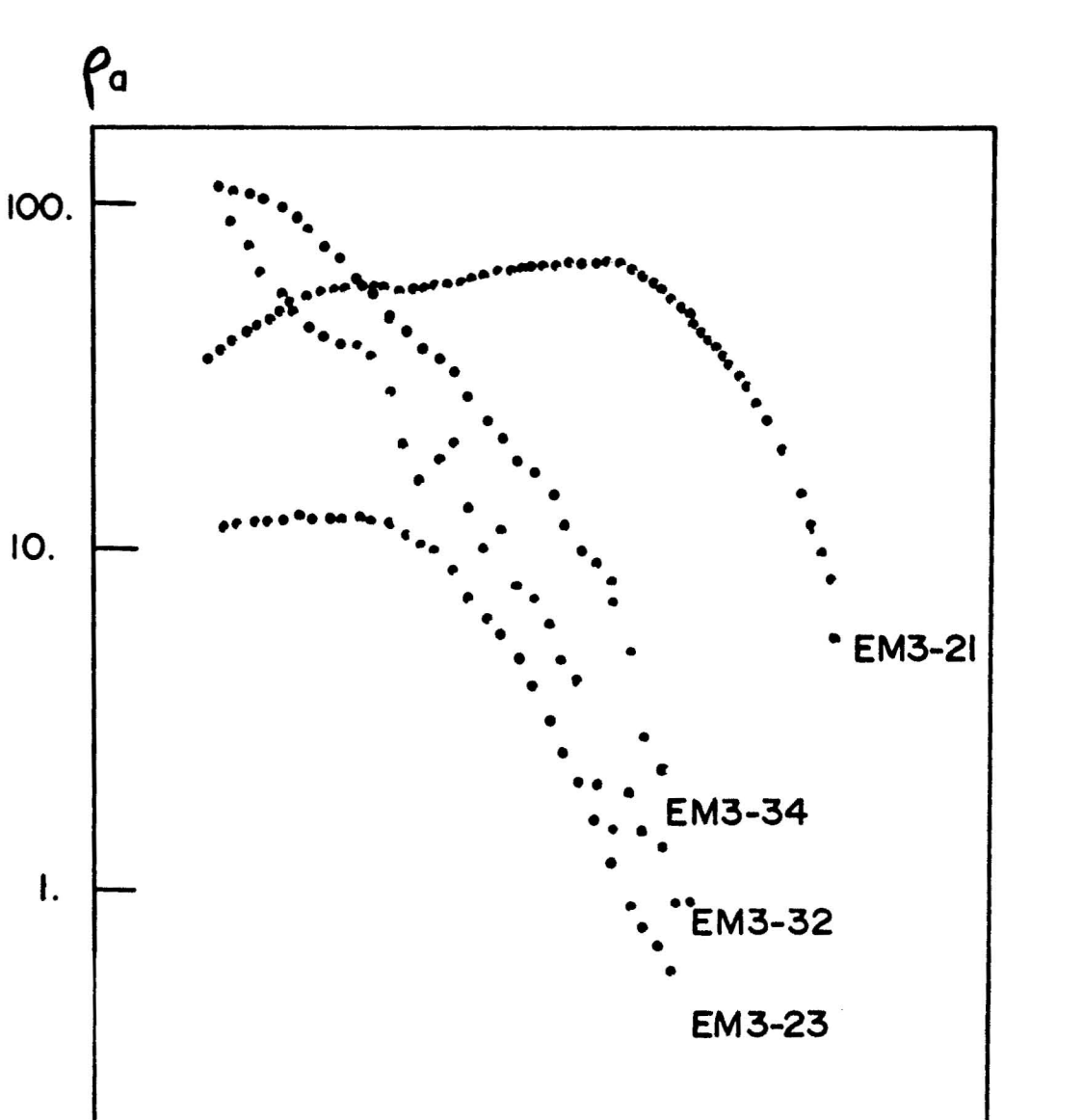
ρa
100.
10.
1.
EM3-21
EM3-34
EM3-32
EM3-23
0.1
1.0
't

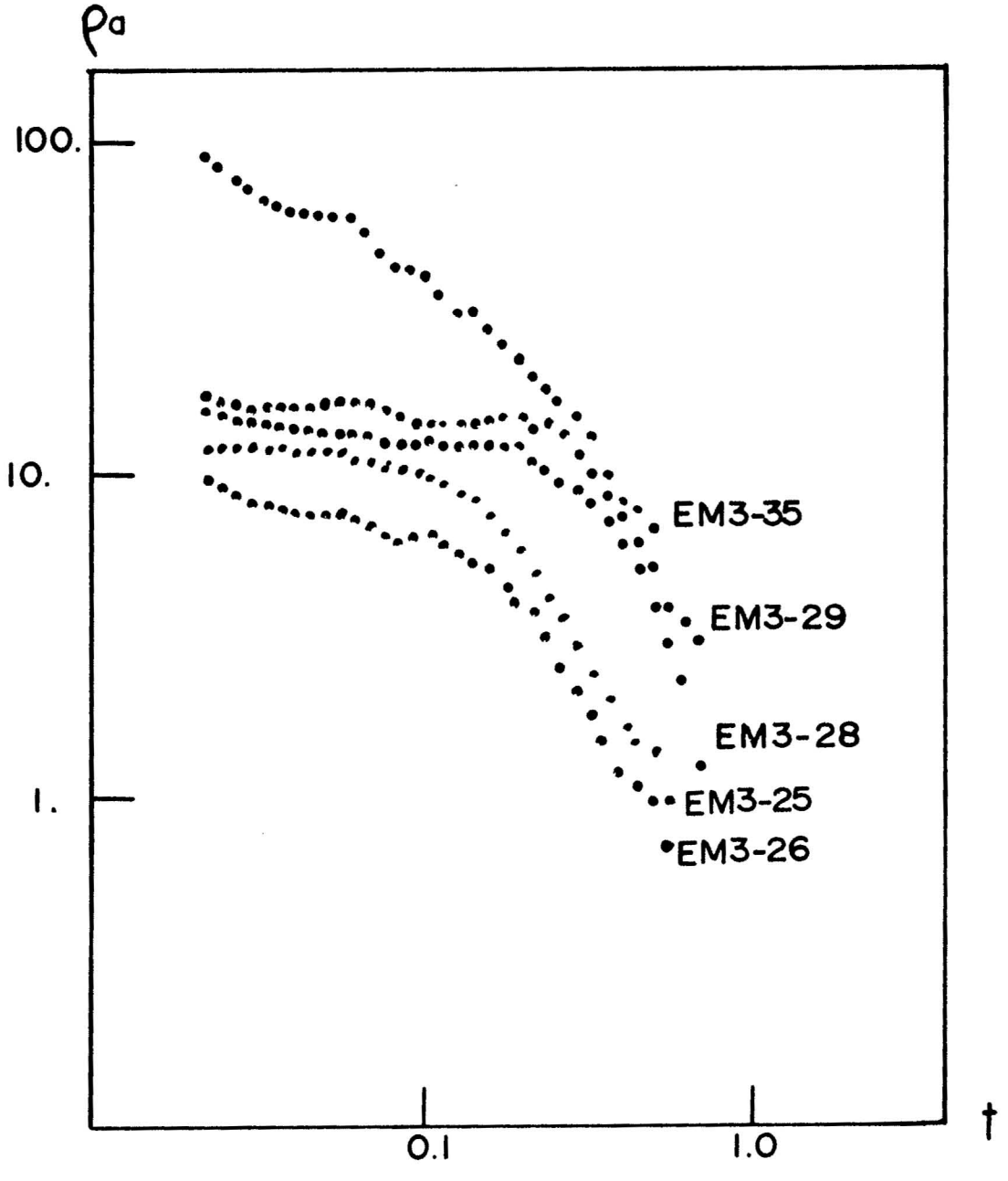
ρa
100.
10.
1.
EM3-35
EM3-29
EM3-28
EM3-25
EM3-26
0.1
1.0
t

APPENDIX C -

CATALOG OF INTERPRETATION COMPUTER PROGRAMS

This catalog contains six computer programs used for time-domain electromagnetic data reduction and interpretation. Preceding each FORTRAN IV program listing is a flow diagram which summarizes the logic.

Program	Purpose
SYSTEM.F4	This program reads in the digitized step-response and prints out a Fourier transform of the response. (Programmed by G. V. Keller).
STACK2.F4	This program: 1) reads in digitized signals and stacks them when necessary, 2) reads in the output of SYSTEM.F4 and removes the step-response of the recording system from the stacked signal through deconvolution, 3) smooths the deconvolved signal, and 4) converts the smoothed, deconvolved voltages to apparent resistivities. (Programmed by G. V. Keller).
TRANS.F4	This program reads in frequencies and the real part of the frequency function, and transforms the function to the time domain using a polygonal-approximation cosine transform method. For this study, this program was used to convert theoretical frequency-domain curves to the time domain for curve matching in the time domain.
ITRAN.F4	This program reads in a time function and transforms the function using a polygonal-approximation transform method. The real part of the frequency function is printed out. For this study, this program was used to convert the deconvolved field

curves to the frequency domain for curve matching in the frequency domain and for use in the program EMINT.F4.

EMFWD.F4 This program reads in geometric parameters and a layered earth model and calculates the real part of the frequency function for line-loop coupling. (Programmed by J. J. Daniels).

EMINT.F4 This program reads in an observed frequency domain curve (real part of line-loop coupling) and a layered earth model. Adjustments are made to the model to find a good fit to the observed curve. (Programmed by J. J. Daniels).

FLOW FOR SYSTEM.F4

1-- Read in number of digitized points (NUM) and sampling interval (DT)

2-- Read in digitized points from step response (Y_k)

3-- Calculate a "frequency" $=(\pi/NUM)*(i)$, $i=1$

4-- Calculate real part of transform for that "frequency"

$$AR_i = \sum_{k=1}^{NUM} Y_k * C_{k+1}$$

where $C_{k+1} = C_k*\cos(\omega) - S_k*\sin(\omega)$

$C_1 = \cos(\omega)$

$S_1 = \sin(\omega)$

5-- Calculate the imaginary part of the transform for that "frequency"

$$AI_i = \sum_{k=1}^{NUM} Y_k * S_{k+1}$$

where $S_{k+1} = S_k*\cos(\omega) + C_k*\sin(\omega)$

6-- Calculate amplitude and phase correction factors.

$$\text{Amplitude}_i = \frac{(AR_1^2 + AI_1^2)^{\frac{1}{2}}}{(AR_i^2 + AI_i^2)^{\frac{1}{2}}}$$

$$\text{Phase}_i = \pi/2 - \text{Tan}^{-1}\ \frac{AI_i}{AR_i}$$

7-- Increase i by one and repeat steps 3 through 6 until i=NUM, print out each amplitude and phase correction factor.

```
COMMENT SUBROUTINE SYSTEM.F4
      DIMENSION Z(100),Y(100),AR(100),C(100),PHC(100),AI(100),TITL(15)

 3004 CONTINUE
      READ (1,77) NUM,DT
      DO 2  I=1,NUM
    2 READ (1,1) Y(I)
    1 FORMAT(F)
   77 FORMAT(I,F)
        WRITE(2,200) NUM
        IF(Y(1).LT.0.0) GO TO 1400
        IF(NUM.LT.21) GO TO 1300
 1300 CONTINUE
        M=NUM
      DO 3008 J=1,M

      DW=3.1416*FLOAT(J)/FLOAT(M)

      C1=COS(DW)

      S1=SIN(DW)

      S2=S1

      C2=C1

      AR(J)=0

      AI(J)=0

      DO 3007 K=1,M

      AR(J)=AR(J)+Y(K)*C2

      AI(J)=AI(J)+Y(K)*S2

      C3=C2*C1-S2*S1

      S3=S2*C1+C2*S1

      S2=S3
```

```
3007 C2=C3

3008 AI(J)=-AI(J)

     AMP=SQRT(AR(1)*AR(1)+AI(1)*AI(1))

     DO 3009 I=1,M,2

     AM=SQRT(AR(I)*AR(I)+AI(I)*AI(I))

     PH=ATAN2(AI(I),AR(I))

     C(I)=AMP/FLOAT(I)/AM

     PHC(I)=1.5708-PH

3009 CONTINUE

     DO 16 I=1,M

     WRITE(2,3001) C(I),PHC(I)
  16 CONTINUE
1400 CONTINUE
       IF(Y(1).LT.0.0) WRITE(2,400)
 100 FORMAT(15A5)
 200 FORMAT(I3)
 300 FORMAT(20F4.0)
 400 FORMAT(' -1')
3001 FORMAT(2E12.5)

     STOP

     END
```

FLOW FOR STACK2.F4

1-- Read in # data points, type of measurement, digitizing interval.

2-- Read in the output of SYSTEM.F4.

3-- Read in title and R, source length, current, and source/receiver angle.

4-- Read in a scaling factor.

5-- Read in voltages for each transient and count the number of transients.

6-- Average each time value for all the transients and calculate a standard deviation.

7-- Test to see if each value is within two standard deviations of the average. Reject values which are not.

8-- Calculate early and late resistance (values not necessary for this interpretation technique).

9-- Print time, # of signals included in the final stack, average, standard deviation, and late and early R.

10--Calculate a geometric factor and store.

11--Convert time signal to amplitude and phase as described in SYSTEM.F4.

12--Remove the step response of the recording system by multiplying the amplitude and amplitude correction factors and by adding the phase and phase correction factors.

13--Reverse the transform process to give deconvolved voltages and times.

14--Make time evenly spaced on a log plot.

15--Use Lagrangian interpolation to find voltages on the

equally-spaced log plot.

16--Replace v with log(v)and t with log(t).

17--Apply a three point ($\frac{1}{2}$,1, $\frac{1}{2}$) weighted average for initial smoothing.

18-- Do a seven-point average for each point to smooth the data.

19--Convert log(t) back to t and log(v) back to v.

20--Multiply voltages by a geometric factor ($2\pi R^4/3AILcos\theta$) to give apparent resistivities.

21--Also calculate ρ_{late}, Δ depth, and Δ conductance which are not used here.

22--Print time, ρ_a, ρ_{late}, Δ depth, and Δ conductance.

```
COMMENT FILE K7,F4 IS INTENDED FOR STACKING OF EM TRANSIENTS
COMMENT        INDEX1 IS NEGATIVE FOR WIRE TO WIRE COUPLING
COMMENT        INDEX1 IS ZERO FOR WIRE TO LOOP COUPLING
COMMENT        INDEX1 IS POSITIVE FOR LOOP TO LOOP COUPLING
COMMENT       FOR01.DAT IS THE FILE FOR INPUT DATA
COMMENT       FOR02.DAT IS THE FILE FOR INPUT DATA
COMMENT       FOR03.DAT IS THE FILE WITH SYSTEM RESPONSE
COMMENT       FOR07.DAT IS THE FILE FOR PLOTTER OUTPUT
COMMENT PROGRAM K7 CALLS K1003 AND K1005 AS SUBPROGRAMS
      DIMENSION XX(20),X(20,100),A5(16),N(100),AV2(100),S(100),
     1A3(6),AV(100),RLATE(100),REARLY(100),Y2(100),C(100)
     2,PHC(100)
      I1=1
      I4=7
      I2=2
      I3=3
      READ (I1,1019) NPNT,INDEX1,DT
      DO 605 I=1,NPNT
  605 READ (I3,606) C(I),PHC(I)
  606 FORMAT(2E12.5)
 1019 FORMAT(I3,I2,F10.0)
 9999 READ (I1,1000) (A5(I),I=1,16)
 1000 FORMAT(16A5)
      WRITE (I2,1001) (A5(I),I=1,10)
 1001 FORMAT(1H1,2X,'ELECTROMAGNETIC INTERPRETATION:
     2EDITED STACKING, OBSERVED VOLTAGES',//,2X,10A5)
      READ(I1,1005)R,A1,A2,CUR,THETA,BETA,(A3(II),II=1,6)
 1005 FORMAT(6F,6A5)
      WRITE(I2,971) R
  971 FORMAT(1X,'OFFSET DISTANCE IS ',F6.0,' METERS')
      WRITE(I2,972) A1
  972 FORMAT(1X,'LOOP AREA IS ',F6.4,' SQUARE KILOMETERS')
      WRITE (I2,973) A2
  973 FORMAT(1X,'SOURCE LENGTH IS ',F5.0,' METERS')
      WRITE (I2,974) CUR
  974 FORMAT(1X,'CURRENT IS ',F5.1,' AMPERES')
      WRITE (I2,975) THETA
  975 FORMAT(1X,'DEFLECTION ANGLE IS ',F4.1,'DEGREES')
      READ(I1,1009) (XX(I),I=1,3)
 1009 FORMAT(2F4.0,F5.0)
      SCALE=XX(3)/(XX(2)-XX(1))
      WRITE (I2,1006) SCALE
 1006 FORMAT(2X,'DIGITIZING SCALE IS ',F7.3,'MICROVOLTS/DIV')
      NCASE=1
      SCALE=ABS(SCALE)
    2 NPNT=0
    3 CONTINUE
      READ(I1,1002) (XX(I),I=1,20)
      IF(XX(1)+100.) 7,8,9
    9 DO 10 I=1,20
      NPNT=NPNT+1
   10 X(NCASE,NPNT)=XX(I)
      GO TO 3
    8 CONTINUE
      NCASE=NCASE+1
      GO TO 2
    7 CONTINUE
      IF(INDEX1)20,21,21
   20 N4=NPNT-1
      DO 22 I=1,NPNT
```

```
      DO 22 J=1,NCASE
   22 X(J,I)=(X(J,I)-X(J,1))*SCALE*.000001
      DO 24 I=1,NCASE
      IF(X(I,3)) 25,24,24
   25 DO 27 J=1,NPNT
   27 X(I,J)=-X(I,J)
   24 CONTINUE
      GO TO 34
   21 CONTINUE
 1002 FORMAT(20F4.0)
      DO 32 I=2,NPNT
      DO 32 J=1,NCASE
   32 X(J,I)=X(J,I)-X(J,1)
      DO 33 I=2,NPNT
      DO 33 J=1,NCASE
   33 X(J,I)=X(J,I)*SCALE*.000001
      DO 34 I=1,NCASE
      IF(X(I,3))35,36,36
   35 DO 37 J=2,NPNT
   37 X(I,J)=-X(I,J)
   36 CONTINUE
   34 CONTINUE
      Z=FLOAT(NCASE)
      DO 310 JPNT=2,NPNT
      AV(JPNT)=0
      DO 309 JCASE=1,NCASE
  309 AV(JPNT)=AV(JPNT)+X(JCASE,JPNT)
  310 AV(JPNT)=AV(JPNT)/Z
      DO 312 JPNT=2,NPNT
      S(JPNT)=0
      DO 311 JCASE=1,NCASE
  311 S(JPNT)=S(JPNT)+(X(JCASE,JPNT)-AV(JPNT))**2
  312 S(JPNT)=SQRT(S(JPNT)/Z)
      WRITE(I2,1007)
      DO 315 JPNT=2,NPNT
      N(JPNT)=0
      AV2(JPNT)=0
       TEST1=2.*S(JPNT)
      DO 322 JCASE=1,NCASE
      TEST2=ABS(X(JCASE,JPNT)-AV(JPNT))
 1007 FORMAT(//2X,'EDITED AND STACKED DATA'//,
     25X,'TIME',3X,'NUMBER',4X,'AVERAGE',6X,'ST. DEV.',
     3 5X,'EARLY R',4X,'LATE R')
       IF(TEST2-TEST1)321,321,322
  321 AV2(JPNT)=AV2(JPNT)+X(JCASE,JPNT)
      N(JPNT)=N(JPNT)+1
  322 CONTINUE
  315 AV2(JPNT)=AV2(JPNT)/FLOAT(N(JPNT))
      CALL K10P1(R,A1,A2,CLR,THETA,BETA,INDEX1,FACTOR,SCALE
     2,XPNT1,XPT2)
      DO 333 JPNT=2,NPNT
  800 FORMAT(12X,'INDEX1=',I,/)
      IF(INDEX1) 601,602,602
  601 DCLEV=(AV2(NPNT-4)+AV2(NPNT-3)+AV2(NPNT-2))/3.
      REARLY(JPNT)= FACTOR*(AV2(JPNT)-DCLEV)
      RLATE(JPNT)= SCALE/(((AV2(JPNT)-DCLEV)*FLOAT(JPNT-1)
     1*DT)**XPNT1)
      GO TO 603
  602 CONTINUE
      REARLY(JPNT)=FACTOR*AV2(JPNT)
```

```
      RLATE(JPNT)=SCALE/(AV2(JPNT)*(FLOAT(JPNT-1)*DT)**XPNT1)
  603 CONTINUE
      IF(RLATE(JPNT))334,334,335
  334 RLATE(JPNT)=0
      GO TO 333
  335 RLATE(JPNT)=RLATE(JPNT)**XPT2
  333 CONTINUE
        DO 101 JPNT=2,NPNT
      TIME=FLOAT(JPNT-1)*DT
      WRITE(I2,1008) TIME,N(JPNT),AV2(JPNT),S(JPNT),REARLY
     2(JPNT),RLATE(JPNT)
 1008 FORMAT(3X,F4.2,4X,I2,4(4X,E10.3))
  101 CONTINUE
      CALL K1003(AV2,NPNT,Y2,C,PHC)
      IF(INDEX1) 701,702,702
  701 DO 704 J=2,NPNT
      DCOLEV=(Y2(NPNT-4)+Y2(NPNT-3)+Y2(NPNT-2))/3.
  704 Y2(J)=Y2(J)-DCOLEV
  702 CONTINUE
      DO 401 I=2,NPNT
      TIME=FLOAT(I-1)*DT
      R1=FACTOR*Y2(I)
      R2=SCALE/(Y2(I)*TIME**XPNT1)
      IF(R2)402,402,403
  402 R2=0
      GO TO 404
  403 R2=R2**XPT2
  404 CONTINUE
  401 CONTINUE
      WRITE(I2,1015) (A5(I),I=1,10)
      DO 501 JPNT=30,NPNT
  501 Y2(JPNT)=AV2(JPNT)
      N3=NPNT-1
      DO 502 JPNT=1,N3
  502 Y2(JPNT)=Y2(JPNT+1)
 1015 FORMAT(//////,2X,10A8)
      CALL K1005(Y2,NPNT,DT,FACTOR,SCALE,2.5,.667,A3)
       GO TO 9999
      STOP
      END
COMMENT PROGRAM TO GNERATE GEOMETRIC FACTORS
C
C
C*************************************************************
      SUBROUTINE K1001(R,A1,A2,CUR,THETA,BETA,INDEX1,FACTOR
     2,SCALE,XPNT1,XPT2)
      IF(INDEX1)10,20,30
   10  XPNT1=1.5
      XPT2=2.0
      X=40.
      SCALE=X**1.5*1.E-12*CUR*A1*A2/12.
      FACTOR=(6.2832*R**3*COS(BETA/57.3))/((3.*SIN(THETA/57.3)**2
     2-2.)*CUR*A1*A2)
      GO TO 100
   20 XPNT1=2.5
      A1=A1*1000000.
      XPT2=.667
      FACTOR=6.2832*R**4/(A1*A2*CUR*COS(THETA/54.))/3.
      SCALE=A1*A2*CUR*.0793E-17
     2*R
```

```
      GO TO 100
   30 XPNT1=2.5
      A1=A1*1000000.
      A2=A2*1000000.
      XPT2=.667
      SCALE=CUR*A1*A2*15.9E-18
      FACTOR=6.2832*R**5*COS(BETA/54.)/9./CUR/A1/A2
  100 CONTINUE
      RETURN
      END
COMMENT SUBROUTINE DECON2
C       C IS THE AMPLITUDE CORRECTION FACTOR
C       PHC IS THE PHASE CORRECTION FACTOR
C       X IS THE STEP RESPONSE FUNCTION
C       NPNT IS THE NUMBER OF POINTS
C*************************************************************
      SUBROUTINE K1003 (X,NPNT,Y2,C,PHC)
            DIMENSION C(100),PHC(100),X(100),A(100),B(100),
     2PHX(100),V(100),Y2(100)
      X(1)=0.
      NUMBER=NPNT
      DO 7 J=1,NUMBER
      W=3.1416*FLOAT(J)/FLOAT(NUMBER)
      C1=COS(W)
      S1=SIN(W)
      C2=C1
      S2=S1
      A(J)=0
      B(J)=0
      DO 6 K=1,NUMBER
      A(J)=A(J)+X(K)*C2
      B(J)=B(J)+X(K)*S2
      C3=C2*C1-S2*S1
      S3=C2*S1+S2*C1
      C2=C3
      S2=S3
    6 CONTINUE
      B(J)=-B(J)
      PHX(J)=ATAN2(B(J),A(J))
      V(J)=SQRT(A(J)*A(J)+B(J)*B(J))
    7 CONTINUE
      DO 8 I=1,NUMBER,2
      V(I)=V(I)*C(I)
      PHX(I)=PHX(I)+PHC(I)
      A(I)=V(I)*COS(PHX(I))
    8 B(I)=V(I)*SIN(PHX(I))
      M2=NUMBER-1
      DO 3012 I=2,M2,2
      I2=I-1
      I3=I+1
      A(I)=(A(I2)+A(I3))/2.
 3012 B(I)=(B(I2)+B(I3))/2.
      DO 10 J=1,NUMBER
      W=3.1416*FLOAT(J)/FLOAT(NUMBER)
      C1=COS(W)
      S1=SIN(W)
      C2=C1
      S2=S1
      Y2(J)=0
      DO 9 K=1,NUMBER
```

```
      Y2(J)=Y2(J)+B(K)*S2
      C3=C2*C1-S2*S1
      S3=C2*S1+S2*C1
      C2=C3
      S2=S3
    9 CONTINUE
      Y2(J)=Y2(J)/FLOAT(NUMBER)*2.
   10 CONTINUE
      RETURN
COMMENT SUBROUTINE TO CONVERT A TRANSIENT TO THE LOG DOMAIN
C      AND SMOOTH.
      END
C      V IS THE TRANSIENT
C      NPNT IS THE NUMBER OF POINTS IN THE TRANSIENT AT FIRST
C      DELTAT IS THE DIGITIZING INTERVAL IN SECONDS
C      FACTOR IS THE EARLY TIME GEOMETRIC FACTOR
C      SCALE IS THE LATE TIME GEOMETRIC FACTOR
C       XPNT1 IS THE EXPONENT ON TIME FOR LATE RESISTIVITY
C       XPT2 IS THE ROOT FOR LATE RESISTIVITY
C        WIRE/LOOP  XPNT1=2.5, XPT2=.6667, CALL K1006
C        WIRE/WIRE  XPNT1=1.5, XPT2=.6667, CALL K1007
C        LOOP/LOOP
C*************************************************************
      SUBROUTINE K1005(V,NPNT,DELTAT,FACTOR,SCALE,XPNT1,XPT2,A5)
      DIMENSION V(100),T(100),X(400),Y1(100),A5(10)
     1,ABCD(16)
     1,SINT(100),DELTA(100)
      I22=2
      I44=7
      NUMBER=NPNT-1
      DO 1 I=1,NPNT
    1 T(I)=FLOAT(I)*DELTAT
      SHIFT=0
      VMAX=V(1)
      VMIN=VMAX
      DO 710 I=2,NUMBER
      IF(V(I)-VMIN)702,702,701
  701 VMAX=V(I)
  702 IF(V(I)-VMIN)703,710,710
  703 VMIN=V(I)
  710 CONTINUE
      SHIFT=0
      IF(VMIN) 711,713,713
  711 SHIFT=.01*(VMAX-VMIN)-VMIN
      DO 712 I=1,NUMBER
  712 V(I)=V(I)+SHIFT
  713 CONTINUE
      DT=ALOG(T(NUMBER)/T(NUMBER-1))
      RANGE=ALOG(T(NUMBER)/T(1))
      NEED =AINT(RANGE/DT)
      DO 11 I=1,NUMBER
      T(I)=ALOG(T(I))
   11 V(I)=ALOG(V(I))
      DO 21 I=1,NEED
      XI=FLOAT(I)
      TIME=XI*DT+T(1)-DT*.99
      J=1
   12 IF(TIME-T(J))14,14,13
   13 J=J+1
      IF(J-NUMBER)12,14,14
```

```
   14 J=J+1
      IF(J-2)15,15,16
   15 X(I)=0
      DO 151 K1=1,3
      TERM=V(K1)
      DO 153 K2=1,3
      IF(K1-K2) 154,153,154
  154 TERM=TERM*(TIME-T(K2))/(T(K1)-T(K2))
  153 CONTINUE
  151 X(I)=X(I)+TERM
      GO TO 21
   16 IF(J-NUMBER+2) 18,17,17
   17 X(I)=0
      N1=NUMBER-2
      DO 171 K1=N1,NUMBER
      TERM=V(K1)
      DO 173 K2=N1,NUMBER
      IF(K1-K2) 174,173,174
  174 TERM=TERM*(TIME-T(K2))/(T(K1)-T(K2))
  173 CONTINUE
  171 X(I)=X(I)+TERM
      GO TO 21
   18 X(I)=0
      N1=J-1
      N2=J+1
      DO 181 K1=N1,N2
      TERM=V(K1)
      DO 183 K2=N1,N2
      IF(K1-K2)184,183,184
  184 TERM=TERM*(TIME-T(K2))/(T(K1)-T(K2))
  183 CONTINUE
  181 X(I)=X(I)+TERM
   21 CONTINUE
      N3=NEED-4
      I2=1
      DO 6655 I=4,N3,4
      N4=I-3
               N5=I+3
      Y1(I2)=0
      DO 7655 I3=N4,N5
 7655 Y1(I2)=Y1(I2)+X(I3)
      Y1(I2)=Y1(I2)/7.
 6655 I2=I2+1
      SINT(1)=1./Y1(1)
      DO 6656 I=2,I2
      DELTA(I)=(2.*EXP(FLOAT(4*I+1)*DT+T(1)))/.1256E-09/Y1(I)
      DELTA(I)=SQRT(ABS(DELTA(I)))/100.
      SINT(I)=(DELTA(I)/Y1(I)-DELTA(I-1)/Y1(I-1))/(DELTA(I)-DELTA(I-1))
 6656 CONTINUE
      INDEX1=-1
      INDEX=1
      NCX=3
      NCY=3
      D=3.33
      XZERO=.01
      YZERO=.1
      IFLAG=0
      WRITE(122,1020)
 1020 FORMAT(1H1,2X,'ELECTROMAGNETIC INTERPRETATION:
     2NON-LINEAR FILTERING'//)
```

```
      WRITE(I22,4444)
      WRITE (I44,998)NCX,NCY,D,XZERO,YZERO
      LASTPL=1
      IGRID=1
      IPOS=1
      INEG=2
      WRITE(I44,910)LASTPL,IGRID,IPOS,INEG
  910 FORMAT(4I2)
 4444 FORMAT(3X,'TIME   EARLY    LATE       DELTA       DELTA',/
     211X,'RESIS.   RESIS.      DEPTH      CONDUCTANCE',//)
  998 FORMAT(2I10,3F10.0)
    7 FORMAT(2E12.5)
      DO 911 I8=1,16
  911 ABCD(I8)=0
      WRITE(I44,912) (ABCD(I8),I8=1,16)
  912 FORMAT(16A5)
      WRITE(I44,912) (A5(I),I=1,16)
      WRITE (I44,913) I2
  913 FORMAT(I3)
  997 FORMAT(5A5,I10)
  909 FORMAT(E12.5)
  908 FORMAT(I1)
      DO 7656 I=1,I2
      TIME=EXP(FLOAT(4*I+1)*DT+T(1))
      VOLT=EXP(Y1(I))-SHIFT
      RATIO=FACTOR*VOLT
      IF(VOLT)301,302,302
  301 VOLT=-VOLT
      RHO=(SCALE/(VOLT*TIME**XPNT1))**XPT2
      RHO=-RHO
      GO TO 303
  302 RHO=(SCALE/(VOLT*TIME**XPNT1))**XPT2
  303 CONTINUE
      WRITE (I44,7) TIME,RATIO
 7656 WRITE (I22,7657) TIME,RATIO,RHO,DELTA(I),SINT(I)
 7657 FORMAT(5X,F6.3,2(5X,F6.2),2(3X,E10.3))
      RETURN
      END
```

FLOW FOR TRANS.F4

1-- Read in resistivities and thicknesses for three layers.

2-- Read in I number of frequencies (W) and corresponding real part (XX) of the frequency function.

3-- Calculate the zero-time value:

$$F_{zero} = \sum_{n=1}^{I-1} 1/\pi \; (XX_{n+1} - XX_n)(W_{n+1} - W_n)$$

4-- Calculate the time-curve from time, t, = 0.0001 to time, t, = 1000.

$$F_j = \sum_{n=1}^{I-1} 2/(\pi t^2) \; \frac{XX_j - XX_{j+1}}{W_{j+1} - W_j} \; (\mathrm{Cos}W_j t - \mathrm{Cos}W_{j+1} t)$$

5-- Calculate the step response by replacing XX_j with $-XX_j/W_j$ and repeat steps 3 and 4.

6-- Print out time and corresponding transform function and step-response function.

```
C:::::::::::::::::::::::::::::::::::::::::::::::::::::::::::::::::::::::::::
C       THIS PROGRAM CALCULATES THE COSINE TRANSFORM OF THE REAL PART
C  OF ANY FUNCTION. A POLYGONAL-APPROXIMATION TRANSFORM
C  METHOD IS USED.  THE STEP RESPONSE IS ALSO CALCULATED.
C:::::::
C  INPUT FILE -- FOR01.DAT      OUTPUT FILE -- FOR02.DAT
C:::::::::::::::::::::::::::::::::::::::::::::::::::::::::::::::::::::::::::
      DIMENSION R(25),D(25),XX(200),YY(200),W(200),F(200),S(200)
      READ(1,101)R(1),D(1),R(2),D(2),R(3)
102   FORMAT(3(3X,E10.3))
101   FORMAT(5F)
      PI=3.1415926
      WRITE(2,71)
      N=3
      WRITE(2,1003) (R(I),D(I),I=1,N)
1003   FORMAT(20X,' RESISTIVITY=',E10.2,5X,'THICKNESS=',E10.3)
      I=1
37      READ(1,102) W(I),XX(I),YY(I)
      IF(W(I).GT.20.0) GO TO 38
      I=I+1
      GO TO 37
71    FORMAT(' TIME-DOMAIN CURVE FROM COSINE TRANSFORM OF H(J)',5X,
     1'STEP RESPONSE OF THE TIME CURVE')
38    WRITE(2,72)
72    FORMAT(6X,'TIME',8X,'AMPLITUDE',30X,'TIME',8X,'AMPLITUDE')
      T=0.0
      FZERO=0.0
C  CALCULATE THE ZERO-TIME VALUE
      DO 4  N=1,I-1
4     FZERO = FZERO +((1.0/PI)*(XX(N+1)-XX(N))*(W(N+1)-W(N)))
7     FORMAT(2E15.7,22X,2E15.7)
C  CALCULATE THE TIME-DOMAIN CURVE
      T=.0001
      DO 6  K=1,1000
      F(K)=0.0
      DO 5  J=1,I-1
5     F(K)=F(K)+(2.0/(PI*T**2))*((XX(J)-XX(J+1))/(W(J+1)-W(J)))*
     1(COS(W(J)*T)-COS(W(J+1)*T))
      T=T*2.0
      IF(T.GT.1000.) GO TO 100
6     CONTINUE
C  CALCULATE THE STEP RESPONSE
100   DO 18  JJ=1,I
18    XX(JJ)=XX(JJ)/(-1.0*W(JJ))
      T=0.0
      SZERO=0.0
      DO 14  N=1,I-1
14    SZERO=SZERO+((1.0/PI)*(XX(N+1)-XX(N))*(W(N+1)-W(N)))
      WRITE(2,7)T,FZERO,T,SZERO
      T=.0001
      DO 16  K=1,1000
      S(K)=0.0
      DO 15  J=1,I-1
15    S(K)=S(K)+(2.0/(PI*T**2))*((XX(J)-XX(J+1))/(W(J+1)-W(J)))*
     1(COS(W(J)*T)-COS(W(J+1)*T))
      WRITE(2,7) T,F(K),T,S(K)
      T=T*2.0
      IF(T.GT.1000.) GO TO 1000
16    CONTINUE
1000  STOP
      END
```

FLOW FOR ITRAN.F4

1-- Read in resistivities and thicknesses for three layers.

2-- Read in I number of times (T) and corresponding values (X) of the time function.

3 -- Calculate the real part of the frequency function from frequency, W, = 0.001 to W = 1000.

$$S_k = \sum_{k=1}^{I+1} 1/w \frac{XX_j - XX_{j+1}}{T_{j+1} - T_j} (\mathrm{Sin}T_j W - \mathrm{Sin}T_{j+1} W)$$

4-- Print out frequency and corresponding real part of the frequency function.

```
C::::::::::::::::
C  THIS PROGRAM CALCULATES THE FOURIER TRANSFORM OF A TIME-DOMAIN
C  FUNCTION USING A POLYGONAL APPROXIMATION TRANSFORM METHOD.
C  THE OUTPUT IS THE REAL PART OF THE FREQUENCY FUNCTION.
C::::::::::::::::
      DIMENSION R(25),D(25),XX(299),T(299),S(299),SS(299)
      READ(1,101)R(1),D(1),R(2),D(2),R(3)
102   FORMAT(2F)
101   FORMAT(5F)
      PI=3.1415926
      WRITE(2,71)
      N=3
      WRITE(2,1003) (R(I),D(I),I=1,N)
1003  FORMAT(' RESISTIVITY=',E10.2,5X,'THICKNESS=',E10.3)
      I=1
37    READ(1,102) T(I),XX(I)
      IF(T(I).GT.10.0)  GO TO 38
      I=I+1
      GO TO 37
71    FORMAT(' FREQUENCY-DOMAIN CURVE FROM SINE TRANSFORM OF H')
38    WRITE(2,72)
72    FORMAT(3X,'FREQUENCY',8X,'AMPLITUDE')
7     FORMAT(2E15.7)
      W=.001
      DO 16  K=1,1000
      S(K)=0.0
      DO 15 J=1,I-1
15    S(K)=S(K)+((XX(J)-XX(J+1))/(T(J+1)-T(J)))*
     1(SIN(T(J)*W)-SIN(T(J+1)*W))
      SS(K)=S(K)/W
      WRITE (2,7) W,SS(K)
      W=W*2.0
      IF(W.GT.1000.) GO TO 1000
16    CONTINUE
1000  STOP
      END
```

FLOW FOR EMFWD.F4

NOTE: For detailed derivation of the equation and program see Daniels (1974).

1-- Read in angle, R, numberof layers, number of frequencies.

2-- Read in thicknesses and resistivities for each layer.

3-- Read in current and source length.

4-- Read in each frequency to be calculated.

5-- Calculate the line-loop coupling using linear filter theory:

$$H_z = \frac{I\ ds\ \sin\theta\ e^{-x}}{2\pi\delta^2} \cdot \sum_{k=1}^{m} H(b_x)d_k -$$

$$\frac{j\ I\ ds\ \delta^2 \sin\theta}{4\pi r^4} \cdot (3-(3+3(1+j)B + 2jB^2)\ e^{-(1+j)B}$$

I -- current

ds -- source length

θ -- source/receiver angle

x -- ln B

δ^2 -- $2\rho_1/\mu\omega$

d_k -- $\mathrm{sinc}(x)*e^x J_1(x)$

j -- $(-1)^{\frac{1}{2}}$

r -- source-receiver separation

λ -- dummy variable of integration

B -- r/δ

J_1 -- Bessel function of the 1st order

b_k -- $e^{-(x-y_k)}$

g -- $\lambda\delta$

y -- $\ln(1/g)$

ρ_1 -- 1st layer resistivity

μ -- $4\pi*10^{-7}$

ω -- frequency

6-- Print out frequency and corresponding H_z.

```
C********************* PROGRAM EMFWD ****************************
C
C       THIS PROGRAM CALCULATES THE VERTICAL H FIELD, THE X-COMPONENT
C   OF THE ELECTRIC FIELD, THE Y-COMPONENT OF THE ELECTRIC FIELD,
C   AND THE COMBINED HORIZONTAL ELECTRIC FIELD COMPONENTS (EC*
C   SIN(2*ANG)EX-COS(2*ANG)EY) FOR A 1,2,OR 3 LAYERED EARTH,  THE SCURCE
C   IS A HORIZONTAL CURRENT DIPOLE
C
C
C      FIELDS FOR A HOMOGENCUS HALF-SPACE (1 LAYER) MAY BE COMPUTED
C   BY USING A TWO LAYER MODEL WITH RHO(2)=RHO(1).  MODELS
C   FOR MORE THAN THREE LAYERS MAY BE COMPUTED SIMPLY BY INCREASING
C   THE DIMENSIONS OF THE ARRAYS.
C
C
C       PROGRAM EMFWD WAS DEVELOPED ON A DEC PDP-10 COMPUTER AT THE
C   COLORADO SCHOOL OF MINES.  FORTRAN PROGRAMING LANGUAGE IS USED
C  THROUGHOUT
C
C
C                       JEFF DANIELS
C                   COLORADO SCHOOL OF MINES
C                       FEBRUARY 1974
C
C
C************************ VARIABLES *********************
C
C  NFW= THE NUMBER OF FREQUENCIES TO BE CALCULATED
C  R= SOURCE-RECEIVER SEPERATION
C  ANG=ANGLE,IN DEGREES, DEFINING SOURCE-RECEIVER ORIENTATION
C  FF=FREQUENCY IN HERTZ
C  F=ANGULAR FREQUENCY
C  N= THE NUMBER OF LAYERS
C  HP(I)= LAYER THICKNESS
C  RH(I)= LAYER RESISTIVITY
C  CH(I)= COEFFICIENTS FOR CALCULATING  THE J1 HANKEL TRANSFORM
C  YH(I)= ABSCISSA VALUES FOR CH(I)
C  CE(I)= COEFFICIENTS FOR CALCULATING THE J0 HANKEL TRANSFORM
C  YE(I)= ABSSCISSA VALUES FOR CALCULATING CE(I)
C  CI = SOURCE-DIPOLE CURRENT
C  DS= SOURCE-DIPOLE LENGTH
C  D = NORMATIZED THICKNESSES
C  RK= NORMALIZED RESISTIVITIES
C  DEL= MODIFIED WAVE NUMBER
C  IIN= INPUT AREA
C  IOUT= OUTPUT AREA
C
C
C*****************************************************************
      COMPLEX H,E,EX,EY
      DIMENSION HPP(3),HP(3)
      COMMON /QC/D(3),RK(3),RH(3),N,DEL,R
      COMMON /CV/CI,DS, ANG,F,X,YH(48),CH(48),YE(61),CE(61),TM
      DATA
     &YH/-4.5307316E 0,-4.3004731E 0,-4.0702146E 0,-3.8399561E 0,
     &   -3.6096976E 0,-3.3794391E 0,-3.1491806E 0,-2.9189221E 0,
     &   -2.6886636E 0,-2.4584051E 0,-2.2281466E 0,-1.9978881E 0,
     &   -1.7676296E 0,-1.5373711E 0,-1.3071126E 0,-1.0768541E 0,
     &   -8.4659563E-1,-6.1633713E-1,-3.8607863E-1,-1.5582013E-1,
     &    7.4438369E-2, 3.0469687E-1, 5.3495537E-1, 7.6521387E-1,
```

```
     &     9.9547237E-1, 1.2257309E 0, 1.4559894E 0, 1.6862479E 0,
     &     1.9165064E 0, 2.1467649E 0, 2.3770234E 0, 2.6072819E 0,
     &     2.8375404E 0, 3.0677989E 0, 3.2980574E 0, 3.5283159E 0,
     &     3.7585744E 0, 3.9888329E 0, 4.2190914E 0, 4.4493499E 0,
     &     4.6796084E 0, 4.9098669E 0, 5.1401254E 0, 5.3703839E 0,
     &     5.6006424E 0, 5.8309009E 0, 6.0611594E 0, 6.2914179E 0/
      DATA
     &CH/3.1010561E-6, 1.8802098E-5, 5.4819540E-5, 9.2891602E-6,
     &   1.5523239E-4, 3.0344652E-5, 3.5338744E-4, 1.4798002E-4,
     &   7.7342377E-4, 5.3570857E-4, 1.7170605E-3, 1.6387239E-3,
     &   3.9247683E-3, 4.5796508E-3, 9.2111468E-3, 1.2130467E-2,
     &   2.1938415E-2, 3.0853660E-2, 5.1973594E-2, 7.4661566E-2,
     &   1.1775455E-1, 1.6353574E-1, 2.3127545E-1, 2.7368461E-1,
     &   2.8059285E-1, 1.2875840E-1,-1.5380437E-1,-4.5659951E-1,
     &  -3.6077766E-2, 4.2985683E-1,-2.1506075E-1,-2.3624312E-2,
     &   8.9316746E-2,-7.4344203E-2, 4.8572965E-2,-3.0088872E-2,
     &   1.8846544E-2,-1.2158687E-2, 8.0708759E-3,-5.4706275E-3,
     &   3.7554604E-3,-2.5929707E-3, 1.7909426E-3,-1.2320277E-3,
     &   8.4095286E-4,-5.6749747E-4, 3.7718405E-4,-1.5891835E-4/
      DATA
     &YE/-6.8348046E 0,-6.6045461E 0,-6.3742876E 0,-6.1440291E 0,
     &   -5.9137706E 0,-5.6835121E 0,-5.4532536E 0,-5.2229951E 0,
     &   -4.9927366E 0,-4.7624781E 0,-4.5322196E 0,-4.3019611E 0,
     &   -4.0717026E 0,-3.8414441E 0,-3.6111856E 0,-3.3809271E 0,
     &   -3.1506686E 0,-2.9204101E 0,-2.6901516E 0,-2.4598931E 0,
     &   -2.2296346E 0,-1.9993761E 0,-1.7691176E 0,-1.5388591E 0,
     &   -1.3086006E 0,-1.0783421E 0,-8.4808358E-1,-6.1782508E-1,
     &   -3.8756658E-1,-1.5730808E-1, 7.2950416E-2, 3.0320892E-1,
     &    5.3346742E-1, 7.6372592E-1, 9.9398442E-1, 1.2242429E 0,
     &    1.4545014E 0, 1.6847599E 0, 1.9150184E 0, 2.1452769E 0,
     &    2.3755354E 0, 2.6057939E 0, 2.8360524E 0, 3.0663109E 0,
     &    3.2965694E 0, 3.5268279E 0, 3.7570864E 0, 3.9873449E 0,
     &    4.2176034E 0, 4.4478619E 0, 4.6781204E 0, 4.9083789E 0,
     &    5.1386374E 0, 5.3688959E 0, 5.5991544E 0, 5.8294129E 0,
     &    6.0596714E 0, 6.2899299E 0, 6.5201884E 0, 6.7504469E 0,
     &    6.9807054E 0/
      DATA
     &CE/7.3260937E-4, 5.6326423E-4, 1.3727237E-4, 7.5331222E-4,
     &   3.5918326E-4, 1.2500608E-3, 7.1530982E-4, 1.5160070E-3,
     &   1.2841617E-3, 2.2497985E-3, 2.1906186E-3, 3.4076782E-3,
     &   3.6321245E-3, 5.2376028E-3, 5.9212519E-3, 8.1315877E-3,
     &   9.5527062E-3, 1.2708615E-2, 1.5305589E-2, 1.9941086E-2,
     &   2.4396626E-2, 3.1333652E-2, 3.8683065E-2, 4.9127993E-2,
     &   6.0824806E-2, 7.6314344E-2, 9.3928346E-2, 1.1545027E-1,
     &   1.3868663E-1, 1.6248847E-1, 1.8114332E-1, 1.8424433E-1,
     &   1.5556741E-1, 6.8592481E-2,-8.8339029E-2,-2.8819226E-1,
     &  -3.5565260E-1,-5.6288677E-2, 4.8186942E-1,-5.1516453E-2,
     &  -2.6102989E-1, 2.1416490E-1,-9.4490687E-2, 2.6196370E-2,
     &  -5.1097828E-4,-6.6032948E-3, 7.5193619E-3,-6.7854344E-3,
     &   5.8044372E-3,-4.9354894E-3, 4.2323106E-3,-3.6733648E-3,
     &   3.2266260E-3,-2.8649137E-3, 2.5677680E-3,-2.3202655E-3,
     &   2.1115187E-3,-1.9334662E-3, 1.7800248E-3,-1.6465436E-3,
     &   1.5468317E-3/


14    FORMAT(1X,I2,1X,'LAYERS',2X,'SOURCE CURRENT=',
     &F8.3,2X,'SOURCE LENGTH=',F8.2,/,'ANGLE=',F8.2,2X,
     &'SOURCE-RECEIVER SEPERATION=',E12.4,/)
15    FORMAT(3X,'LAYER',3X,'RESISTIVITY',3X,'THICKNESS')
16    FORMAT(1X,I5,4X,E11.5,3X,E10.4)
```

```
10    FORMAT(//,3X,'FREQUENCY',4X,'H(REAL)',6X,'H(IMAG)',6X,'EC
     &(RFAL)',5X,'EC(IMAG)',/,3X,'FREQUENCY',4X,'EX(REAL)',
     &5X,'EX(IMAG)',5X,'EY(REAL)',5X,'EY(IMAG)',//)
12    FORMAT(5(1X,E12.6))
 5    FORMAT(1F)
 1    FORMAT(2F,2I)
28    FORMAT(2F)
 3    FORMAT(2F)
      IIN=3
      IOUT=8
      READ(IIN,1) ANG,R,N,NFW
      DO 11 LT=1,N
11    READ(IIN,28) HP(LT),RH(LT)
      READ(IIN,3) CI,DS
      WRITE(IOUT,14) N,CI,CS,ANG,R
      WRITE(IOUT,15)
      WRITE(IOUT,16) (LT,RH(LT),HP(LT),LT=1,N)
      NB=2*N
      TM=12.566371E-7
      ANG=(3.1415927/180.)*ANG
      DO 2 JJ=1,N
 2    RK(JJ)=RH(1)/RH(JJ)
      WRITE(IOUT,10)
      DO 20 I=1,NFW
      READ(IIN,5) FF
      F=6.2831853*FF
      DEL=SQRT(2.*RH(1)/(TM*F))
      DO 6 JJ=1,N
 6    D(JJ)=2.*HP(JJ)/DEL
      X=ALOG(R/DEL)
      CALL FV(E,H,EX,EY)
      WRITE(IOUT,12) FF,H

20    CONTINUE
      END
      SUBROUTINE FV(EC,H,EX,EY)
C
C***************SUBROUTINE FVALUE ******************************
C  THIS SUBROUTINE CALCULATES THE CONVOLUTION SUMS FOR EX,
C  EY, EC, AND HZ ELECTROMAGNETIC FIELD COMPONENTS
C
C********************** VARIABLES ******************************
C
C  SUM= CONVOLUTION SUM FOR HZ
C  SUEY1,SUEY0, SUEX1, SUEX0 AS DEFINED ON PAGE 10 OF THESIS
C  SUEY1= CONVOLUTION SUM FOR EY1
C  SUEY0= CONVOLUTION SUM FOR EX1
C  SUEX1= CONVOLUTION SUM FOR EX3
C  SUEX0= CONVOLUTION SUM FOR EX2
C  H1= CLOSED-FORM HOMOGENEOUS HALF-SPACE EXPRESSION FOR HZ
C  EX= X-COMPONENT OF THE ELECTRIC FIELD FOR A LAYERED EARTH
C  EY= Y-COMPONENT OF THE ELECTRIC FIELD FOR A LAYERED EARTH
C  EX1= CLOSED-FORM EXPRESSION FOR A HOMOGENOUS HALF-SPACE
C        (X-COMPONENT)
C  EY1= CLOSED-FORM EXPRESSION FOR A HOMOGENOUS HALF-SPACE
C       (Y-COMPONENT)
C  E= CLOSED-FORM EXPRESSION FOR A HOMOGENOUS HALF-SPACE
C       ( COMBINED ELECTRIC FIELD)
C  EC= COMBINED ELECTRIC FIELD FOR A LAYERED EARTH
C  F1= LAYERED EARTH CORRECTION FACTOR
```

```
C   Z1= LAYERED EARTH CORRECTION FACTOR
C   V1= NORMALIZED FIRST LAYER PSEUDO WAVE NUMBER
C
C
C*****************************************************************

      COMMON /CV/ CI,DS,ANG,F,X,YH(48),CH(48),YE(61),CE(61),TM
      COMMON /QC/ D(3),RK(3),RH(3),N,DEL,R
      COMPLEX H,V1,F1,SUM,H1,Z1,E1,EC,C1,C2,
     &EX1,EX0,EY1,EY0,SUEX1,SUEY1,SUEX0,SUEY0,EX,EY
      SUEX1=CMPLX(0.0,0.0)
      SUEY1=CMPLX(0.0,0.0)
      SUEX0=CMPLX(0.0,0.0)
      SUEY0=CMPLX(0.0,0.0)
      SUM=CMPLX(0.0,0.0)
      BB=EXP(X)
      C1=CMPLX(0.0,1.0)
      C2=CMPLX(1.0,1.0)
C*************************************
CALCULATE THE J1 HANKEL TRANSFORMS
C*************************************
      DO 8 J=1,49
      Y=EXP(-(X-YH(J)))
      CALL CALC(F1,Z1,V1,Y)
      EX1=C1*V1*(Z1-1)+2.*V1*(1-F1)/((Y+V1*F1)*(Y+V1))
      SUEX1=SUEX1+CH(J)*EX1
      H=Y*Y*V1*(1.-F1)
      H=H/((Y+V1*F1)*(Y+V1))
      SUM=SUM+CH(J)*H
 8    CONTINUE
      SUEY1=SUEX1
      H=(1/BB)* CI*DS*SIN(ANG)*SUM/(6.2831853*DEL*DEL)
      R2=R*R
      H1=3.-(3.+3.0*C2*BB+2.*C1*BB**2)*CEXP(-C2*BB)
      H1=(-C1*CI*DS*DEL*DEL*SIN(ANG)*H1)/(12.566371*R2*R2)
12    FORMAT(2(1X,E14.8))
      H=H+H1
      SUM=CMPLX(0.0,0.0)
C*************************************
CALCULATE THE J0 HANKEL TRANSFORMS
C*************************************
      DO 4 I=1,61
      Y=EXP(-(X-YE(I)))
      CALL CALC(F1,Z1,V1,Y)
      EY0=Y*(C1*V1*(Z1-1.)+2.*V1*(1.-F1)/((Y+V1)*(Y+V1*F1)))
      EX0=(COS(ANG)**2/DEL)*EY0-(1/DEL)*2.*Y*V1*(1.-F1)/
     &((Y+V1*F1)*(Y+V1))
      SUEX0=SUEX0+CE(I)*EX0
      SUEY0=SUEY0+CE(I)*EY0
      EC=C1*V1*Y*(Z1-1.0)/2.0
      EC=EC-Y*V1*(1.0-F1)/((Y+V1*F1)*(Y+V1))
 4    SUM=SUM+CE(I)*EC
      EC=C1*TM*F*CI*DS*SIN(2.*ANG)*SUM/(12.566371*DEL*BB)
      E1=-.500*(1+C2*BB)*CEXP(-C2*BB)
      E1=CI*DS*RH(1)*SIN(2.*ANG)*E1/(6.2831853*R*R2)
      EC=E1+EC
      EX=(C1*TM*F*CI*DS/(12.566371*BB))*(SUEX0-COS(2.*ANG)
     &*SUEX1/R)
      EY=(C1*TM*F*CI*DS/(12.566371*BB))*SIN(2.*ANG)*(-SUEY1/R
     &+SUEY0/(2.*DEL))
```

```
      EX1=CI*DS*RH(1)*((3*COS(ANG)**2-2)+(1.+(1+C1)*BB)*CEXP(-C2*BB)
     &)/(6.2831853*R*R2)
      EY1=3.*RH(1)*CI*DS*SIN(ANG)*COS(ANG)/(6.2831853*R*R2)
      EX=EX+EX1
      EY=EY+EY1
      RETURN
      END



      SUBROUTINE CALC(F1,Z1,V1,Y)
C*****************************************************
C SUBROUTINE CALC CALCULATES THE LAYERED EARTH CORRECTION FACTORS
C (F1 AND Z1) FOR UP TO 3 LAYERS**************************
      COMMON /QC/ D(3),RK(3),RH(3),N,DEL,R
      COMPLEX V1,F1,V2,AEX,Z1
      Y2=Y*Y
      T=2.*RK(N)
      V2=CSQRT(CMPLX(Y2,T))
      DO 9 LL=2,N
      IF(LL.GT.2) GO TO 4
      F1=CMPLX(1.0,0.0)
      Z1=CMPLX(1.0,0.0)
 4    I=N-LL+1
      DD=D(I)
      T=2.*RK(I)
      V1=CSQRT(CMPLX(Y2,T))
      AEX=(1.-CEXP(-V1*DD))/(1.+CEXP(-V1*DD))
      F1=(V2*F1+V1*AEX)/(V1+V2*F1*AEX)
      Z1=(V2*RH(I+1)*Z1+V1*RH(I)*AEX)/(V1*RH(I)+V2*RH(I+1)*Z1*AEX)
 9    V2=V1
      RETURN
      END
```

FLOW FOR EMINT.F4

NOTE: For detailed derivation and discussion of the program see Daniels (1974).

1-- Read in angle, R, current, source length, number of frequencies, and 21.

2-- Read in frequency and Real (HZ) pairs from the observed curve.

3-- Read in the parameters that may be varied.

4-- Read in estimated resistivities and thicknesses.

5-- Read in a normalization factor.

6-- Calculate theoretical curve from the model of Step 4 using the method described for EMFWD.F4.

7-- Calculate a RMS error, ϕ, = $\sum_{i=1}^{n} (Y_{observed} - Y_{model})^2$

8-- Calculate a correction vector (δ).

9-- Calculate new parameters: $P_{new} = P_{old} + \delta$

10-- Calculate a new theoretical curve.

11-- Repeat steps 7 through 10 until ϕ is small enough or five times.

12-- The smallest ϕ and the adjusted resistivity and thickness values are printed out.

```
C****************** PROGRAM EMINT ******************************
C       THIS PROGRAM USES MARQUARDT'S ALGORITHM TO ADJUST FIRST
C  GUESS PARAMETERS TO FIT THE OBSERVED DATA.  THE SOURCE IS
C  ASSUMED TO BE A CURRENT DIPOLE.  RECEIVER COMPONENTS WHICH THIS
C PROGRAM WILL FIT ARE CHOSEN BY THE VARIABLE NCOMP LISTED BELOW.
C
C        PROGRAM EMINT WAS DEVELOPED ON A DEC PDP-10 COMPUTER
C  AT THE COLORADO SCHOOL OF MINES,  FORTRAN PROGRAMMING LANGUAGE IS
C  USED THROUGHOUT THE PROGRAM.
C
C
C
C                         JEFF DANIELS
C                    COLORADO SCHOOL OF MINES
C                       FEBRUARY 1974
CC****************************** VARIABLES  *********************
C NCOMP=21 ← REAL PART OF HZ CALCULATED
C ANG= ANGLE (IN DEGREES) DEFINING THE SOURCE-RECEIVER ORIENTATION
C R= SOURCE-RECEIVER SEPERATION
C CI= SOURCE CURRENT
C DS= SOURCE LENGTH (IN METERS)
C YNORM= NORMALIZATION FACTOR FOR THE INPUT Y VALUES ( E.G. IF
C       THE AVERAGE VALUE FOR 20 EX VALUES (AT 20 DIFFERENT FREQUENCIES)
C       IS .10070E-10, YNORM SHOULD BE .10070E-10)
C IE= THE NUMBER OF X-Y PAIRS OF VALUES TO BE INPUT
C X(I)= THE ITH FREQUENCY
C Y(I)= THE ITH VALUE OF THE ELECTROMAGNETIC FIELD COMPONENT
C        CORRESPONDING TO THE ITH FREQUENCY
C N= THE NUMBER OF LAYERS IN THE FIRST-GUESS MODEL
C HP(I)= ITH LAYER THICKNESS
C RH(I)= ITH LAYER RESISTIVITY
C ** CHOICE OF PARAMETERS TO BE VARIED **
C IFXE(J)=0 THE JTH PARAMETER IS NOT VARIED
C IFXE(J)=1 THE JTH PARAMETER IS VARIED
C TWO LAYER ORDER:
C   J=1 ← R; J=2 ← RH(1); J=3 ← HP(1); J=4 ← RH(2)
C THREE LAYE  ORDER:
C  J=1 ← R; J=2 ← RH(1); J=3 ← HP(1); J=4 ← RH(2);J=5 ← HP(2);
C  J=6 ← RH(3)
C***************************************************************
      COMMON /CV/ CI,DS,ANG,FX,XX,TM
      COMMON /QC/ DD(3),RKK(3),RHH(3),N,DEL,RR
      DIMENSION X(25),Y(25),B(7),WTS(25),
     &BDB(7),ATA(7,7),IFXE(6),HP(3),RH(3)
      REAL LAM
      IN=1
C***************************************
C READ IN THE DATA UNDER THE LOGICAL UNIT "IN"
C***************************************
      READ(IN,1)ANG,R,CI,DS,IE,N,NCOMP
      NFW=IE
 7    FORMAT(E)
 1    FORMAT(4F,3I)
      READ(IN,9)(X(I),Y(I),WTS(I),I=1,NFW)
9     FORMAT(2(3X,E14.3),2X,F3.1)
 2    FORMAT(2F)
      ANG=(3.1415927/180.)*ANG
      NB=2*N
      READ(IN,8) (IFXE(J),J=1,NB)
 8    FORMAT(I6)
```

```
      READ(IN,2) (HP(LT),RH(LT),LT=1,N)
      READ(IN,7) YNORM
      DO 4 JJ=1,NFW
4     Y(JJ)=Y(JJ)/YNORM
      NPAR=NR
      B(1)=R
      DO 3 JCT=1,N
      NCT=2*JCT
      B(NCT)=RH(JCT)
      B(NCT+1)=HP(JCT)
3     CONTINUE
      CALL NONLS2(NPAR,IFXE,IE,X,Y,WTS,B,NCOMP,YNORM)
      END



      SUBROUTINE NONLS2 (NPAR,IFXE,IE,X,Y,WTS,B,NCOMP,YNORM)
C******************** SUBROUTINE NONLS2 ****************************
C  THIS SUBROUTINE CONTROLS THE LEAST-SQUARES CURVE FITTING
C ALGORITHM AS OUTLINED BY MARQUARDT (1963)
C
C
C    THIS IS A MODIFIED VERSION OF THE ORIGINAL
C GEOPHYSICS LEAST-SQUARES PROGRAM WRITTEN BY JORGE
C PARRA.
C
C
C**********LEAST SQUARES SUBROUTINE****************************
C  NVAR=# OF UNFIXED PARAMETERS
C  NPAR=# OF UNKNOWN PARAMETERS OF F > LINOUT
C  NPTS=#OF OBSERVATION POINTS
C  IW=OUTPUT (FLAG:-1=NO OUTPUT,0,1,2=OUTPUT)
C  FAIL=OUTPUT(0,1,2=CONVERGENCE;3,4,5=NO CONVERGENCE)
C  MAXITR=THE MAXIMUM # OF ITERATIONS ALLOWED
C  IFXE=ACCURACY(IFXE(K)=1,THE KTH PARAMETER IS ALLOWED TO VARY;
C       IFXE(K)=0, THE KTH PARAMETER IS FIXED AT ITS INPUT VALUE)
C  NEXT=,
C  LINMIN=?
C  X(IE,2)=DOUBLY DIMENSIONED ARRAY HOLDING THE OBSERVATIONS
C          (INDEPENDENT VARIABLES) AS ROWS OF X
C  Y(IE)= ARRAY HOLDING THE DEPENDENT VARIABLE OBSERVATIONS
C  WTS=ARRAY HOLDING THE RELIABILITY WEIGHTS FOR EACH POINT
C      /IF WTS=? THE WEIGHT =1.0/
C  ATA=A* MATRIXFROM MARQUARDT'S FORMULATION
C  B=HOLDS THE INITIAL ESTIMATES OF THE PARAMETERS. IF IFAIL=0
C    OR 1, B HOLDS THE CONVERGED PARAMETER SET
C  BDB= THE FINAL CORRECTION VECTOR TO THE CONVERGED PARAMETERS
C  IP=10**-5
C  LAM=MARQUARDT'S DAMPING CONSTANT
C  PHI=(Y(OBS)-Y(MODEL))**2
C  DAC=.05 / PARABLOIC MINIMUMIZATION
C  FVALUE=SUBROUTINE THAT CALCULATES THE MODEL
C  PARVAL=SUBROUTINE THAT CALCULATES THE FIRST DERIVATIVE OF THE
C         MODEL
C  ANS=CORRECTION VECTOR AT THE POINTS OF LINEAR MINIMUMIZATION
C     *************************************************************

      DIMENSION ATF(7),ANS(7),ANS1(7),EX(7)
      DIMENSION X(25),Y(25),B(7),BDB(7),WTS(25),ATA(7,7)
      REAL LAM,L00,L10,NORM
```

```
      DIMENSION INX(7),IFXE(7)
        INTEGER FAIL
1003  FORMAT(4(2X,E14.8))
C**********************************
C  SET THE CONSTANT VALUES
C**********************************
      LAM= 0.01
      NPTS=IE
      ID=NPAR
      MAXITR=6
      EP=1.E+0
      NEXT=0
      GAMA0=45.
        IW=3
      ITER=0
      TOLR=1.E-8
      IOUT=2
      IR=3
C     DETERMINE THE PARAMETERS TO BE VARIED.
C
      NVAR=0
      DO 10 I=1,NPAR
      BDB(I)=B(I)
      ANS(I)=0.E0
      ANS1(I)=0.E0
      IF(IFXE(I).LE.0) GO TO 10
      NVAR=NVAR+1
      INX(NVAR)=I
10    CONTINUE
3001  FORMAT(I)
      IF(IW.GE.0) WRITE(IOUT,11700) NPAR,NVAR,NPTS,MAXITR,IW,LINMIN,EP,
     *DAC
C
C       EXAMINE THE WTS ARRAY
C
      NORM=0.E0
      DO 40 I=1,NPTS
      IF(WTS(I)) 20,30,40
20    WTS(I)=1.E0/WTS(I)**2
      GO TO 40
30    WTS(I)=1.E0
40    NORM=NORM+WTS(I)
        NORM=FLOAT(NPTS)/NORM
      IF(NORM.EQ.1.E0) GO TO 60
      DO 50 I=1,NPTS
50    WTS(I)=WTS(I)*NORM
C
C     CALCULATE THE INITAL SUM OF SQUARES
C
60    PHI=0.E0
      IF(IW.GT.0) WRITE(IOUT,10200)
      DO 70 I=1,NPTS
      NPVFC=1
      CALL EMCALC (X,B,IE,I,EX,FV,IFXE,NPVFC,NCOMP,YNORM)
      SS=Y(I)-FV
      IF(IW.GT.0) WRITE(IOUT,10000) X(I),Y(I),FV,SS
 70   PHI=PHI+SS**2*WTS(I)
C**********************************
C       START THE DAMPED GAUSSIN PROCEDURE
C**********************************
```

```
C
80      ITER=ITER+1
        IF(IW.GT.0) WRITE(IOUT,11800)
        IF(ITER.GT.MAXITR) GO TO 380
        DO 90 I=1,NPAR
90      BDB(I)=B(I)
        DO 100 I=1,NVAR
        ATF(I)=0.E0
        DO 100 J=I,NVAR
100     ATA(I,J)=0.E0
C*************************************
C         GENERATE THE ATA AND ATF ARRAYS
C*************************************
        DO 110 I=1,NPTS
        NPVFC=1
        CALL EMCALC(X,B,IE,I,EX,FV,IFXE,NPVFC,NCOMP,YNORM)
        NORM=WTS(I)*(Y(I)-FV)
        NPVFC=0
        CALL EMCALC(X,B,IE,I,EX,FV,IFXE,NPVFC,NCOMP,YNORM)
        DO 110 L=1,NVAR
        J=INX(L)
        ATF(L)=ATF(L)+NORM*EX(J)
        DO 110 M=L,NVAR
        K=INX(M)
        ATA(L,M)=ATA(L,M)+EX(J)*EX(K)*WTS(I)
110     CONTINUE
        IF(IW.GT.0) WRITE(IOUT,11500) ITER,PHI,(B(I),I=1,NPAR)
C*********************************************
C       PERFORM A LOCAL SCALING ON THE ATA MATRIX TO AID CALCULATIONS.
C*********************************************
        DO 120 I=1,NVAR
        IF(ATA(I,I).EQ.0.D0) GO TO 410
120     EX(I)=SQRT(ATA(I,I))
        DO 140 I=1,NVAR
        ATF(I)=ATF(I)/EX(I)
        DO 140 J=I,NVAR
        IF(I.EQ.J) GO TO 130
        ATA(I,J)=ATA(I,J)/(EX(I)*EX(J))
        GO TO 140
130     ATA(I,I)=1.E0
140     CONTINUE
C*************************************************************
C       DETERMINE A VALID LAMDA FOR THE SCALED PARTIAL MATRIX.
C   GAMA=DIRECTION VECTOR ANGLE
C   PHI1=SS ERROR FOR NEW LAMBDA
C*************************************************************

        FAC=1.E+0
        CALL NEWLAM(ATA,LAM,BDB,ATF,ANS,EX,GAMA,FVALUE,PHI1,X,Y,WTS,B,
       *ID,IE,NVAR,NPTS,NPAR,IFAL,INX,IFXE,IR,NCOMP,YNORM)
        IF(IW.GT.0) WRITE(IOUT,10600) LAM,PHI1,GAMA
C*********************************************************
C   EP= RELATED TO THE FIRST GUESS (CONTROLS LAMBDA SO THAT
C       LAMBDA DOESN'T GET TOO LARGE) EXAMPLE:EP=.5 THEN THE
C       GREATEST CHANGE THAT THE PARAMETERS CAN HAVE IS 50% OF
C       THE ORIGINAL FIRST GUESS
C*********************************************************
        IF(IFAL-1) 150,390,400
150     DO 160 I=1,NVAR
        IF(ABS(ANS(I)).GT.(TOLR+EP*ABS(B(INX(I))))) GO TO 180
```

```
160   CONTINUE
      IF(PHI.LT.PHI1) GO TO 440
      DO 170 I=1,NVAR
170   B(INX(I))=B(INX(I))+ANS(I)
      PHI =PHI1
      GO TO 440
180   IF(PHI1.GE.PHI) GO TO 220
      IF(LAM.LE.TOLR) GO TO 320
      DO 1213 JP1=1,NVAR
1213  B(JP1)=BDB(JP1)
      PHI=PHI1
      LDO=LAM/10.0E0
      CALL NEWLAM(ATA,LDO,BDB,ATF,ANS1,EX,GAMA,FVALUE,PHI2,X,Y,WTS,B,
     *ID,IE,NVAR,NPTS,NPAR,IFAL,INX,IFXE,IR,NCOMP,YNORM)
      IF(IW.GT.0) WRITE(IOUT,10700) LDO,PHI2,GAMA
      IF(IFAL-1) 190,390,400
190   IF(PHI2.GE.PHI1) GO TO 320
200   LAM=LDO
      DO 1207 JP1=1,NVAR
1207  B(JP1)=BDB(JP1)
      PHI=PHI2
      DO 210 I=1,NVAR
210   ANS(I)=ANS1(I)
      PHI1=PHI2
      GO TO 320
220   LDO=LAM/10.0E0
      CALL NEWLAM(ATA,LDO,BDB,ATF,ANS1,EX,GAMA,FVALUE,PHI2,X,Y,WTS,B,
     *ID,IE,NVAR,NPTS,NPAR,IFAL,INX,IFXE,IR,NCOMP,YNORM)
      IF(IW.GT.0) WRITE(IOUT,10700) LDO,PHI2,GAMA
      IF(IFAL-1) 230,390,400
230   IF(PHI2.LT.PHI) GO TO 200
      L10=LAM
240   L10=L10*10.E0
      CALL NEWLAM(ATA,L10,BDB,ATF,ANS,EX,GAMA,FVALUE,PHI3,X,Y,WTS,B,
     *ID,IE,NVAR,NPTS,NPAR,IFAL,INX,IFXE,IR,NCOMP,YNORM)
      IF(L10.GT.1.E+6) STOP
      IF(IW.GT.0) WRITE(IOUT,10900) L10,PHI3,GAMA
      IF(IFAL-1) 250,390,400
250   IF(PHI3.GE.PHI.AND.L10.GT.1.E+3) GO TO 360
      IF(PHI3.GE.PHI) GO TO 260
      PHI1=PHI3
      PHI=PHI3
      DO 1208 JP1=1,NVAR
1208  B(JP1)=BDB(JP1)
      LAM=L10
      GO TO 320
260   IF(GAMA.GE.GAMA0) GO TO 240
      FAC=FAC/2.E0
      DO 270 I=1,NVAR
270   ANS(I)=ANS(I)/2.E0
      DO 280 I=1,NVAR
      IF(ABS(ANS(I)).GT.(TOLR+EP*ABS(B(INX(I))))) GO TO 290
280   CONTINUE
      GO TO 430
290   DO 300 I=1,NVAR
300   BDB(INX(I))=B(INX(I))+ANS(I)
      PHI3=0.D0
      DO 310 I=1,NPTS
      NPVFC=1
      CALL EMCALC(X,BDB,IE,I,EX,FV,IFXE,NPVFC,NCOMP,YNORM)
```

```
310   PHI3=PHI3+(Y(I)-FV)**2*WTS(I)
      IF(IW.GT.0) WRITE(IOUT,10300) FAC,PHI3
      GO TO 250
320   CONTINUE
      IF(IW.LE.1) GO TO 360
      IF(NVAR.EQ.NPAR) GO TO 340
      DO 330 I=1,NPAR
330   EX(I)=0.E0
340   DO 350 I=1,NVAR
350   EX(INX(I))=ANS(I)
      WRITE(IOUT,11600) (EX(I),I=1,NPAR)
360   CONTINUE
      GO TO 440
380   IF(IW.GE.0) WRITE(IOUT,12300)
      FAIL=2
      GO TO 450
390   IF(IW.GE.0) WRITE(IOUT,12000)
      FAIL=3
      RETURN
400   IF(IW.GE.0) WRITE(IOUT,11900) GAMA,LAM
      FAIL=4
      RETURN
410   IF(IW.GE.0) WRITE(IOUT,11400) I,(B(K),K=1,NPAR)
      FAIL=6
      RETURN
420   IF(IW.GE.0) WRITE(IOUT,10500)
      FAIL=5
      RETURN
430   IF(IW.GT.0) WRITE(IOUT,12400)
      FAIL=1
      GO TO 450
440   IF(ITER.LE.4) GO TO 80
C*************************************
C     THE PROCEDURE HAS CONVERGED
C*************************************
      FAIL=0
      IF(IW.GE.0) WRITE(IOUT,11800)
      IF(IW.GE.0) WRITE(IOUT,11800)
      IF(IW.GE.0) WRITE(IOUT,12200) ITER
 450  IF(IW.GE.0) WRITE(IOUT,12100) PHI,(B(I),I=1,NPAR)
C*************************************************
C     CALCULATE THE STANDARD ERROR, USE NPTS-NVAR-NEXT AS THE DF.
C*************************************
        NORM=SQRT(PHI/FLOAT(NPTS-NVAR-NEXT))
C*************************************************
C     REMAKE THE PARTIAL MATRIX INSTEAD OF USING THE RE-SCALED MATRIX.
C     THIS COULD EASILY BE CHANGED.
C*************************************************
      DO  460 I=1,NPAR
460   BDB(I)=0.E0
      DO 470 I=1,NVAR
      DO 470 J=I,NVAR
470   ATA(I,J)=0.E0
      DO 480 I=1,NPTS
      NPVFC=0
      CALL EMCALC(X,B,IE,I,EX,FV,IFXE,NPVFC,NCOMP,YNORM)
      DO 480 L=1,NVAR
      J=INX(L)
      DO 480 M=L,NVAR
      K=INX(M)
```

```
480   ATA(L,M)=ATA(L,M)+EX(J)*EX(K)*WTS(I)
      CALL INVRT (NVAR,ATA,ID,IFU)
      IF(IFU.EQ.1) GO TO 420
      DO 490 I=1,NVAR
      EX(I)=SQRT(ATA(I+1,I))
 490  BDB(INX(I))=NORM*EX(I)
C*********************************
C     CALCULATE THE CORRELATION MATRIX
C*********************************
      DO 500 I=1,NVAR
      DO 500 J=I,NVAR
500   ATA(I,J)=ATA(J+1,I)/(EX(I)*EX(J))
      IF(IW.LT.0) RETURN
C*****************************************************
C       PRINT THE PARAMETERS AND THE STANDARD ERRORS ASSOCATED TO THEM
C*****************************************************
      WRITE(IOUT,11300) (INX(I),B(INX(I)),BDB(INX(I)),I=1,NVAR)
      IF(NVAR.EQ.1) GO TO 520
      IF(FAIL.EQ.2) GO TO 540
C*************************
C     PRINT THE CORRELATION MATRIX
C*********************************
      WRITE(IOUT,11200)
      DO 510 I=1,NVAR
510   WRITE(IOUT,11000) I,(ATA(J,I),J=1,I)
C*************************
C     PRINT THE INVERSE MATRIX
C*********************************
      WRITE(IOUT,11800)
      WRITE(IOUT,11800)
520   WRITE(IOUT,11100)
      M=NVAR+1
      DO 530 I=2,M
      K=I-1
530   WRITE(IOUT,10400) I,(ATA(I,J),J=1,K)
540   CONTINUE
      WRITE(IOUT,11800)
      WRITE(IOUT,11800)
      WRITE(IOUT,10100)
      DO 550 I=1,NPTS
      NPVFC=1
      CALL EMCALC(X,B,IE,I,EX,FV,IFXE,NPVFC,NCOMP,YNORM)
      SS=Y(I)-FV
550   WRITE(IOUT,10000) X(I),Y(I),FV,SS
      WRITE(IOUT,12500) YNORM
      RETURN
10000 FORMAT(4E14.8)
10100 FORMAT(1H0,'FINAL DEVIATIONS'/1H ,1X,'FREQUENCY',3X
     &,'OBS',13X,'CAL',12X,'O-C')
10200 FORMAT(1H0,'INITIAL DEVIATIONS'/1H ,13X,'OBS',13X,'CALC',12X,
     *'O-C')
10300 FORMAT(1H0,'FAC=',E14.8,6X,'  PHI(FAC) = ',F14.8)
10400 FORMAT(1H ,'ROW ',I2/(1H ,8E15.6))
10500 FORMAT(1H0,'FINAL A TRANSPOSE A IS NOT POSITIVE DEFINE')
10600 FORMAT(1H0,' IN-L = ',E14.8,'     PHI(IN-L) = ',E14.8,
     *'      GAMA = ',F10.4)
10700 FORMAT(1H0,' L/10 = ',E14.8,'     PHI(L/10) = ',E14.8,
     *'     GAMA = ',F10.4)
10800 FORMAT(3H0L ,7E14.8/(3H   ,16X,6E14.8))
10900 FORMAT(1H0,' L*10 = ',E14.8,'      PHI(L*10) V ',E14.8,
```

```
     *'   GAMA = ',F10.4)
11000 FORMAT(1H ,'ROW',I2/(1H ,8E15.6))
11100 FORMAT(1H0,  ' INVERSE MATRIX - LOWER TRIANGULAR PORTION')
11200 FORMAT(1H0,'CORRELATION MATRIX LOWER TRIANGULAR PORTION ROW BY ROW
     *PRINT')
11300 FORMAT(1H0,'  VARIABLE',6X,'PARAMETER VALUE',5X,'STANDARD ERROR'/
     * (1H0,4X,I2,9X,E15.6,7X,E10.4))
11400 FORMAT(1H0,'THE DIAGONAL ELEMENT RESULTING FROM THE PARTIAL WRT
     *B(',I2,') IS = 0.D'/1H ,'THE POINT AT WHICH THE FAILURE OCCURED
     *IS'/(1H ,7E14.8))
11500 FORMAT(1H0,'ITERATION ',I3/1H ,7E14.8/(1H ,16X,6E14.8))
11600 FORMAT(1H0,'DIR-VEC',5X,6E14.8/(1H0,12X,6E14.8))
11700 FORMAT(1H1,T3,'NPAR',T11,'NVAR',T19,'NPTS',T27,'MAXITR',T37,'IW',
     *T42,'LINMIN',T56,'EP',T71,'DAC'/1H ,T4,I2,T12,I2,T20,I2,T29,
     *I2,T37,I2,T44,I2,T53,E10.4,T68,E10.4)
11800 FORMAT(1H0/)
11900 FORMAT(1H0,'GAMA = ',E14.8,' WHEN LAM = ',E14.8/
     *1H ,'THERE PROBABLY EXISTS EXCESSIVELY HIGH CORRELATIONS BETWEEN
     * THE PARAMETERS')
12000 FORMAT(1H0,'THE (ATA +LAM*I) MATRIX FAILED TO BE POS.DEF.')
12100 FORMAT(1H0,7E14.8/(1H ,16X,6E14.8))
12200 FORMAT(1H0,'OPTIMAL POINT REACHED IN ',I5, ' ITERATIONS')
12300 FORMAT(1H0,'MAXIMUM NUMBER OF ITERATIONS REACHED-BEST POINT PRIN
     *TED'/)
12400 FORMAT(1H0,'THE DELTA-B VECTOR REDUCED TO CONVERGENCE LEVEL WHILE
     *GAMA LESS THAN GAMA0.'/1H ,'THE POINT IS PROBABLY OPTIMAL WITHIN
     *ROUNDING ERRORS.')
12500 FORMAT(1X,'NORMALIZATION FACTOR = ',E14.8)
      END


      SUBROUTINE NEWLAM(ATA,LAM,B1,ATF,ANS,EX,GAMA,FVALUE,PHI,
     &X,Y,WTS,B,ID,IE,NVAR,NPTS,NPAR,IFAL,INX,IFXE,IR,NCOMP,YNORM)
C******** SUBROUTINE NEWLAM **********************************
C       SUBROUTINE NEWLAM CALCULATES THE NEW LAMBDA FOR THE LEAST
C  SQUARES PROCEDURE CONVERGENCE ACCORDING TO THE ALGORITHM
C  STATED BY MARQUARDT (1963).
C
C
C                ORIGINAL PROGRAMER   JORGE PARRA
C                MODIFIED BY          JEFF DANIELS
C
C*************************************************************
      DIMENSION ATA(7,7),B1(7),ATF(7),ANS(7),EX(7)
      DIMENSION Y(IE),X(IE),WTS(IE),B(7)
      DIMENSION INX(20),IFXE(7)
      REAL LAM
      CON=57.295779E0
      IFAL=0
      DO 10 I=1,NVAR
      ATA(I,I)=1.E0
10    ATA(I,I)=ATA(I,I)+LAM
      ERRORX=.001E+0
      CALL DSOL (ATA,ATF,ANS,25,NVAR,ERRORX,10,IDET,1,IFAIL)
1005   FORMAT(I5)
1006   FORMAT(3(4X,E14.8))
      IF(IFAIL.EQ.1) GO TO 20
      IFAL=1
      RETURN
 20   DO 30 I=1,NVAR
```

```
30      ANS(I)=ANS(I)/EX(I)
        IFAIL=0
        IF(NVAR.NE.1) GO TO 40
        GAMA=0.E0
        GO TO 70
40      SUM1=0.E0
        SUM2=0.E0
        SUM3=0.E0
        DO 50 I=1,NVAR
        SUM1=SUM1+ANS(I)*ATF(I)
        SUM2=SUM2+ATF(I)**2
50      SUM3=SUM3+ANS(I)**2
        COSGAM=SUM1/SQRT(SUM2*SUM3)
          UV=SQRT(1.E0-COSGAM*COSGAM)
          GAMA=ATAN(UV/COSGAM)*CON
        IF(COSGAM.GT.0.E0) GO TO 60
        GAMA=180.E0-GAMA
        IF(LAM.LT.1.E0) GO TO 60
        IFAIL=1
60      IF(IFAIL.EQ.0) GO TO 70
        IFAL=2
        RETURN
70      DO 80 I=1,NVAR
        K=INX(I)
80      B1(K)=B(K)*ANS(I)
        PHI=0.E0
        DO 90 I=1,NPTS
        NPVFC=1
        CALL EMCALC(X,B1,IE,I,EX,FV,IFXE,NPVFC,NCOMP,YNORM)
90      PHI=PHI+(Y(I)-FV)**2*WTS(I)
        RETURN
        END
        SUBROUTINE INVRT(N,A,IE,IFL)
C*****************SUBROUTINE INVRT*****************************
C   THIS PROGRAM PERFORMS A MATRIX INVERSION ON THE
C TWO DIMENSIONAL ARRAY A.
C**************************************************************


        DIMENSION A(7,7)
        IFL=2
        DO 40 I=1,N
        I1=I+1
        DO 40 J=I,N
        J1=J+1
        X=A(I,J)
        K=I-1
10      IF(K.LT.1) GO TO 20
        X=X-A(J1,K)*A(I1,K)
        K=K-1
        GO TO 10
20      IF(J.NE.I) GO TO 30
        IF(X.LE.0.E0) GO TO 90
        Y=1.E0/SQRT(X)
        A(I1,I)=Y
        GO TO 40
30      A(J1,I)=X*Y
40      CONTINUE
        NL=N-1
        DO 60 I=1,NL
```

```
      KL=I+1
      DO 6Ø J=KL,N
      Z=A(J,I)*E0
      J1=J+1
      K=J-1
5Ø    IF(K.LT.I) GO TO 6Ø
      Z=Z-A(J1,K)*A(K+1,I)
      K=K-1
      GO TO 5Ø
6Ø    A(J1,I)=Z*A(J1,J)
      J1=N+1
      DO 8Ø I=1,N
      DO 8Ø J=I,N
      Z=0.D0
      KL=J+1
      DO 7Ø K=KL,J1
7Ø    Z=Z+A(K,J)*A(K,I)
8Ø    A(KL,I)=Z
      RETURN
9Ø    IFL=1
      RETURN
      END
```

```
      SUBROUTINE DSOL (A,B,X,NAMAX,NA,ERRORX,MAXIT,K,IENTRY,ISING)
C
C     THIS SUBROUTINE SOLVES A SET OF SIMULTANEOUS LINEAR EQUATIONS
C     USING CROUTS FACTORIZATION WITH PARTIAL PIVOTING, EQUILIBRATION,
C     ITERATIVE IMPROVEMENT, AND DOUBLE PRECISION OF PRODUCTS TO REDUCE
C     ROUND-OFF ERROR.
C
C     SUBROUTINE PARAMETERS  ..........................................
C     A       = THE COEFFICIENT MATRIX
C     B       = THE CONSTANT VECTOR
C     X       = THE SOLUTION VECTOR (INFORMATION RETURNED)
C     NAMAX   = THE NUMBER OF ROWS IN THE DIMENSION OF A IN
C               THE CALLING PROGRAM.
C     NA      = THE NUMBER OF ROWS IN A
C     ERRORX  = THE MAXIMUM ALLOWABLE ERROR BETWEEN SUCCESSIVE ITERATIONS
C     MAXIT   = THE MAXIMUM ALLOWABLE NUMBER OF ITERATIONS
C     K       = THE ACTUAL NUMBER OF ITERATIONS PERFORMED (INFORMATION RE
C     IENTRY  = 1 (FIRST CALL TO SUBROUTINE)
C             = 2 (SUBSEQUENT CALLS WITH UNCHANGED A)
C     ISING   = 1  THE MATRIX IS NON-SINGULAR (INFORMATION RETURNED)
C             = 2  THE MATRIX IS SINGULAR, PROCEDURE DISCONTINUED.
C     .................................................................
C     IF A SINGULAR MATRIX IS ENCOUNTERED THE PROCEDURE IS DISCONTINUED
C     AND ERROR MESSAGES ARE PRINTED OUT.
C     IF A SOLUTION IS REQUIRED FOR THE SAME A-MATRIX, BUT FOR DIFFERENT
C     B-VECTORS, THE SUBROUTINE MAY BE SUBSEQUENTLY DIRECTED TO ENTRY
C     POINT -- TWO.
C     .................................................................
C                       PROGRAMED BY
C                    DONALD SNYDER 1968
C                  COLORADO SCHOOL OF MINES
C
```

```
C
      DOUBLE PRECISION S
      DIMENSION A(7,7),B(7),X(7),BIGB(7,7),Q(7),R(7)
      DIMENSION IPIV(10)
      IOUT=2
C
      GO TO (100,200),IENTRY
C
C     ENTRY -- ONE  ..................................................
  100 CONTINUE
C
C     STORE MATRIX A IN ARRAY BIGB
      DO 101 I=1,NA
      DO 101 J=1,NA
  101 BIGB(I,J)=A(I,J)
C
C     DETERMINE ELEMENT WITH MAXIMUM MODULUS IN EACH ROW. STORE IN Q.
      DO 103 I=1,NA
      PLAINQ=0.0
      DO 102 J=1,NA
      TEST=ABS(A(I,J))
      IF (TEST.GT.PLAINQ) PLAINQ=TEST
  102 CONTINUE
      Q(I)=PLAINQ
C     BOX 13 -- CHECK FOR SINGULARITY  ...............................
      IF (PLAINQ.LT.0.1E-30) GO TO 301
C
  103 CONTINUE
C
C
C     DETERMINE THE ELEMENTS OF THE LOWER TRIANGULAR FACTOR OF A
C     STORE OVER BIGB
      DO 110 IR=1,NA
      AMAX=0.0
      IRMAX=IR
      LIM=IR-1
      DO 106 I=IR,NA
      S=DBLE(BIGB(I,IR))
      IF (IR.EQ.1) GO TO 105
      DO 104 J=1,LIM
  104 S=S-BIGB(I,J)*BIGB(J,IR)
  105 BIGB(I,IR)=SNGL(S)
      TEST=ABS(BIGB(I,IR)/Q(I))
      IF (TEST.LE.AMAX) GO TO 106
      AMAX=TEST
      IRMAX=I
  106 CONTINUE
C
C     BOX 37 - CHECK FOR SINGULARITY  ................................
      IF (AMAX.LT.0.1E-30) GO TO 302
C
      Q(IRMAX)=Q(IR)
      IPIV(IR)=IRMAX
C
C     INTERCHANGE THE IR AND IRMAX ROWS OF BIGB
      DO 107 I=1,NA
      PLAINQ=BIGB(IR,I)
      BIGB(IR,I)=BIGB(IRMAX,I)
  107 BIGB(IRMAX,I)=PLAINQ
C
```

```
C       DETERMINE THE ELEMENTS OF THE UPPER TRIANGULAR FACTOR OF A
C       STORE OVER BIGB
        IF (IR.EQ.NA) GO TO 110
        LOW=IR+1
        DO 109 I=LOW,NA
        S=DBLE(BIGB(IR,I))
        IF (IR.EQ.1) GO TO 109
        DO 108 J=1,LIM
  108   S=S-BIGB(IR,J)*BIGB(J,I)
  109   BIGB(IR,I)=SNGL(S/DBLE(BIGB(IR,IR)))
  110   CONTINUE
C
C       FACTORIZATION IS COMPLETE. NOW FIND SOLUTION
C
C       ENTRY -- TWO  .....................................................
  200   CONTINUE
C
C       PRESET ITERATION PARAMETERS, AND INITIALIZE SOLUTION AND ERROR VEC
        K=0
        IFIN=0
        ISING=1
        DO 201 I=1,NA
        X(I)=0.0
  201   R(I)=B(I)
  202   CONTINUE
C
C       PERFORM FORWARDS SUBSTITUTION
        DO 204 I=1,NA
        L=IPIV(I)
        S=DBLE(R(L))
        R(L)=R(I)
        IF (I.EQ.1) GO TO 204
        LIM=I-1
        DO 203 J=1,LIM
  203   S=S-BIGB(I,J)*R(J)
  204   R(I)=SNGL(S/DBLE(BIGB(I,I)))
C
C       PERFORM BACKWARDS SUBSTITUTION
        I=NA+1
        DO 206 N=1,NA
        I=I-1
        S=DBLE(R(I))
        IF (I.EQ.NA) GO TO 206
        LOW=I+1
        DO 205 J=LOW,NA
  205   S=S-BIGB(I,J)*R(J)
  206   R(I)=S
C
C       COMPUTE NORMS
        ANORMX=0.0
        ANORME=0.0
        IF (K.EQ.0) GO TO 212
        DO 207 I=1,NA
        TEST=ABS(X(I))
        IF (TEST.GT.ANORMX) ANORMX=TEST
        TEST=ABS(R(I))
        IF (TEST.GT.ANORME) ANORME=TEST
  207   CONTINUE
C
        IF (K.NE.1) GO TO 208
```

```
C
C       BOX 94 - CHECK FOR SINGULARITY  ..............................
        IF ((ANORME/ANORMX).GT.0.5) GO TO 303
C
  208 IF ((ANORME/ANORMX).LT.ERRORX) IFIN=1
  210 CONTINUE
C
C       COMPUTE CURRENT APPRCXIMATE SOLUTION
        DO 211 I=1,NA
211     X(I)=X(I)+R(I)
C
C       COMPUTE ERROR AND STORE BACK IN R
        DO 213 I=1,NA
        S=DBLE(B(I))
        DO 212 J=1,NA
  212 S=S-A(I,J)*X(J)
213     R(I)=SNGL(S)
        K=K+1
        IF (IFIN.EQ.1) RETURN
        IF (K.LT.MAXIT) GO TO 202
C
C       PRINT ERROR MESSAGE AND RETURN
        WRITE(IOUT,11) MAXITR
        RETURN
  301 IBOX=13
        GO TO 304
  302 IBOX=37
        GO TO 304
  303 IBOX=94
304     WRITE(IOUT,12) IBOX
        ISING=2
C
   11 FORMAT(1H0,53HSOLUTION HAS NOT CONVERGED TO DESIRED ACCURACY AFTER
     1,I5,11H ITERATIONS)
   12 FORMAT(1H0,31HSINGULAR MATRIX DETECTED AT BOX,I3)
C
        RETURN
        END


        SUBROUTINE EMCALC(FF,B,IE,I,DERIV,FV,IFXE,NPVFC,NCOMP,YNORM)
C********************* SUBROUTINE EMCALC ******************
C THIS SUBROUTINE HANDLES BOTH THE CALCULATION OF THE FORWARD
C SOLUTION AND THE PARTIAL DERIVATIVES OF THE FORWARD
C SOLUTION WITH RESPECT TO THE LAYERED EARTH PARAMETERS
C AND THE SOURCE RECEIVER SEPERATION.
C
C*********************VARIABLES*****************************
C  FF= FREQUENCY IN HERTZ
C  F= ANGULAR FREQUENCY
C  D(I)= NORMALIZED THICKNESS FOR THE I-TH LAYER
C  RK(I)= NORMALIZED RESISTIVITIES FOR THE I-TH LAYER
C  DEL= MODIFIED WAVE NUMBER
C
C
C*************************************************************

        COMPLEX  H,E
        COMMON /PD/ EXX(6),HX(6),DINX(6),KFXE(6),EC,HZ,ECR,ECI,HZR,HZI
       &,EXR(6),EXI(6),HXR(6),HXI(6)
```

```
      COMMON /QC/DD(3),RKK(3),RHH(3),N,DEL,RR
      COMMON /CV/CI,DS, ANG,F,XX,TM
      COMMON /PART/ RK(3),RH(3),HP(3),HPP(3),D(3),
     &X,R,NB
      DIMENSION B(7),FF(25),DERIV(7),IFXE(6)

      R=B(1)
      NB=2*N
      DO 1 JCT=1,N
      NCT=2*JCT
      RH(JCT)=B(NCT)
      HP(JCT)=B(NCT+1)
 1    CONTINUE
      DO 3 JC=1,NB
 3    KFXE(JC)=IFXE(JC)
      TM=12.566371E-7
      F=FF(I)*6.2831853
      DEL=SQRT(2.*RH(1)/(TM*F))
      DO 2 JJ=1,N
      D(JJ)=2.*HP(JJ)/DEL
 2    RK(JJ)=RH(1)/RH(JJ)
      X=ALOG(R/DEL)
      P=1.001
      RR=R
      XX=X
      DO 9 J=1,N
      RHH(J)=RH(J)
      RKK(J)=RK(J)
 9    DD(J)=D(J)
      CALL FVAL(E,H,NCOMP)
      EC=CABS(E)
      HZ=CABS(H)
      ECR=REAL(E)
      ECI=AIMAG(E)
      HZR=REAL(H)
      HZI=AIMAG(H)
      IF(NPVFC.EQ.0) GO TO 17
      IF(NCOMP.EQ.21) FV=HZR/YNORM
17    CONTINUE
      IF(NPVFC.EQ.1) GO TO 4
      CALL PARDER (IFXE,DERIV,NCOMP,YNORM)
 4    CONTINUE
      RETURN
      END



      SUBROUTINE PARDER(IFXE,DERIV,NCOMP,YNORM)
C*******SUBROUTINE PARDER*******************************
C THIS SUBROUTINE CONTROLS THE PARTIAL DIFFERENTATION WRT THE
C LAYERING PARAMETERS (RESISTIVITY AND THICKNESS)
C*****************************************************************
      COMMON /PD/ EXX(6),HX(6),DINX(6),KFXE(6),EC,HZ,ECR,ECI,
     &HZR,HZI,EXR(6),EXI(6),HXR(6),HXI(6)
      COMMON /QC/ DD(3),RKK(3),RHH(3),N,DEL,RR
      COMMON /CV/CI,DS,ANG,F,XX,TM
      COMMON /PART/ RK(3),RH(3),HP(3),HPP(3),
     &D(3),X,R,NB
      DIMENSION DERIV(7),IFXE(6)
      COMPLEX H,E
```

```
      JP=1
      IF(IFXE(JP).EQ.0) GO TO 6
      P=1.001
      RR=P*R
      XX=ALOG(RR/DEL)
      DIMX(JP)=RR-R
      CALL FVAL(E,H,NCOMP)
      EXX(JP)=CABS(E)
      HX(JP)=CABS(H)
      EXR(JP)=REAL(E)
      EXI(JP)=AIMAG(E)
      HXR(JP)=REAL(H)
      HXI(JP)=AIMAG(H)
      XX=X
      GO TO 7
    6 EXX(JP)=EC
      HX(JP)=HZ
      EXR(JP)=ECR
      EXI(JP)=ECI
      HXR(JP)=HZR
      HXI(JP)=HZI
    7 JP=JP+1
      DO 12 J=1,N
      IF(IFXE(JP).EQ.0) GO TO 8
      RHH(J)=P*RH(J)
      RKK(J)=RHH(1)/RHH(J)
      DIMX(JP)=RHH(J)-RH(J)
      CALL FVAL(E,H,NCOMP)
      EXX(JP)=CABS(E)
      HX(JP)=CABS(H)
      EXR(JP)=REAL(E)
      EXI(JP)=AIMAG(E)
      HXR(JP)=REAL(H)
      HXI(JP)=AIMAG(H)
      RHH(J)=RH(J)
      RKK(J)=RK(J)
      GO TO 13
    8 EXX(JP)=EC
      HX(JP)=HZ
      EXR(JP)=ECR
      EXI(JP)=ECI
      HXR(JP)=HZR
      HXI(JP)=HZI
   13 JP=JP+1
      IF(J.EQ.N) GO TO 12
      IF(IFXE(JP).EQ.0) GO TO 10
      HPP(J)=P*HP(J)
      DD(J)=2.*HPP(J)/DEL
      DIMX(JP)=HPP(J)-HP(J)
      CALL FVAL(E,H,NCOMP)
      EXX(JP)=CABS(E)
      HX(JP)=CABS(H)
      EXR(JP)=REAL(E)
      EXI(JP)=AIMAG(E)
      HXR(JP)=REAL(H)
      HXI(JP)=AIMAG(H)
      HPP(J)=HP(J)
      DD(J)=2.*HP(J)/DEL
      GO TO 12
   10 EXX(JP)=EC
```

```
      HX(JP)=HZ
      EXR(JP)=ECR
      EXI(JP)=ECI
      HXR(JP)=HZR
      HXI(JP)=HZI
12    JP=JP+1
 5    CONTINUE
      CALL FINDIF (NB,NCOMP,DERIV)
      DO 19 JPZ=1,NB
19    DERIV(JPZ)=DERIV(JPZ)/YNORM
 4    CONTINUE
      RETURN
      END

      SUBROUTINE FINDIF (NB,NCOMP,DERIV)
C*************SUBROUTINE FINDIF*******************************
C THIS SUBROUTINE CALCULATES THE PARTIAL DERIVATIVES OF THE
C PARAMETERS USING FINITE DIFFERENCES
C***********************************************************

      COMMON /PD/ EX(6),HX(6),DINX(6),INX(6),EC,HZ,ECR,ECI,HZR,HZI,
     &EXR(6),EXI(6),HXR(6),HXI(6)
      DIMENSION DERIV(7)
      DO 1 JP=1,NB
      IF(INX(JP).EQ.0) GO TO 2
1005  FORMAT(3(2X,E14.8))
      GO TO 6
 6    IF(NCOMP.NE.21) GO TO 7
      DERIV(JP)=(HXR(JP)-HZR)/DINX(JP)
      GO TO 1
 7    IF(NCOMP.NE.31) GO TO 1
      DERIV(JP)=(HXI(JP)-HZI)/DINX(JP)
      GO TO 1
 2    DERIV(JP)=0.0
 1    CONTINUE
      RETURN
      END

      SUBROUTINE FVAL (EC,H,NCOMP)
C***************SUBROUTINE FVAL *****************************
C THIS SUBROUTINE CALCULATES THE FORWARD SOLUTION ON COMMAND FROM
C EMCALC USING LINEAR DIGITAL FILTER THEORY
C
C************************VARIABLES****************************
C  CH= COEFFICIENTS FOR CALCULATING THE J1 HANKEL TRANSFORM
C  YH= ABCISSA VALUES FOR CH
C  CE= COEFFICIENT FOR CALCULATING THE J0 HANKEL TRANSFORM
C  YE= ARCISSA VALUES FOR CALCULATING CE
C  SUM= CONVOLUTION SUM FOR HZ
C  SUEY1,SUEX1,SUEY0,SUEX0, ARE AS DEFINED ON PAGE 10 OF THESIS
C  SUEY1= CONVOLUTION SUM FOR EY1
C  SUEX1= CONVLOUTION SUM FOR EX3
C  SUEY0= CONVOLUTION SUM FOR EX1
C  SUEX0= CONVOLUTION SUM FOR EX2
C  H1= CLOSED FORM HOMOGENCUS HALF-SPACE EXPRESSION FOR HZ
C  EX1= CLOSED FORM EXXPRESSION FOR A HOMOGENOUS HALF-SPACE
C       ( X-COMPONENT)
C  EY1= CLOSED FORM EXPRESSION FOR A HOMOGENOUS HALF-SPACE
C       (Y-COMPONENT)
C  EX= X-COMPONENT OF THE ELECTRIC FIELD FOR A LAYERED EARTH
```

```
C   EY= Y-COMPONENT OF THE ELECTRIC FIELD FOR A LAYERED EARTH
C   EC= COMBINED ELECTRIC FIELD FOR A LAYERED EARTH
C   F1= LAYERED EARTH CORRECTION FACTOR
C   Z1= LAYERED EARTH CORRECTION FACTOR
C   V1= NORMALIZED FIRST LAYER PSEUDO WAVE NUMBER
C
C
C*****************************************************************

      COMMON /CV/ CI,DS,ANG,F,X,TM
      COMMON /QC/ D(3),RK(3),RH(3),N,DEL,R
      COMPLEX EX1,EX0,EY1,EY0,SUEX1,SUEX0,SUEY1,SUEY0,EX,EY
      COMPLEX H,V1,F1,SUM,Z1,E1,EC,H1,C1,C2
      DIMENSION YH(48),CH(48),YE(61),CE(61)
      DATA
     &YH/-4.5307316E 0,-4.3004731E 0,-4.0702146E 0,-3.8399561E 0,
     &   -3.6096976E 0,-3.3794391E 0,-3.1491806E 0,-2.9189221E 0,
     &   -2.6886636E 0,-2.4584051E 0,-2.2281466E 0,-1.9978881E 0,
     &   -1.7676296E 0,-1.5373711E 0,-1.3071126E 0,-1.0768541E 0,
     &   -8.4659563E-1,-6.1633713E-1,-3.8607863E-1,-1.5582013E-1,
     &    7.4438369E-2, 3.0469687E-1, 5.3495537E-1, 7.6521387E-1,
     &    9.9547237E-1, 1.2257309E 0, 1.4559894E 0, 1.6862479E 0,
     &    1.9165064E 0, 2.1467649E 0, 2.3770234E 0, 2.6072819E 0,
     &    2.8375404E 0, 3.0677989E 0, 3.2980574E 0, 3.5283159E 0,
     &    3.7585744E 0, 3.9888329E 0, 4.2190914E 0, 4.4493499E 0,
     &    4.6796084E 0, 4.9098669E 0, 5.1401254E 0, 5.3703839E 0,
     &    5.6006424E 0, 5.8309009E 0, 6.0611594E 0, 6.2914179E 0/
      DATA
     &CH/3.1010561E-6, 1.8802098E-5, 5.4819540E-5, 9.2891602E-6,
     &   1.5523239E-4, 3.0344652E-5, 3.5338744E-4, 1.4798002E-4,
     &   7.7342377E-4, 5.3570857E-4, 1.7170605E-3, 1.6387239E-3,
     &   3.9247683E-3, 4.5796508E-3, 9.2111468E-3, 1.2130467E-2,
     &   2.1938415E-2, 3.0853660E-2, 5.1973594E-2, 7.4661566E-2,
     &   1.1775455E-1, 1.6353574E-1, 2.3127545E-1, 2.7368461E-1,
     &   2.8059285E-1, 1.2875840E-1,-1.5380437E-1,-4.5659951E-1,
     &  -3.6077766E-2, 4.2985683E-1,-2.1506075E-1,-2.3624312E-2,
     &   8.9316746E-2,-7.4344203E-2, 4.8572965E-2,-3.0088872E-2,
     &   1.8846544E-2,-1.2158687E-2, 8.0708759E-3,-5.4706275E-3,
     &   3.7554604E-3,-2.5929707E-3, 1.7909426E-3,-1.2320277E-3,
     &   8.4095286E-4,-5.6749747E-4, 3.7718405E-4,-1.5891835E-4/
      DATA
     &YE/-6.8348046E 0,-6.6045461E 0,-6.3742876E 0,-6.1440291E 0,
     &   -5.9137706E 0,-5.6835121E 0,-5.4532536E 0,-5.2229951E 0,
     &   -4.9927366E 0,-4.7624781E 0,-4.5322196E 0,-4.3019611E 0,
     &   -4.0717026E 0,-3.8414441E 0,-3.6111856E 0,-3.3809271E 0,
     &   -3.1506686E 0,-2.9204101E 0,-2.6901516E 0,-2.4598931E 0,
     &   -2.2296346E 0,-1.9993761E 0,-1.7691176E 0,-1.5388591E 0,
     &   -1.3086006E 0,-1.0783421E 0,-8.4808358E-1,-6.1782508E-1,
     &   -3.8756658E-1,-1.5730808E-1, 7.2950416E-2, 3.0320892E-1,
     &    5.3346742E-1, 7.6372592E-1, 9.9398442E-1, 1.2242429E 0,
     &    1.4545014E 0, 1.6847599E 0, 1.9150184E 0, 2.1452769E 0,
     &    2.3755354E 0, 2.6057939E 0, 2.8360524E 0, 3.0663109E 0,
     &    3.2965694E 0, 3.5268279E 0, 3.7570864E 0, 3.9873449E 0,
     &    4.2176034E 0, 4.4478619E 0, 4.6781204E 0, 4.9083789E 0,
     &    5.1386374E 0, 5.3688959E 0, 5.5991544E 0, 5.8294129E 0,
     &    6.0596714E 0, 6.2899299E 0, 6.5201884E 0, 6.7504469E 0,
     &    6.9807054E 0/
      DATA
     &CE/7.3260937E-4, 5.6326423E-4, 1.3727237E-4, 7.5331222E-4,
     &   3.5918326E-4, 1.0930608E-3, 7.1530982E-4, 1.5160070E-3,
```

```
     &    1.2841617E-3, 2.2497985E-3, 2.1906186E-3, 3.4076782E-3,
     &    3.6321245E-3, 5.2376028E-3, 5.9212519E-3, 8.1315877E-3,
     &    9.5527062E-3, 1.2708615E-2, 1.5305589E-2, 1.9941086E-2,
     &    2.4396626E-2, 3.1333652E-2, 3.8683065E-2, 4.9127993E-2,
     &    6.0824806E-2, 7.6314344E-2, 9.3926346E-2, 1.1545027E-1,
     &    1.3868663E-1, 1.6248847E-1, 1.8114332E-1, 1.8424433E-1,
     &    1.5556741E-1, 6.8592481E-2,-8.8339029E-2,-2.8819226E-1,
     &   -3.5565260E-1,-5.6288677E-2, 4.8186942E-1,-5.1516453E-2,
     &   -2.6102989E-1, 2.1416490E-1,-9.4490687E-2, 2.6196370E-2,
     &   -5.1097828E-4,-6.6032948E-3, 7.5193619E-3,-6.7854344E-3,
     &    5.8244372E-3,-4.9354894E-3, 4.2323106E-3,-3.6733648E-3,
     &    3.2266260E-3,-2.8649137E-3, 2.5677680E-3,-2.3202655E-3,
     &    2.1115187E-3,-1.9334662E-3, 1.7800248E-3,-1.6465436E-3,
     &    1.3468317E-3/
      SUEX1=CMPLX(0.0,0.0)
      SUEY1=CMPLX(0.0,0.0)
      SUEX0=CMPLX(0.0,0.0)
      SUEY0=CMPLX(0.0,0.0)
      SUM=CMPLX(0.0,0.0)
      BB=EXP(X)
      C1=CMPLX(0.0,1.0)
      C2=CMPLX(1.0,1.0)
C*****************************************
CALCULATE THE FIRST ORDER HANKEL TRANSFORMS
C*****************************************
      DO 8 J=1,48
      Y=EXP(-(X-YH(J)))
      CALL CALC(F1,Z1,V1,Y)
      EX1=C1*V1*(Z1-1)+2.*V1*(1-F1)/((Y+V1*F1)*(Y+V1))
      SUEX1=SUEX1+CH(J)*EX1
      H=Y*Y*V1*(1.-F1)
      H=H/((Y+V1*F1)*(Y+V1))
      SUM=SUM+CH(J)*H
 8    CONTINUE
      SUEY1=SUEX1
      H=(1/BB)* CI*DS*SIN(ANG)*SUM/(6.2831853*DEL*DEL)
      R2=R*R
      H1=3.-(3.+3.0*C2*BB+2.*C1*BB**2)*CEXP(-C2*BB)
      H1=(-C1*CI*DS*DEL*DEL*SIN(ANG)*H1)/(12.566371*R2*R2)
12    FORMAT(2(1X,E14.8))
      H=H+H1
      IF(MOD(NCOMP,10).EQ.1) GO TO 6
      SUM=CMPLX(0.0,0.0)
C*****************************************
CALCULATE THE ZEROTH ORDER HANKEL TRANSFORMS
C*****************************************
      DO 4 I=1,61
      Y=EXP(-(X-YE(I)))
      CALL CALC(F1,Z1,V1,Y)
      EY0=Y*(C1*V1*(Z1-1.)+2.*V1*(1.-F1)/((Y+V1)*(Y+V1*F1)))
      EX0=(COS(ANG)**2/DEL)*EY0-(1/DEL)*2.*Y*V1*(1.-F1)/
     &((Y+V1*F1)*(Y+V1))
      SUEX0=SUEX0+CE(I)*EX0
      SUEY0=SUEY0+CE(I)*EY0
      EC=C1*V1*Y*(Z1-1.0)/2.0
      EC=EC-Y*V1*(1.0-F1)/((Y+V1*F1)*(Y+V1))
 4    SUM=SUM+CE(I)*EC
      EC=C1*TM*F*CI*DS*SIN(2.*ANG)*SUM/(12.566371*DEL*BB)
      E1=-.5*0+(1+C2*BB)*CEXP(-C2*BB)
      E1=CI*DS*RH(1)*SIN(2.*ANG)*E1/(6.2831853*R*R2)
```

```
      EC=E1+EC
      EX=(C1*TM*F*CI*DS/(12.566371*BB))*(SUEX0-COS(2.*ANG)
     &*SUEX1/R)
      EY=(C1*TM*F*CI*DS/(12.566371*BB))*SIN(2.*ANG)*(-SUEY1/R
     &+SUEY0/(2.*DEL))
      EX1=CI*DS*RH(1)*((3*COS(ANG)**2-2)+(1.+(1+C1)*BB)*CEXP(-C2*BE)
     &)/(6.2831853*R*R2)
      EY1=3.*RH(1)*CI*DS*SIN(ANG)*COS(ANG)/(6.2831853*R*R2)
      EX=EX+EX1
      EY=EY+EY1
      IF(NCOMP.GE.10.AND.NCOMP.LE.30) GO TO 7
      IF(NCOMP.GE.40.AND.NCOMP.LE.60) GO TO 11
      IF(NCOMP.GE.70.AND.NCOMP.LE.90) GO TO 9
 7    EC=EC
      GO TO 6
11    EC=EX
      GO TO 6
 9    EC=EY
 6    CONTINUE
      RETURN
      END



      SUBROUTINE CALC(F1,Z1,V1,Y)
C*************************************************
C SUBROUTINE CALC CALCULATES THE LAYERED EARTH CORRECTION FACTORS
C (F1 AND Z1) FOR UP TO 3 LAYERS*********************
      COMMON /BC/ D(3),RK(3),RH(3),N,DEL,R
      COMPLEX V1,F1,V2,AEX,Z1
      Y2=Y*Y
      T=2.*RK(N)
      V2=CSQRT(CMPLX(Y2,T))
      DO 9 LL=2,N
      IF(LL.GT.2) GO TO 4
      F1=CMPLX(1.0,0.0)
      Z1=CMPLX(1.0,0.0)
 4    I=N-LL+1
      DD=D(I)
      T=2.*RK(I)
      V1=CSQRT(CMPLX(Y2,T))
      AEX=(1.-CEXP(-V1*DD))/(1.+CEXP(-V1*DD))
      F1=(V2*F1+V1*AEX)/(V1+V2*F1*AEX)
      Z1=(V2*RH(I+1)*Z1+V1*RH(I)*AEX)/(V1*RH(I)+V2*RH(I+1)*Z1*AEX)
 9    V2=V1
      RETURN
      END
```

REFERENCES

Cagniard, L., 1953, Basic theory of the magneto-telluric method of geophysical prospecting: Geophysics, v. 18, no. 3.

Daniels, J. J., 1974, Interpretation of electromagnetic soundings using a layered-earth model: Thesis - 1627, Colorado School of Mines, Golden, Colorado.

Davis, D. and Yamanaga, G., 1968, Preliminary report on the water resources of the Hilo-Puna area, Hawaii: Hawaii Division of Water and Land Development Circ. C45.

Department of Land and Natural Resources, 1970, An inventory of basic water resources data: Island of Hawaii: Division of Water and Land Development Report R34.

Duncan, George, 1942, The dug well at Olaa Mill: Volcano Letter 477.

Finch, R. H., 1925, The earthquakes at Kapoho, Island of Hawaii, April, 1924: Bull. Seismol. Soc. Am., v. 15, no. 2.

_____ 1946, The Puna Rift of Kilauea: Volcano Letter 493.

Fisher, W. A., Davis, D. A., and Sousa, T. M., 1966, Fresh-water springs of Hawaii from infrared images: U. S. Geol. Survey Hydrol. Inv. Atlas HA-218.

Frischknect, F. C., 1967, Field about an oscillating magnetic dipole over a two-layer earth, and application to ground and airborne electromagnetic survey: Colorado School of Mines Quart., v. 62, no. 1.

Heirtzler, J. P., Peter, G., Talwani, M., and Zurflueh, J. P., 1962, Magnetic anomalies caused by two-dimensional structure: their computation by digital computers and their interpretation, Cambridge, Mass., Columbia Univ. Tech. Rept. 6.

Isaev, G. A., Kaufman, A. A., and Rabinovich, B. I., 1971, The late stage in short-separation transient sounding: (in Russian) Geologi i geofiziki, no. 1, p. 119-123.

Jackson, D. B., and Keller, G. V., 1972, An eletromagnetic sounding survey of the summit of Kilauea Volcano, Hawaii: Jour. Geophys. Research, v. 77, no. 26.

Kalakaua, David, 1888, Legends and myths of Hawaii: Tokyo, Chas. Tuttle Co.

Kaufman, A. A., and Morozova, G. M., 1970, Theoretical basis for transient sounding at short spacings: (in Russian) Novosjbirsk, Nauka Siberian Dept.

Keller, G. V., 1968, Electrical prospecting for oil: Colorado School of Mines Quart., v. 63, no. 2.

_____ 1970, Induction methods in prospecting for hot water: Pisa, Italy, Proc. United Nations Symposium on the Devel. and Utilization of Geothermal Resources.

Keller, G. V., and Frischknect, F. C., 1966, Electrical methods in geophysical prospecting: London, Pergamon Press.

King, C. A., 1971, Time-domain electromagnetic coupling: Thesis-1427, Colorado School of Mines, Golden, Colorado.

Kinoshita, W., Krivoy, H., Mabey, D., and Macdonald, G., 1965, A gravity survey of the Island of Hawaii: U. S. Geol. Survey Prof. Paper 475-C.

Krivoy, H. L., and Eaton, J. P., 1961, Preliminary gravity survey of Kilauea Volcano, Hawaii: U. S. Geol. Survey Prof. Paper 424-D.

Macdonald, G. A., 1949, Petrography of the Island of Hawaii: U. S. Geol Survey Prof. Paper 214-D.

_____ 1965, Hawaiian calderas: Pacific Sci., v. 19, no. 3.

_____ 1973, Geological prospects for development of geothermal energy in Hawaii: Pacific Sci., v. 27, no. 3.

Macdonald, G. A., and Eaton, J. P., 1964, Hawaii volcanoes during 1955: U. S. Geol. Survey Bull. 1171.

Malahoff, A. and McCoy, F., 1967, Geologic structure of the Puna submarine ridge, Hawaii: Jour. Geophys. Reserach, v. 72, no. 2.

Moore, J. G., and Richter, D. H., 1962, The 1961 flank eruption of Kilauea Volcano, Hawaii: Am. Geophys. Union Trans., v. 43, no. 4.

Moore, J. G., and Krivoy, H. L., 1964, The 1962 flank eruption of Kilauea: Jour. Geophys. Research, v. 69, no. 10.

Papóulis, A., 1962, The Fourier integral and its applications: New York, McGraw-Hill Book Co.

Popular Mechanics, 1908, Locate ores by wireless electric waves: Popular Mechanics, v. 10, no. 1, p. 33-34.

Pritchard, J. I., 1971, The theory of electromagnetic soundings in the frequency-domain: Thesis-1364, Colorado School of Mines, Golden, Colorado.

Silva, L. R., 1969, Two-layer master curves for electromagnetic sounding: Thesis-1250, Colorado School of Mines, Golden, Colorado.

Stearns, H. T., 1966, Geology of the state of Hawaii: Palo Alto, California, Pacific Books.

Stearns, H. T., and Macdonald, G. A., 1946, Geology and groundwater resources of the Island of Hawaii: Hawaii Division of Hydrography Bull. 9.

Vacquier, V., Steenland, N. C., Henderson, R. G., and Zietz, I., 1951, Interpretation of aeromagnetic maps: Geol. Soc. Am. Mem. 47.

Vanyan, L. L., et al., 1967, Electromagnetic depth soundings: New York, Consultants Bureau.

Wentworth, C. K., 1947, Factors in the behavior of ground water in a Ghyben-Herzberg system: Pacific Sci., v. 1, no. 3.